DESIGN AND IMPLEMENTATION OF FOUR ELECTRODE BASED IMPEDIMETRIC SENSORS

A DISSERTATION

Submitted in partial fulfillment of the
requirements for the award of the degree

of

MASTER OF TECHNOLOGY

in

ELECTRONICS AND COMMUNICATION ENGINEERING

(With Specialization in Microelectronics and VLSI)

by

SANJANA AFRIN RAISA

DEPARTMENT OF ELECTRONICS AND COMMUNICATION

INDIAN INSTITUTE OF TECHNOLOGY, ROORKEE

ROORKEE-247667 (INDIA)

JUNE 2019

CANDIDATE'S DECLARATION

I hereby declare that the work which is presented in this project, entitled, "**DESIGN AND IMPLEMENTATION OF FOUR ELECTRODE BASED IMPEDIMETRIC SENSORS"**, submitted in partial fulfillment of the requirement for the award of the degree of **Master of Technology** in "Microelectronics And VLSI " in Department of Electronics And Communication, Indian Institute of Technology, Roorkee (India) , is an authentic record of my own work carried out under the supervision and guidance of Dr. Sanjeev Kumar Manhas, Associate Professor, Department of Electronics And Communication, Indian Institute of Technology Roorkee, Roorkee (India).

I also declare that I have not submitted the matter embodied in this report for award of any other degree.

Date:

Place: Roorkee, India

SANJANA AFRIN RAISA

(17534008)

CERTIFICATE

This is to certify that the above statement made by the candidate is correct to the best of my knowledge.

Date:

Dr. Sanjeev Kumar Manhas

Associate Professor,
Department of Electronics and Communication Engineering,
Indian Institute of Technology,
Roorkee-247667

ACKNOWLEDGEMENT

I am using this opportunity to express my gratitude to Dr. Sanjeev Kumar Manhas, Associate Professor, Department of Electronics and Communication Engineering, Indian Institute of Technology, Roorkee, who supported me throughout the course of this thesis work. I am thankful for his aspiring guidance, invaluably constructive criticism and friendly advice during the seminar work. I am sincerely grateful to him for sharing his truthful and illuminating views on a number of issues related to the work.

Last but not the least I am also grateful to all the faculty members of Department of Electronics And Communication, Indian Institute of Technology, Roorkee.

I extend my thanks to Dr Rangadhar Pradhan of Nanotech Department of Indian Institute of Technology, Roorkee, for his valuable guidance all through the project and also to all fellow members of Sponsored Research Lab, ECE Department, Indian Institute of Technology, Roorkee, who have given their full cooperation and suggestions for my seminar work.

Thank you.

Date:

Place: Roorkee, India (**SANJANA AFRIN RAISA**)

ABSTRACT

The continuous development of cell based microelectronic sensing devices has been a significant milestone in the drug discovery and in depth bio-analytical researches on living cell behavior and its physiology. Along with time, conventional cell based sensors have faced some limitations which paved the way to shift towards Electric Cell Substrate Impedance Sensor which ensures non invasive, real time and label free impedance sensing of the living cells as well as lower cost and higher accuracy. The low impedance of the sensing device plays a vital role in measuring the accurate impedance of living cells. With that aim, an optimized, non invasive four electrode based Electric Cell-substrate Impedance Sensing (ECIS) device has been designed, fabricated and then characterized in this work. The ECIS device is designed with gold electrodes and the impedance of the designed device has been simulated by varying different parameters and was compared and verified with equivalent electrical circuit parameters. The designed device was further fabricated with gold on a glass substrate and was characterized with biocompatible Phosphate Buffer Solution (PBS) where the obtained design parameters from the simulations were applied. The measured impedance data were compared with equivalent circuit models with an electrochemical impedance spectroscopy analysis software to realize the feasibility and error percentage of the device. The output impedance data of the fabricated device fitted well with the simulated data which was later used for the realization of the equivalent circuit model of this electrochemical system as well as the mathematical equations between the impedance, phase angle and the area of electrode for the device which can be used for further researches of cell impedances in future works.

CONTENTS

Particulars **Page No.**

LIST OF FIGURES

LIST OF TABLES

CHAPTER 1

INTRODUCTION

The invention of cell based biosensors is indeed a significant breakthrough in the research arena of microelectronics, nanotechnology and bio-electronic devices which opened the passage for in-depth studies on the functionality of living cells promising a reliable solution of cancer research, stem cell research and drug discoveries. For the last two decades it has been implemented extensively in studies and researches for the detection of cellular anomaly, food and environmental toxicity, pharmaceutical effect analysis, cancer research, stem cell research and various medical diagnoses etc. But along with time with the continuous increase in the demand for non invasive cell based sensors, smaller sensor area and also different issues like less accuracy and reliability issue of other cell based sensors in use have shifted the focus to Electric Cell Impedance Sensor which is one of the promising cell based biosensors nowadays which ensures faster response, lower cost, higher accuracy of the sensor mechanisms overcoming all the limitations of current biosensors in use.

1.1 Micro/Nano Cell Based Biosensors

Micro/Nano cell based biosensors are devices which can analyze the physiological and biochemical signals from living cells, employing the living immobilized functional cells as primary sensing elements [2]. These special devices are able to detect the microenvironment in the intracellular as well as in the extracellular level using the living cells as detectors along with microelectronic transducers or sensors. As a result of the interaction between the cell and the applied input stimulus, the produced response by the living cell, is taken out as the output of the cell-based biosensors. The main two parts of cell-based biosensors are,

a) The living cell which acts as the primary transducer sensing the element, receiving and producing the signals.

b) The electrical circuit containing the microelectronic sensors which is used to convert the physiological signals of the living cell to electrical signals.

In the basic mechanism of the cell-based biosensors, the surface of a transducer is used for the culture of the living cell in which the input stimulus is applied, while a different transducer, having the potential sensing or chemical sensing ability is connected with the external circuit for the output. When any external stimuli (electrical or chemical) is applied on the living cell which acts as the primary sensor, the secondary sensor provides electrical signals such as extracellular changes of ions, action potential or impedance changes resulted because of the changes in their cellular metabolism on the application of the stimuli .[1]

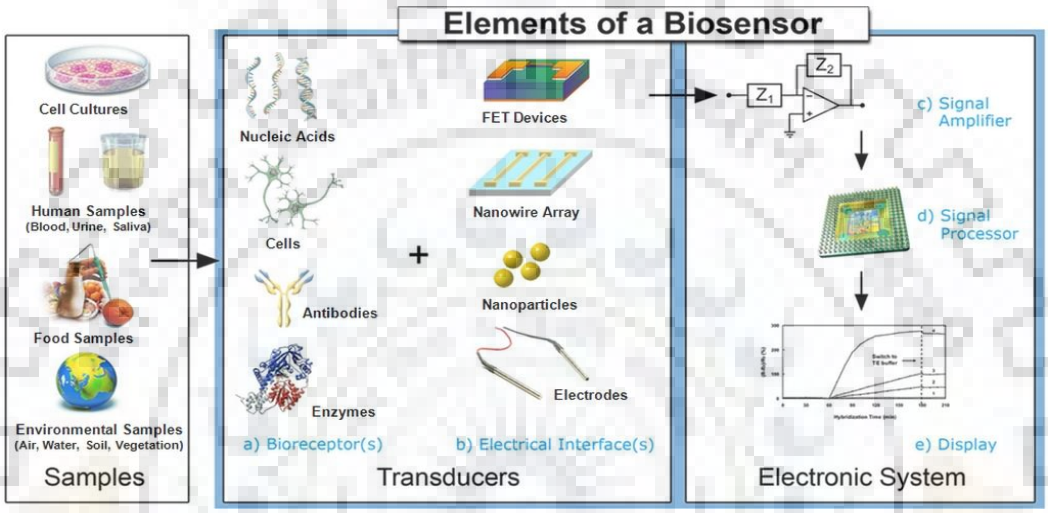

Figure 1.1: Biosensors Based on Microelectronic Devices [3].

To detect the physiological and functional information of the living cell, cell-based biosensors can be used profusely in fields like medical sciences, pharmaceutical researches, environmental monitoring etc with promises of rapid response, high sensitivity and in depth knowledge of the researches.[1]

1.2 Features of Cell Based Biosensors

- **Employment of the Living Cell**

  Two integral parts of cell based biosensors are

  1) Micro/Nano devices as transducers to sense the electrical response of cells.

  2) The living cells or molecules as sensing elements.

With the help of some biocompatible compounds these device can detect if there is any change in the living cell or it is perished the abrupt changes can be detected by the sensors.[1, 2]

- **Micro Ranged Size of Sensors**

  The size of the transducers used for biosensors ranges from 10 to 100 of times in the order of microns. So, they are almost equal in size to the living cells or molecules which enable these transducers to merge with the living cell/cell membrane for an efficient sensing mechanism and signal transmission. [2]

- **Reduction of Sample and Reagent Usage**

  As the transducers used are in the Micro/Nano scale, the use of sample and reagent are greatly reduced. [2]

- **More Tolerant to Solute Inhibition, Ph, and Temperature**

  Compared to enzyme electrodes, cell-based biosensors are more tolerant to suboptimal pH and temperature values. Also, in the case of solute inhibition, the biosensors are less sensitive. However, care should be taken so that the narrow range is not surpassed in case of the cells dying.[10]

- **Longer Lifetime**

  The use of cell based biosensors ensures longer living time for the cells of experimentation compared to enzymatic sensors.[10]

- **Fast Responses**

  As discussed in [10], living cells have special bio-features which enable them to respond speedily when used as sensing materials incorporated with microelectronic sensing devices.

- **Easier to Immobilize the Cell**

  The living cells and molecules must be immobilized around or on the sensitive surface of the transducers for the purpose of efficient coupling of cells/molecules with Micro/Nano devices[10]. This mechanism cooperates in that process also.

1.3 Different Types of Sensors Used in Cell Based Sensors

A number of sensors with various mechanisms have been invented to convert the physiological data to electrical signals in the cell-based researches. The secondary transducer of cell-based biosensors prevalent in the current years are FET – Field Effect transistors, MEA – Microelectrodes array, QCM – Quartz Crystal Microbalance, ECIS – Electric Cell-Substrate Impedance Sensor, LAPS – Light Addressable Potentiometric Sensor etc which can be employed for various analysis of the living cell.

1.3.1 Microelectrodes Array (MEA)

Microelectrode arrays (MEAs) contain multiple (tens to thousands) microelectrodes in array. The technology they use is "micromachining" and they are fabricated by depositing Gold, Platinum, Iridium (other metals can be used too) on glass/silicon substrate for the fabrication of electrodes[7]. However, some drawbacks of MEA are,

- Requires higher selectivity, thinner and sharper structure of electrodes. [11]
- Increased electrode impedance due to the small tip exposures.[11]
- The substrate surface for depositing the metal gets eroded easily if it is in contact with the solution for an extended period.[7]
- Using MEA as a sensor, the cell – electrode gap is tough to regulate.[1]

1.3.2 Cell Based Field Effect Transistor Sensors

Cell based Field Effect Transistor sensors are able to detect ionic concentration variations around the gate area and the corresponding cell membrane potential. If variation is detected in the ion concentration, the dielectric layer's surface potential will be lifted, thus inducing the density change for the mobile defect electrons [7]. Sensitive films such as Silicon-nitride and Silicon-dioxide are deposited on the gate-area and these films are enclosed by various types of electrogenic cells.

The drawbacks are:

- The sensors are not enough suitable for the environment which consists of the wet environment, which is mandatory for the biocompatibility of the device with the living cells. [12]
- In FET, some additional amplifying circuitries are always accompanied with the fabrication of this "silicon-based chip". Thus, compared to glass chips, the whole process is much more complicated. [5]
- The sensing device can be used to measure only a few analytes. [12]
- There are detection inconsistencies which are a result of various factors such as – pH level, ionic stretch, temperature, etc. [2]

1.3.3 LAPS – Light Addressable Potentiometric Sensor

LAPS use light emitting diode (LED) for monitoring cellular metabolism. This sensor is usually as an EIS – Electrolyte/Insulator/Semiconductor sensor where the silicon chip is kept separated from the electrolyte solution using the insulating layer [1]. An LED is connected at the back of the sensor chip producing a photocurrent emitting a pulsating infrared light. The electric field which is generated on application of a dc voltage changes in correspond to the changes of the photocurrent. Therefore, the output is obtained when corresponding fluctuations occur in the photocurrent, which are induced from the biological behaviors which modify the interface's electrochemical parameters.[1]

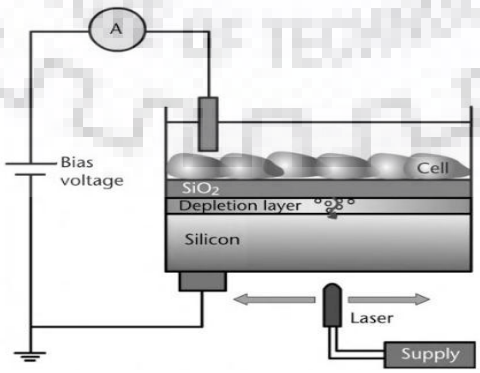

Figure 1.2: Light Addressable Potentiometric Sensor (LAPS)[1].

Drawbacks:

- LAPS based sensors are generally slow.[13]
- Issues with miniaturization and integration with microfluidic devices.[13]

1.3.4 QCM – Quartz Crystal Microbalance

Based on the piezoelectric effect, the QCM sensors can identify minute changes in mass and it does so by using the shifts in oscillation frequency of a crystal induced by pressure changes [1]. These frequency shifts are a result of mass loading that creates pressure changes on the crystal surface. The primary advantage of QCM over other sensors is the high sensitivity, noninvasiveness, long measurement periods ,detection rage from small molecules to array of cells etc. [1]

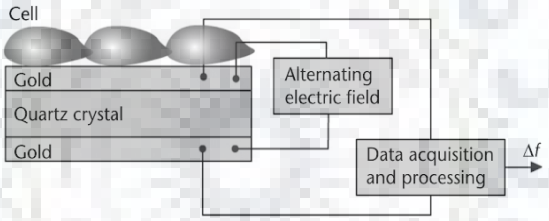

Figure 1.3: Quartz Crystal Microbalance (QCM) [2].

The drawbacks are as discussed in[14]

- Can be an expensive mechanism to get the actual data.
- It still needs further improvement to ensure higher accuracy.
- Data collection is more time consuming for this sensor.

1.4 Key Limitations of Conventional Cell Based Biosensor Devices

- Devices are required to be free of labels and also, they should be non-invasive.
- The cell metabolism and a biocompatible environment must be maintained
- Needs to be sufficiently miniaturized

- The cells which are functional and living must be immobilized on the transducer surface in such a way as to not limit their biological functions.
- Improvement is needed to be highly sensitive and responsive
- Current data collection procedure is quite time consuming which needs to provide data on real time.
- In some of the sensors there is uncertainty in getting the actual data, which needs to be fixed.
- The efficiency of the overall device needs improvement.
- Overall cost of the device should be minimized.

The above limitations can be solved by using ECIS – Electric Cell-substrate Impedance Sensors instead.

1.5 ECIS – Electric Cell-substrate Impedance Sensor

ECIS – Electric Cell-substrate Impedance Sensor was first invented by Dr. I Giaever and Dr. C. R. Keese in 1984. The sensor, *in vitro* (in a well-defined laboratory environment), is a non-invasive, label free, biophysical impedance-measuring system that is able to do so in real time. It is used to study cell behavior and characteristics in adherent cell layers. By this electrochemical technique the impedance of living cells can be measured by which further bioanalytic study of cell behavior, morphological changes of cell, cell locomotion, growth, attachment, cytoxicity etc can be accomplished and output information can be quantified in micrometer to around nanometer range.

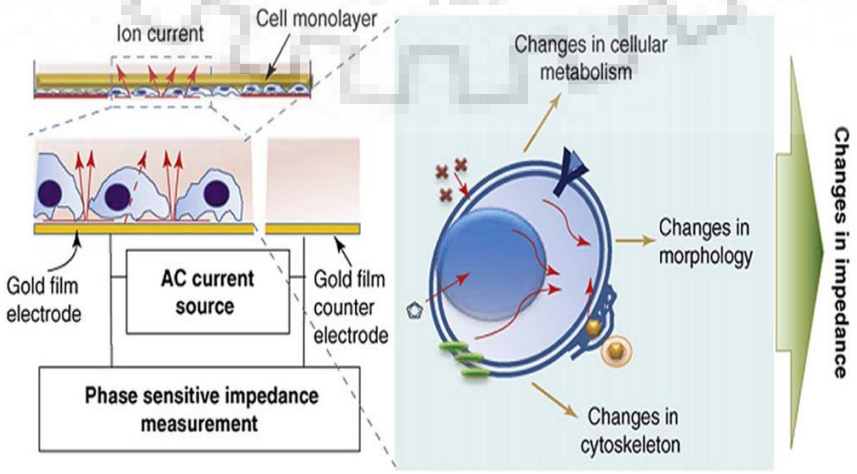

Figure 1.4: ECIS–Electric Cell Substrate Impedance Sensor[1].

1.5.1 ECIS – Principles and Structures

In ECIS technique the fabrication of the microelectrodes is done on a sensor surface on which the living cells are also cultured. The electrodes are supplied with a small AC current and the resulting voltage is measured using an impedance measuring device which is phase sensitive. The impedance developed due to the resistive and capacitive properties of the living cells, blocks the current as the cells having insulating characteristics grow and cover electrode surface. This increases the total impedance of the electrodes. Thus, along with increased number of cells on the electrode surface, the total area for passing the ion current is increased as well as the impedance. Therefore, when lower frequency is applied to measure the impedance of cells, the current passes through the cell to cell junctions or the gaps between the cells, providing the cell-electrode interface information. Whereas, when higher frequency is applied the current is able to pass through the cell membrane, passing through the cell body. Thus with higher frequency current, the cell membrane information and its structural whereabouts can be known.[1]

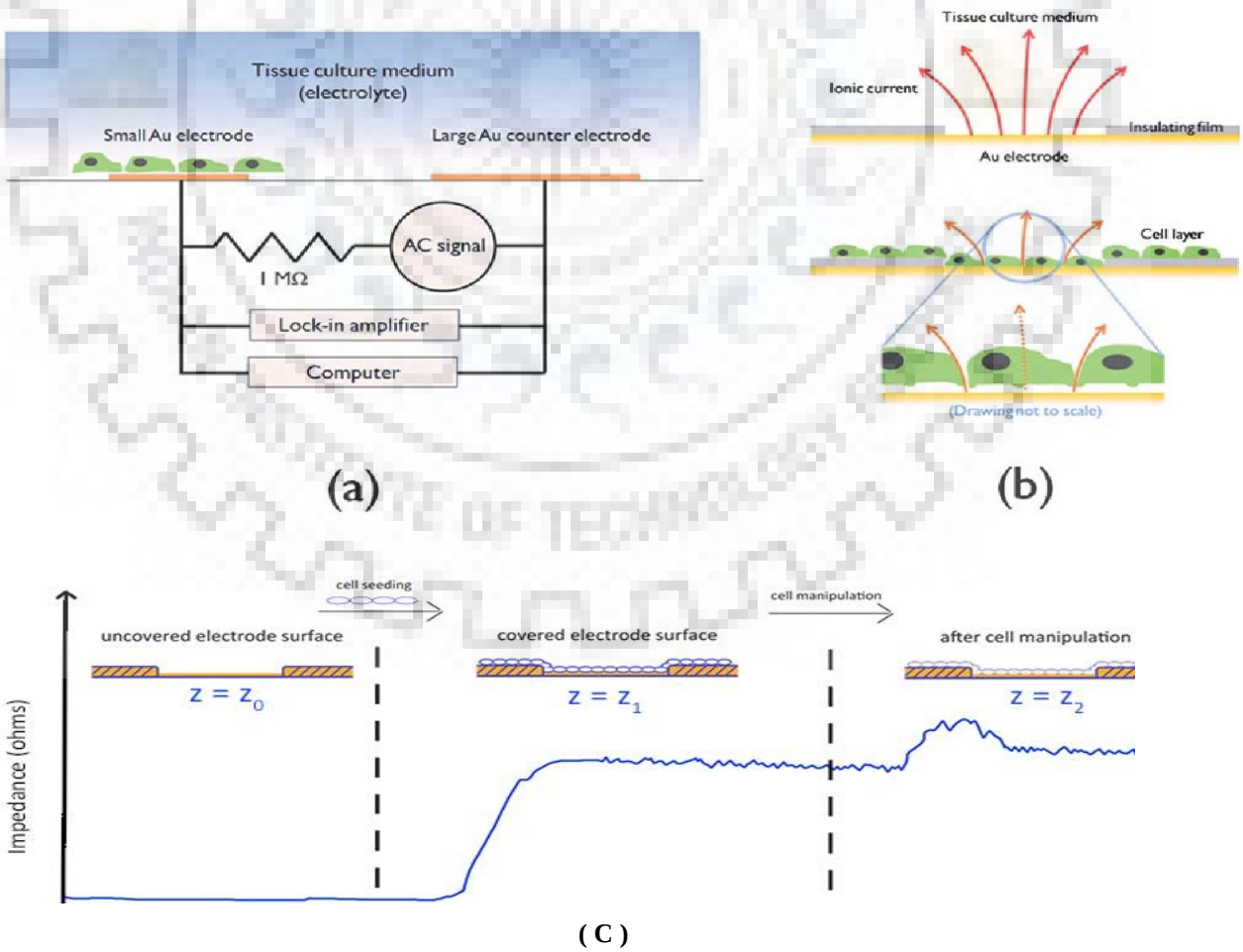

Figure 1.5 (a), (b): ECIS– Electric Cell-Substrate Impedance Sensor [6] (c) Impedance Vs Time Curve [38].

In Electric Cell-substrate Impedance Sensor system, the cells are cultured in a special cell culture chambers on a planar metallic film of electrode surface. Due to the insulating properties of the cell membranes, they act as insulators increasing the total impedance when accompanied with the sensing ECIS device. Impedance increases with the cell growth covering the electrodes. The impedance for the current depends on few things,

1) The number of cells covering the electrode
2) The morphology of the cells
3) The way the cells are attached

Thus, the three-dimensional shape of the cells mainly determines the measured impedance. When different stimulus (chemical or electrical) is given to cells the change in their functions accordingly changes in their cell morphology or cell shape. Thus the impedance data generated in real time reflect the cell behaviors which is studied for different bioanalytic purposes[15,38].

1.5.2 Electrical Properties of a Living Cell and Cell Impedance

If perceived from an electrical point of view, a living cell may be seen as a cytoplasm, which is an ion-rich conductive center submerged in an ion rich "intercellular fluid" – another conductive medium and separating them is the cell membrane – a relatively non-conductive barrier. The ion-rich cytoplasm and extracellular fluid are defined by their ability for conducting charges; hence they are modeled as resistors. Also, charge barriers like the bilayered cell membrane may be modeled as capacitors – as they store charges in between their two insulating membranes like the capacitors. Since impedance is a function of the input electrical signal and input frequency range, forming output frequency spectrum, the electrochemical mechanism consisting of living cells and biocompatible sensors the impedance measurement technique is known as Electrochemical Impedance Spectroscopy or EIS techniques. [16]

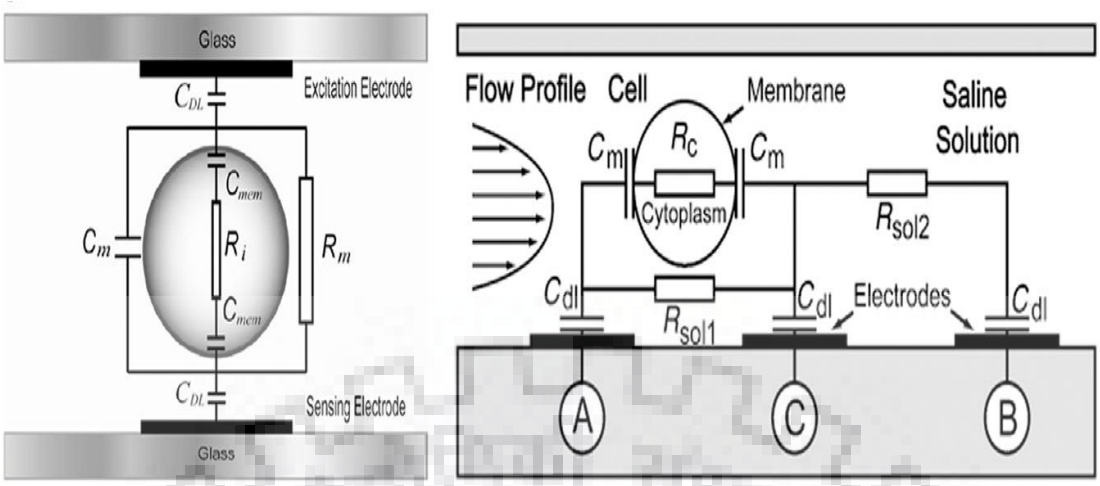

Figure 1.6: Electrical model of a living cell with an ECIS sensor [5].

1.6 Application of ECIS Sensors

The ECIS sensors are being widely used for the advanced and in-depth studies of the cell behavior and characteristic recently. But there is a huge range of scope for improvements. Following applications of the ECIS sensor are prevalent in the recent days:

1) **In Depth Study of Living Cell**

   The ECIS method has been used for many investigations. Few examples include – **cell physiology, cell proliferation, cell growth, cell motility, cell toxicity and endothelial cells testing** (by finding impedance measurements of the barrier function. It is an alternative to animal testing). [38]

2) **Cancer Research**

   The study of invasive nature of cancer cells also incorporates the use of the ECIS sensors recently as explained in [17].

3) **Stem Cell Biology**

   In stem cell researches the ECIS can put a wide impact. There are many devices available to study stem cells, most of them are not capable for further use. However, ECIS allows for further use and research due to its label-free, non-invasive nature.[18]

4) In Study of Neural Network of Human Brain

The ECIS technique has been used in the study of neural cells of brain of human beings as explained in[19, 20].

5) In Study of Tissue Health

In ECIS, the "recovery-after-wounding" feature allow tissue repair through the discovery of molecules. The impedance spectrum of ECIS can identify mild, reversible pressure damage of human tissue [16].

6) Drug Discovery

The implementation of this sensor in the in-depth study of cell will help to the drug discoveries for cancer and other deadly diseases.

7) Food Safety

At the cellular level, multiple variety of chemical and biological analytes have been discovered through use of ECIS each of which has the potential to be a valuable resource in applications for food safety and to find food borne bacteria.[2, 21]

8) Environmental Monitoring

In environment monitoring they are also being employed in some of the recent studies.[2]

1.7 Motivation for using Electric Cell Impedance Sensors

- **Non-invasive Method**

ECIS is a noninvasive sensing technique to monitor cell behavior, physiology and characteristics. This criterion of ECIS makes it compatible to carry out long term measurements of cell characteristics. So, this type of sensor is very promising for neuron studies. This sensing mechanism is adopted in the neural network based sensors which also cooperates in the formation of neural networks on solid surface and their chemical sensing [2, 7].

- **High Sensitivity**

  Being highly sensitive, it is able to precisely identify cellular behavior in different stimulations. As such, it is able to efficiently monitor cellular behavior in various conditions in real-time [5].

- **Real Time Monitoring**

  ECIS device ensures real time monitoring. Since living cells responds very sensitively to the metabolic changes or on application of bio/chemical/physical stimuli, ECIS devices being highly sensitive, are capable of providing real-time monitoring and information of these cell responses. Cell mobility, morphology, proliferation, function, cytotoxicity, attachment, growth etc are the examples of the studies using ECIS devices [15].

- **Ensures Simplified Mechanism**

  In comparison with the other sensors like patch clamp and fluorescent microscopy, the ECIS has the advantage of better performance. For example, through the implementation of MEMS (micro-electromechanical systems) mechanisms and nanoscale technologies, it ensures a simpler, automatic and high-through approach for cells behavior researches.[1]

- **Use of Living Cell**

  ECIS based biosensors employ living cells which carry various natural bio molecules on their surface. Whereas, usual biosensors use antibodies which cannot provide the exact biophysical information of the cells.[22]

- **Detection of Non-visible Cell Damage**

  This ECIS device is flexible enough to detect invisible tissue damage that induced by some pressure and do so in a non invasive way. [16]

- **Cost Effective**

  The use of functional living cells means they do not require isolation in this mechanism, thus driving down the cost.[10]

- **Easy to Fabricate**

  The process is easier to fabricate.

- **Portable**

  Because of their miniaturized sized they are easily portable. [23]

1.8 Organization of Thesis

The thesis has been divided into five chapters.

Chapter 1 – provides the information about the applications, limitations of conventional electric cell impedance biosensors and introduction of Electric Cell Impedance Sensors as the solution to those.

Chapter 2 – describes the basic concept and working principle of ECIS devices as well as the methodology for the design, characterization and fabrication of the proposed four electrode ECIS device.

Chapter 3 – comprises the design, simulations and optimization of design for the four electrode ECIS device. Also, the values of the different electric components for the circuit and error percentage for different designs of the device are extracted and the feasibility for the optimized design of the device has been verified.

Chapter 4 – describes the fabrication and the characterization of the designed device. Also, the data obtained from the characterized device have been further analyzed and an equation for the impedance, phase and area of electrode has been obtained.

Chapter 5 – covers the conclusion and future scopes, followed by references.

CHAPTER 2

BASIC PRINCIPLE, STRUCTURE AND OPERATION OF FOUR ELECTRODE ECIS DEVICE

2.1 Theory and Electrical Analysis of ECIS

The living cells are generally storages of ions, fluids and numerous biochemical compounds which can electrochemically react with any flow of electrons or ions passing through them. More specifically the living cell can act as an insulator due the insulating properties of its cell membrane and cytoplasm which generally blocks the flow of electric currents through them. Implementing this property of living cell cells are grown on the top surface of electrodes preferably of gold, silver or platinum etc in ECIS mechanism and a small alternating current (10^2 -10^6 Hz) is applied on the electrodes and passed through the cells. This adjoining with the insulating property of the living cells, provides a way to measure the impedance of the cells grown on the top of the electrodes. The impedance measurement basically depends on two indicators of cell behavior — Resistance (R) and Capacitance (C). The cell membrane acting as the charge storing capacitance can change the impedance of the system when current is passed through it. The resistive nature of the cell is influenced due to the barrier function of the cells as discussed by [9] in his paper.

This resistive and capacitive nature of the living cell can make a significant electrical response on application of electrical inputs. Therefore studying the variation in the impedance of the overall sensing system along with the living cells attached on it, on application of an AC current, the cell nature, shape, characteristics and behavior of living cells can be understood.

2.1.1 Equivalent Circuit Model of a Living Cell

Capacitance of Cell Membrane

The membrane or covering of a cell is considered to be a capacitor of higher capacitance and lower conductivity but of complex nature. The cell membrane mainly is formed by phospholipids a biochemical compound inside it. As [24] discussed the phospholipid molecules composing the cell membrane are arranged in two layers, commonly known as the phospholipid bilayer which are about 7 nm thick. Each phospholipid molecule has a head and two tails. The head is hydrophilic that is, it attracts water and the tails are hydrophobic or water repelling. The cell membrane is arranged in such a way that the lesser conducting water repelling tails are on the interior, in between of the two layers of the heads, whereas the more conductive water attracting heads point outwards, toward either the cytoplasm or the intercellular fluid in between the cells. Thus the structure of membrane of cell resembles with a typical capacitor with two conducting layer outwards and a conducting layer in between as shown in the figure.

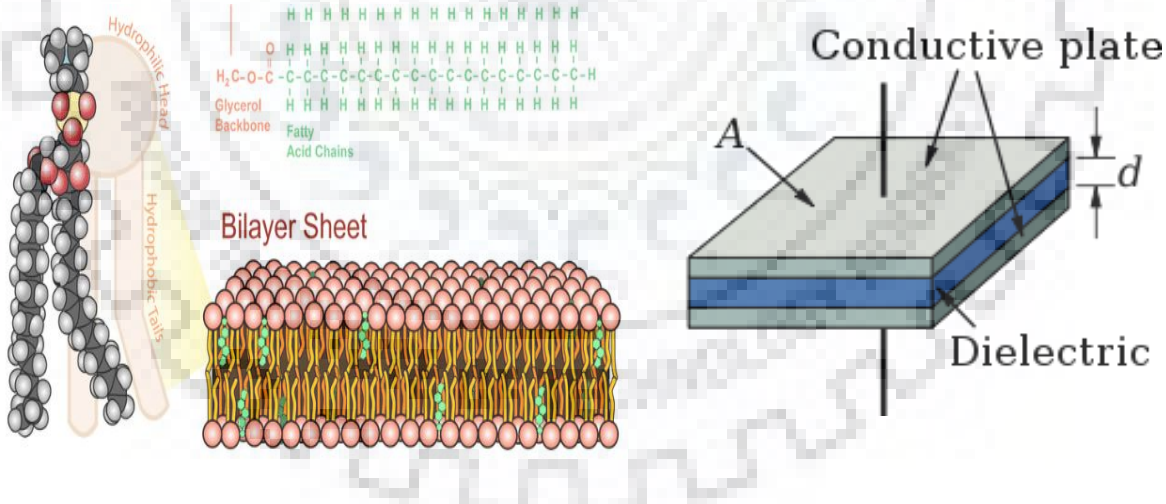

Figure 2.1: Cell Membrane of a Cell [39] and an Electric Capacitor [40].

Hence the capacitance (C) can be described as the separation of the ions at the insulating double-layer of the cell membrane causing ion polarization. The phospholipid bilayer typically has very low conductivity of about 10^{-6} S/m. The hydrophilic heads of phospholipids of the cell membrane induces the formation of a hydration on its surface.

Hence induces the whole cell with a certain amount of charge. Since the width of the cell membrane is very small, the capacitance developed there is of a high value (about 1 $\mu F/cm^2$) [2]. Moreover this capacitance is considered to be frequency dependent as discussed in [1] as well due the responsive nature of the cell membrane on application of electrical input with various frequency.

Equivalent Circuit Model of a Living Cell with an ECIS Device

The electrical properties of a living cell can be interpreted with an equivalent electrical circuit model when it is analyzed with an impedance measurement system. Because of the properties of the cell membrane, the typical circuit for the cells consists of a parallel connection of resistor R_{cell} and capacitor C_{cell}. R_{cell} is the action of the cell against the current flow influenced by the barrier function of the cell. On the basis of the complexity of the surroundings and the equivalent circuit models the ECIS electrodes and the attached cells can be interpreted as capacitance, a resistance-capacitance complex or a constant phase element (CPE) [5]. As discussed in [1] the total mechanism of ECIS can be compared with a standard equivalent circuit basing on the researches of Giever and Keese.

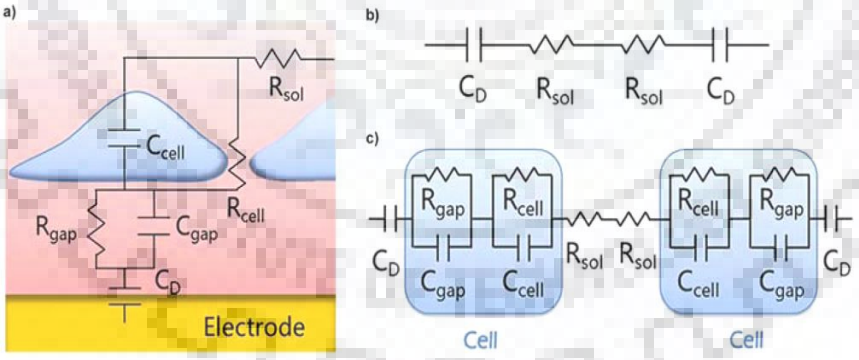

Figure 2.2: a) Equivalent Circuit Model of a Living cell b) Circuit without cell attachment to electrode c) Circuit with cell attachment [7].

The equivalent circuit for measuring cell impedance by an ECIS sensor device as shown in the Figure 2.2(b) is basically an R-C circuit for the case of a noncell attachment on the electrode. The sensor device consists of two surfaces – one of the solid or metallic electrode material and the other is the fluidic solution of the electrolyte. In the electrode/electrolyte

interface a double layer capacitance C_D is developed generally known as Helmholtz double-layer interface capacitance. It is created from the ions and molecules interactions at the electrolyte/electrode interface. In the electrolytic solution of the ECIS device another resistance called the solution resistance or the R_{sol} is formed. It is basically the resistance of the cell culture medium. When cells are grown on electrode surface, the resistance and capacitance of the living cells are added with that of the ECIS device resistance and capacitance. Hence the equivalent circuit model simplifies as depicted in Fig. 2.2(c). Here, the overall capacitance increases as the cell capacitance (C_{cell}), cell resistance (R_{cell}) , cell gap capacitance (C_{gap}) and cell gap resistance (R_{gap}) between the cell and substrate come into picture. Since the cell capacitance basically dominates in the overall system the reactance X hence can be described by the capacitance of the cell membrane.

$$\mathbf{X(f) \approx \frac{1}{(2 * \pi * f * C_{Cell})}} \qquad \mathbf{(1)}$$

For the reactance X, which is frequency dependant, various values of reactance as well as resistance can be obtained for different values of frequency f. Hence the information of different cell structure and functions can be known analyzing the impedance, capacitance and phase shift for the overall system from that calculation.

2.1.2 Frequency Dependence of Cells

Since the cells grown on the electrode surface influences the current flow depending on the input frequency, the principle to extract the information of the impedance (Z), into two indicators of cell behavior (R and C) also depends on the input frequency. Based on the different researches following observations have been found:

- At lower frequencies (10^2 to10^4 Hz), the ability of the alternating current to pass through cell is less, as the cell membrane which largely resists the current flow through it (reactance as given $X_c = \frac{1}{2\pi fc}$), allowing the current to flow mostly around the cells through the intercellular space between the cells. As a result, current flow between the cells is then mainly resisted by the intercellular fluid between the cells (measured as resistance) at lower frequency.

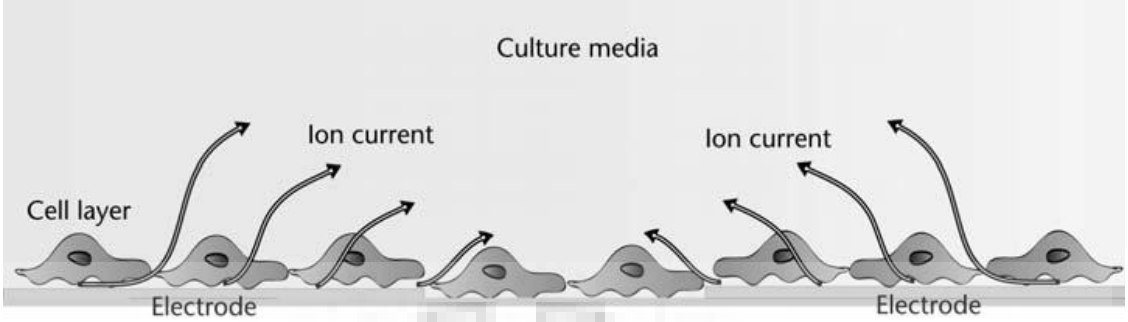

Figure 2.3: The movement of currents of high and low frequency through a living cell.[1].

- For higher input frequency (more than 10^4 Hz), the capacitance gets shorted, effectively removing the charge transfer resistance, leaving only the solution resistance in the equivalent circuit model. Thus the input current gets the ability to pass through the cell body due to lower impedance. [9]

2.2 Basic Equations of Electrochemical Impedance Spectroscopy

2.2.1 Equations of Cell Impedance: The Complex Impedance

The capacitive and inductive properties of cells influence the phase shift of the input voltage and current of the cells. The cell impedance and the impedance of ECIS sensor together give the overall impedance of the electrochemical system. The impedance (Z) of the ECIS device is expressed as the ratio of the phasors of the voltage and current, following Ohm's law:

$$\mathbf{Z\,(\,j\omega) = \frac{V\,(\,j\omega)}{I(\,j\omega)} = Z_r\,(\omega) + j\,Z_i\,(\omega)} \qquad \mathbf{(2)}$$

Here I denotes the input alternating current. The output voltage is denoted by V. The value of $j = \sqrt{-1}$ and angular frequency is denoted by, $\omega = 2\pi f$. The input frequency is f. The real and imaginary parts of the impedance, give magnitude and the phase shift (θ) of the impedance, Z[25]. The expression for excitation signal as a function of time can be given as:

$$\boldsymbol{E_t = E_0 \sin(\omega t)} \qquad \mathbf{(3)}$$

Here, the potential is denoted by E_t, at time t. The amplitude of the signal is termed by E_0. The response signal I_t with a phase shift of θ , can be expressed as:

$$I_t = I_0 \sin(\omega t + \theta) \qquad (4)$$

Thus the impedance then can be shown with terms, magnitude of impedance, Z_0 and phase shift, θ as follows:

$$Z = \frac{E_t}{I_t} = \frac{E_0 \sin(\omega t)}{I_0 \sin(\omega t + \theta)} = Z_0 \frac{\sin(\omega t)}{\sin(\omega t + \theta)} \qquad (5)$$

When cells, being cultured in cell culture media get connected with an ECIS device, the flow of the input current is changed on the impact of the cultured cell on the electrode of the ECIS device. Therefore the impedance of the overall system is also changed. Hence, the comparison of the device impedance and device with cell impedance can give the exact value of the cell impedance. The impedance and phase shift value provide the value of the resistance and the capacitance after proper analysis. Also the obtained data, can be further analyzed to know about the structural and functional characteristics of the cells.

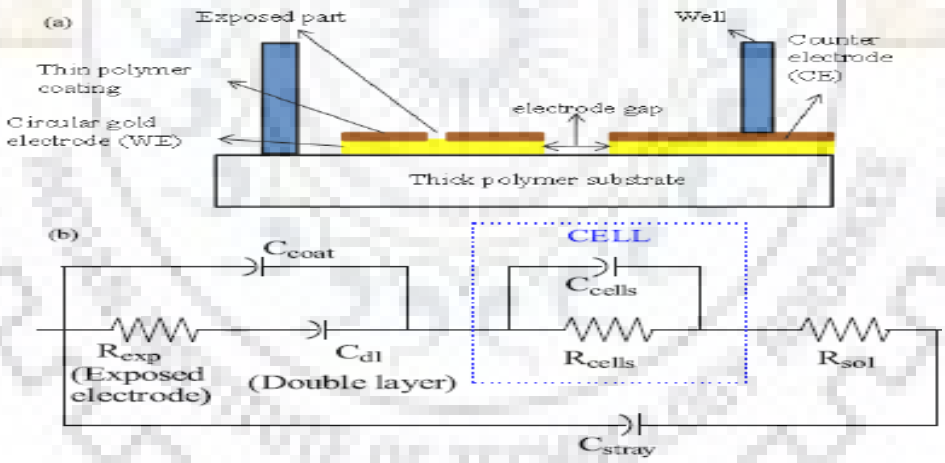

Figure 2.4: Equivalent Circuit of ECIS with a Living Cell [8].

For the cell membrane's conductivity is very low, input current with high frequency gets to pass through the cell body. Input current with low frequency cannot pass through the cell body; hence pass through the intercellular fluid, in the extracellular gaps. Therefore, the equivalent circuit of the cells attached on the electrodes is interpreted by a parallel connection of equivalent resistances and capacitances of the cell membrane, extracellular gap and intercellular fluid. Here, R_{exp}, C_{coat}, and C_{dl} are the charge transfer resistance at the interface

of the electrode and electrolyte surface, coating capacitance. C_{dl} denotes the double layer capacitance at the interface of electrode/electrolyte, respectively. Solution resistance of the electrolyte is denoted by R_{sol}. Since the values of the cell membrane resistance and cytoplasm capacitance are very low, they are excluded from analysis of the equivalent circuit.

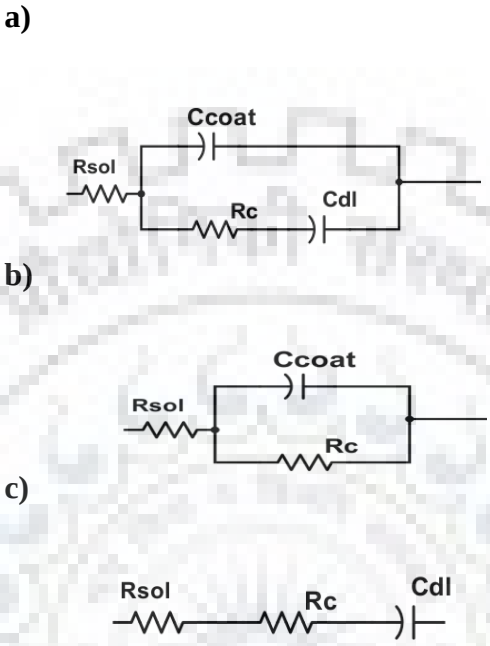

Figure 2.5 :Circuits considering different surroundings of the cell [8] .

The equivalent circuit for the ECIS device can be shown as Fig. 2.5(a). For higher frequency (typically above 100 kHz) the double layer capacitance C_{dl}, acts as a short circuit path. Its value is generally of μF range hence it can be neglected. So the circuit can be modified as Fig. 2.5(b), and the consequent expressions for the magnitude of the impedance and the phase shift of the equivalent circuit , as per [8] are:

$$|Z| = \sqrt{\left(R_{sol} + \frac{R_c}{1+\omega^2 R_c^2 C_{coat}^2}\right)^2 + \left(\frac{\omega R_c^2 C_{coat}}{1+\omega^2 R_c^2 C_{coat}^2}\right)^2} \quad (6)$$

$$Z_r(\omega) = R_{sol} + \frac{R_c}{1+\omega^2 R_c^2 C_{coat}^2} \quad (7)$$

$$\theta = -\tan^{-1}\frac{\omega R_c^2 C_{coat}}{R_{sol}+R_c+1+\omega^2 R_{sol} R_c^2 C_{coat}^2} \quad (8)$$

Equation (2) comprehends that R_{sol} mostly dominates the real part of impedance (Zr (ω)), when input frequency is high. Also for higher frequency, (Zr (ω)) is relatively constant.

For lower input frequencies, the coating capacitance has a high reactance, hence acts as an open circuit. So, as shown in Fig. 2.5(c) the final circuit becomes a simple RC series circuit with equations of magnitude of impedance and phase as below

$$|Z| = \sqrt{(R_{sol}+R_c)^2 + \left(\frac{1}{\omega C_{dl}}\right)^2} \quad (9)$$

$$\theta = -\tan^{-1}\frac{1}{\omega C_{dl}(R_{sol}+R_c)} \quad 10)$$

Therefore as the frequency increases, |Z| decreases and θ from its negative value move towards zero. The peak angular frequency in the Nyquist curve for the RC circuit corresponds to

$$\omega_{peak} = \frac{1}{(R_c+R_{sol})C_{dl}} \quad (11)$$

Hence, the value of the double layer capacitance (C_{dl}) can also be extracted by substituting R_{sol} and R_c values. When cells are added considering the negligible effect of C_{dl} and coating capacitance, for the medium range of frequency, the equivalent circuit can be considered as fig 2.6. The Nyquist curve of this circuit gets a peak angular frequency as below

$$\omega_{peak-cell} = \frac{1}{(R_c+R_{sol})C_{cell}}\left(1+\frac{R_{cell}}{R_c+R_{sol}}\right) \quad (12)$$

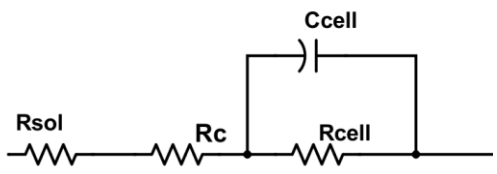

Figure 2.6: Equivalent circuit after adding cell for lower frequency [4].

Substituting the obtained R_c and R_{sol} values, R_{cell}, C_{cell} values of the cell can be estimated[26] .As discussed in [16] cell damage or death causes deformation of the structure of cell membrane. As a result, through cell membrane, the ions and current are able to flow. Hence, a damaged cell thus shows high electrical conductivity, with less storing capacity of charge. Therefore, the cell acts more as a resistor then as a capacitor.

Some of the studies found that, the cell reactance exhibits an increase for epidermal proliferation and decrease for loss of cell or infection. This interprets that, healthier cell membranes are indicated by larger phase angle, whereas damaged cell membrane can be understood from reduced phase angle [16, 27].

2.2.2 Capacitance Measurement

As per [9] , for ECIS mechanism , the capacitance can be described as the charge storing capability of the electrode-substrate and cell-substrate interfaces in their respective surfaces. With no cell attached, the sensing device has a total capacitance equal to the equivalent capacitance of the electrodes. When cells are cultured on electrode surface, C_T - the total capacitance becomes the combination of C_e - the capacitance of electrodes and C_c – capacitance of cell. Therefore, the total capacitance of the device with the cells cultured on the electrode surface simplifies as series connection of two capacitors by following equation

$$\frac{1}{C_T} = \frac{1}{C_e} + \frac{1}{C_c} \qquad (13)$$

Thus, with the increase of cell number on electrode surface, increase of the cell capacitance, Cc is observed, as a function of increasing cell area and hence the total capacitance of the ECIS device, C_T decreases.

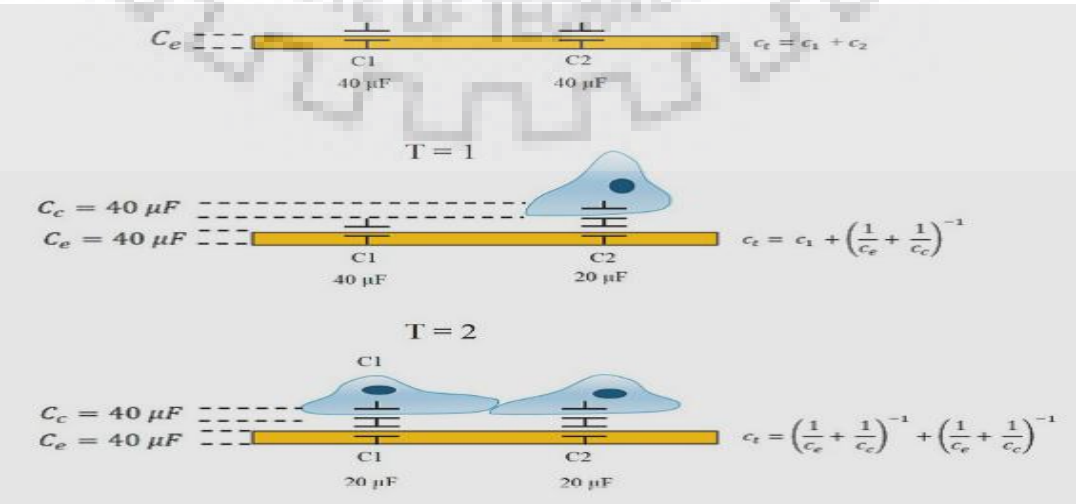

Figure 2.7: Capacitance Measurement [9].

In figure 2.7 the capacitance of the ECIS with and without cells on the electrode for different time has been shown. For T = 0, the sum of the electrode capacitances- C_e , connected in parallel connection forms the total capacitance- C_T .With the growth of the cells on the electrode surface, at T=1, the capacitance of the cells - C_c add along with the electrodes capacitance. Finally, the sum of the series connection of the electrode and cell capacitance at, T=2 , denotes the total capacitance of the overall system.

2.2.3 Impedance of Constant Phase Element

The ECIS device when works in an EIS system the overall capacitance due to the passivation coating, interface capacitance and double layer capacitance behave mainly as a constant phase element (CPE) rather than an ideal capacitor [28]. The capacitance of the gold electrodes is generally of small value in pF range (around 10 pF) .Therefore it can be taken as negligible for ECIS device in very high frequency (more than 50 MHz) as the capacitances are shorted in the equivalent circuit. The impedance of the CPE are expressed by the following model parameters α and Q as per this equation

$$Z_{CPE} = 1/Q(j\omega)^{\alpha} \qquad (14)$$

Here Q is magnitude of the capacitance. By α the fractional exponent of CPE is denoted, where the value of α is, $-1 < \alpha < 1$. When α = 0.9-1.0, CPE acts as an ideal capacitor having units capacitance and the system is expressed by a single time-constant .Also the Nyquist plot gives perfect semicircle shape. Whereas in real case when α is smaller depression is observed in the Nyquist semicircle.[28] When α = 0, CPE acts as a resistor. In this work the value as per[4, 8] has been taken , α = 1,assuming CPE acting as a capacitor.

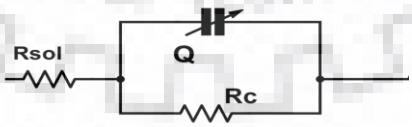

Figure 2.8: Equivalent Circuit for ECIS device with CPE [4].

Therefore considering the resistances and the CPE present in the ECIS device, figure 2.8 interprets the equivalent circuit of the ECIS device and the following equation expresses the overall impedance of the device considering the electrolyte/electrode surface

$$\boldsymbol{Z = R_{sol} + \left[\left(\frac{1}{R_c}\right) + Q(j\omega)^{\alpha}\right]^{-1}} \qquad \textbf{(15)}$$

Where R_{sol} represents the solution resistance, R_c is the charge transfer resistance, caused by the transfer of electrons at electrode/electrolyte interface. Q and α are the magnitude and the fractional exponent of CPE respectively. R_{sol} can be also expressed by

$$R_{sol} = \rho L/A \qquad (16)$$

Here, ρ is the resistivity of the electrolyte, L denotes the length between the counter and working electrode and A expresses the surface area of the electrodes. The expression for the charge transfer resistance, R_c is as below

$$R_c = \left[\left(\frac{KT}{q}\right)\left(\frac{1}{zJA}\right)\right] \qquad (17)$$

z is the ions exchanged during the charge transfer and T is the temperature. Both of the equations portrays that the resistances are inversely proportional to the electrodes areas which should be kept in considerations for the experimental outputs.

2.3 Basic Design and Structure of ECIS

To measure the impedance of the living cells, the structure and size of the sensor should be compatible to the structure of the living cell. The size of the cell is typically (>10u) few times of tens of micron. As cells are cultured in a cell-culture medium, two principle key factors influence the design of an ECIS device: the characteristics of electrodes through which electric potential is applied to the cell medium system and the capability of the device to incorporate the electrodes with the cell along their culture medium.

2.3.1 Arrangements of Electrodes used in ECIS Design

For designing an ECIS device two types of arrangements of the electrodes are prevalent. These two designs have both advantages and disadvantages. So depending on the specific applications the electrodes are to be used accordingly.

a) Monopolar Electrode

A separate electrode acts as the working electrode on which electric potential is applied and another electrode will act as the counter electrode which gets the current flowed through the working electrode and is grounded. The current density and therefore the voltage drop will be very high at the small working electrode, which influences the total impedance changes as well as discussed in [1].

Figure 2.9: Monopolar Electrode with a Counter Electrode and Interdigitated Electrode. [1]

Advantage: It has a simple layout and it is suitable for high resolution and high quality microfabrication application.

b) Interdigitated Electrode

It has basically two closely placed branches of electrodes each containing unit fingers of electrodes. A number of electrode fingers, which are working independently and equally spaced in parallel are connected to a terminal strip to form one branch of an electrode. Another similar branch of electrode facing oppositely forms the interdigitated system together. The two branches having the same dimensions in geometry contribute equally in the electrical measurements. The cells are grown in any of the electrodes and the impedance change of the overall system is measured. But in some cases the exact outputs are not always obtained as per studies.

2.3.2 Types of Electrodes on the Basis of Functions

Other than this depending on their functions there are different types of electrodes. In the electrochemical impedance spectroscopy 2-, 3-, 4- electrode configurations are used in the measurement system. Basically the main electrodes are

1. Working electrode
2. Reference electrode
3. Counter electrode (added in 3 and 4- electrode configuration)
4. Sensing electrode (added in 4- electrode configuration)

1. **Working Electrode**

   The electrode the potential of which is to be measured is termed as working electrode (WE). The living cells are grown basically over the WE. The electrical input is applied on this terminal to pass the electric signal to the living cells for obtaining their electrical responses. The supplied current flows to another electrode from the living cell known as the counter electrode.

2. **Reference Electrode**

   The potential of working electrode and all other electrodes is measured with respect to the reference electrode (RE). RE has a constant known and stable potential. A constant voltage or current is applied between the working and reference electrodes and the corresponding potential is to be measured. It basically interprets the potential at the interface of the metal and the liquid electrolytic solution and it should be of very low impedance. [29]

3. **Counter Electrode**

   The electrode which completes the path of current flow, from the working electrode with the living cell in between, to itself, is termed as counter electrode (CE). The potential of CE changes with respect to the amount of current comes to it from the WE. The CE is connected to an external instrument so that any current comes in WE will be taken by the CE.

4. **Sensing Electrode**

   In four electrode ECIS device the sensing electrode is decoupled from the working electrode as a separate electrode to increase the sensitivity of the device. The potential drop of the sample is basically measured between the inner sensing electrode and reference electrode whereas input current is flowed through the WE and CE.

2.3.3 Design Considerations for ECIS Devices

- The distance between the electrodes is very important as there can be electrochemical reaction between the electrode/electrolyte surfaces also with the living cells. To avoid any contamination between the ions of the electrodes and cells, all the electrodes are placed at a distance of 100 um from each other. As in [30] the gap between the electrodes plays a vital role in the performance of electrodes. So to avoid any unnecessary REDOX reactions initiated at the counter electrode proper gap should be maintained.

- The electrode material should be electrochemically inert with the electrolytic solution and with the living cells. For this thesis work, the material for the electrodes was chosen to be noble material, gold for its inertness to the electrolytic solution. Therefore, any unnecessary electrochemical reaction in the electrode/electrolyte surface could be avoided.

- Since the sensing mechanism should exhibit very high and acute sensitivity on the smallest change in the impedance of the living cell the 4 electrode ECIS device can provide a better result with respect to 3- electrode as the sensing electrode is added in the device mechanism which will help to sense the data by the sensor independently, increasing the accuracy.

- Different geometry of the sensor can be used .Such as with the dimension of the square electrode as 50um,100um,150um,200um.Depending on the cell and cell function the area of the electrodes can be varied.

Few important considerations for designing and fabricating of ECIS devices are:

- The region of interest for extracting cell impedance data is usually between 10^4 and 10^7 Hz, as discussed by [31] which provides significant information about the cell membrane impedance.

- Biocompatibility and sterility of the electrodes, maintenance of the physiochemical environment for the living cell, low parasitic capacitance in the obtained data should be ensured. Also a good packaging which interconnects the measuring device and the cell culture system protecting the living system from the external disturbances etc should be kept in the consideration for the design and fabrication of the ECIS device.

2.4 Device Fabrication of ECIS

In ECIS based biosensors, culture of living cells is accomplished on the sensing device consisting of conductive and insulating materials. Typically, an impedance-based biosensor comprises:

- Electrodes on insulating substrate
- Biocompatible electrolytic solution
- Culture media for cells
- And electrical connection with the measurement system.

2.4.1 Material Selection for the Substrate and Electrodes

i) Electrode Material

The electrode materials used for the fabrication are usually Au, Pt, and iridium tin oxide (ITO). [32]The electrode materials should be biocompatible and with superior electrochemical properties. Au is generally used in this case for its inertness in electrochemical, biocompatibility and can be modified easily in microfabrication processes [33]. Besides, Au is chemically inert with the living cells and the liquid electrolytic surfaces. Other materials including Ag/AgCl [34], Pt [35, 36], Ni [37], ultra-

nano crystalline diamond [38] etc have been used as the electrode material in different researches.

ii) **Substrate Material for Electrode**

As discussed in [1, 39] the materials of the substrate on which the electrode material to be deposited can be glass, sapphire, silicon dioxide on silicon, ceramics, polymer, fiberglass or any other insulating materials. Glass and silicon are mostly used as the substrate materials for cell impedance sensors. The transparency of the glass substrate makes it suitable for the microscopic experiments. The silicon chips cannot ensure this transparency , therefore only through one direction the observation is possible [5]. Still it is in use in cell based FET sensors.

iii) Insulating Material

SiO_2 or SU-8 generally used as the insulating layer for defining the active metallic electrode area and connecting leads, isolating them from the electrolytic solution. Thus the impedance signals can be extracted from the active electrode area only, keeping high signal to noise ratio, reducing background noise. [5, 40, 41]

iv) **Electrolyte Solutions**

Electrolyte solutions such as KCl or NaCl, PBS (Phosphate Buffer Saline) solution have been used in different researches [5]. PBS contains (NaCl, KCl, Na_2HPO_4 and KH_2PO_4) [42].

v) **Bio Compatible Material for Culture Media**

As per [5] [43]explained the materials used to culture the cells must be biocompatible to keep the biological characteristics of the living cells properly. Polydimethylsiloxane (PDMS) is commonly used forming encapsulated micro fluidic devices. The biocompatibility, flexibility in shape, and ability for bonding easily with glass or silicon substrates make PDMS suitable for this purpose. Also Phosphate Buffer Saline (PBS) is used for the culture media.

2.4.2 Fabrication Processes

For the fabrication of the ECIS device following fabrication steps are followed in different researches. [5]

i) Metal Deposition

For deposition of metal sputtering or thermal evaporation is adopted for adhesive materials like Cr (or Ti) (30nm)[44] and electrode material Au (300nm) or Pt. Glass is generally used as substrate material. Cr or Ti is used as the adhesive for depositing Au on glass.

ii) Lithography

On the deposited metal layer, the electrodes, contact pads and connecting leads are patterned as per the mask of the design of the device adopting lithography and etching process as discussed by [4].

iii) Vapor Deposition of Insulation layer

For depositing the insulating layer on the Au electrode surface chemical vapor deposition (CVD), physical vapor metal deposition (PVD)[44] is followed. As the insulating material, polymer or passivation layer of SiO_2 (also in some researches $SiO_2/Si_3N_4/SiO_2$) or any negative photoresist like SU-8 are used on the connecting leads to isolating the active electrode area from the electrolytic solution.

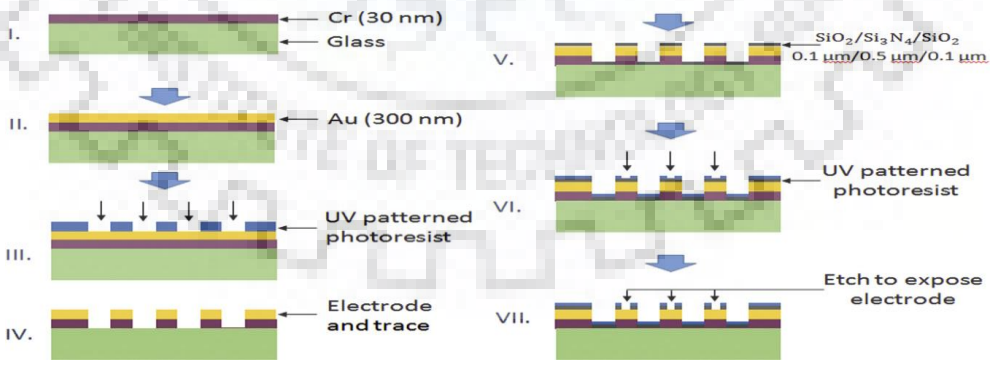

Figure 2.10: A Typical Electrode Fabrication Process Flow [5].

iv) Etching: Wet , reactive ion etching ,plasma etching etc are followed to remove the insulation layer, hence exposing active electrodes area and the contact pads.[32]

2.5 Gaps and Challenges Identified for ECIS Devices

- **Maintaining Natural Environmental Conditions for Living Cell**

  The maintenance of natural living conditions for a cell requires precise control of physical and chemical constraints and it has to be a continuous process to keep the cell alive for a long period of time [13]. A particularly difficult parameter is the creation of a hydrophobic environment, which is essential to keep the receptors of the cell membrane functioning so that they are able to analyze various chemical signals. Besides, to immobilize membrane receptors on transducer surface, hence maintaining the natural cell membrane structure and functions, hydrophobic environment is required [2]. This process however, can be aided by Polydimethylsiloxane (PDMS) – a silicon based polymer, as it offers various advantages over the silicon and glass ones such as – being more flexible, transparent, fabrication friendly, inexpensive and also it is completely biocompatible (as it is not toxic) [33].Also PBS can be a solution[45].

- **Higher Double Layer Capacitance**

  The double layer capacitance at the electrode/electrolyte interface causes higher parasitic impedance which is another challenge for ECIS devices. It incorporates errors in the measured data [4]. The deposition of SiO_2 or SU8 as the insulating material can help eradicating this high double layer capacitance.

- **Effects of Parasitic Capacitance**

  Another concern in designing ECIS device is reducing the parasitic capacitance, caused by the passivated metallic connecting leads, which connect the electrodes and contact pads[46]. Varying width of the lead trace and area of electrodes can be a solution. The microelectrodes if optimized by increasing the thickness or decreasing the area of the passivation layer can help in decreasing the parasitic capacitance caused by this.

- **Fringe Effects by Electrodes**

  Electrodes when spaced closely can incorporate fringe effects which affect the actual electric field. In this case keeping distance of 100µm can be a solution.

- **Decrease of Effective Cells with Miniaturization**

  Since a large number of cells are grown in a small area of electrode, the total impedance of electrodes increases with the increase of cell number in the electrode area. However, the number of effective cells reduces with the decrease of width and length of the electrodes, which decreases device performance. Also reuse of the experiment system with the cell is reduced. Hence, a tradeoff between the number of effective cells and sensor sensitivity should be considered in designing sensors [1].

2.6 Objective of the Project

As per the above gaps identified a four electrode ECIS device with an optimized design and biocompatible microfabrication can ensure a better solution eradicating all these drawbacks, which is the aim of this project.

CHAPTER-3
DESIGN AND SIMULATION OF FOUR ELECTRODE ECIS DEVICE IN COMSOL MULTIPHYSICS AND ZSIMPWIN

3.1 OUTLINE FOLLOWED FOR THE PROJECT WORK

As per the literature review by different researches on ECIS this dissertation work is planned in two phases.

I. Software simulation

II. Lab experimentation

Based on the above design requirements steps to implement for the project work was accomplished as follows:

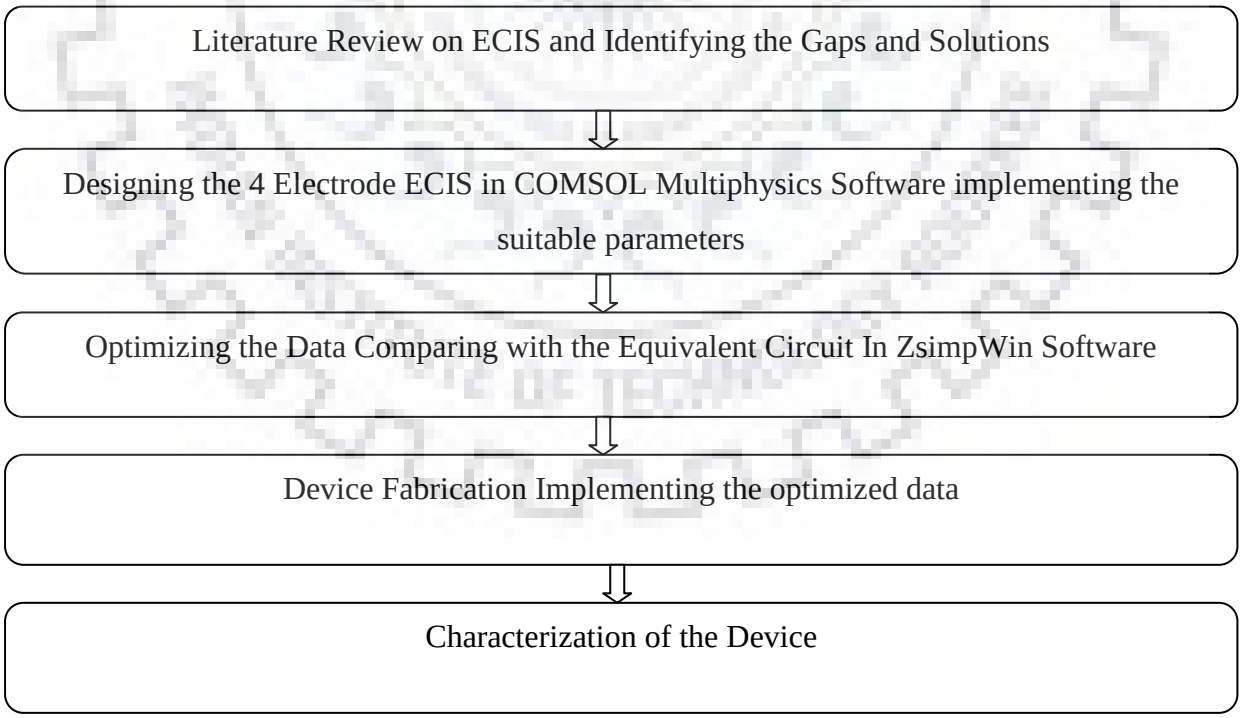

Figure 3.1: Overall Outline of the Project Work.

From the literature review of ECIS the 4 Electrode ECIS device was designed and optimized in COMSOL Multiphysics using suitable parameters and from there the impedance and phase plots were obtained for different geometries and dimensions. For the electrode gold was selected as the material and for the electrolyte Phosphate Buffer Saline (PBS) was chosen assigned with given parameters. Then using the ZSimpWin software plots were then compared with the equivalent circuit models. From the output of the comparison of equivalent circuit models the impedance, capacitance, and admittance for the given designs were obtained. Analyzing those outputs the optimized values for the voltage applied, thickness of electrodes and surface area of the electrolyte were determined. Finally with the optimized data of the parameters the 4 electrode ECIS device was fabricated using Au as the sensor material and characterization with PBS was done accordingly. After this characterization the sensor can be used for further Drug Delivery Study by using the blood cells, cancer cell lines etc.

3.2 METHODOLOGY

3.2.1 ECIS DEVICE DESIGN IN COMSOL MULTIPHYSICS

In this thesis work the four electrode ECIS device has been designed in COMSOL Multiphysics software and following that was fabricated accordingly based on the optimized design parameters obtained from the software simulation. The device includes four sensors- the working electrode -WE, reference electrode -RE, counter electrode -CE and the sensing electrode -SE.

The sensing electrode is decoupled from the working electrode unlike 3 electrode device as an extra electrode basically for the improvement of sensing the cell impedance. The material of the squares has been taken as gold and the circular part surrounding the electrode squares has been taken for the PBS solution.

The potential drop of the sample is basically measured between the inner SE and RE whereas the current is passed between WE and CE. Gold has been chosen as the electrode material for being a noble material and chemically inert with the living cells. Also at the electrode/electrolyte interface, it prevents any electrochemical reaction hence any additional effect on the bioimpedance for that was ignored. [4]

To avoid any cross contamination between the ions of the electrodes and cells, all the electrodes has been designed with a 100 µm distance of from each other. The geometrical dimensions of all the four electrodes were same and square shaped. The dimension of the square electrodes were 50×50 µm, 100×100 µm, 150×150 µm; 200 × 200 µm titled as the Design 1, Design 2, Design 3, Design 4 respectively .All the electrodes were connected to the contact pads from which the external electrical input was supplied. A 100 µm width metal interconnection line was used to connect each electrode with the contact pad having a dimension of 1000 µm x 1000 µm.

3.2.2 Equations Used in COMSOL Multiphysics

COMSOL Multiphysics software is generally used for simulating various physics applications using finite element method and various numerical approaches. In this work the AC/DC module has been selected for conducting the simulations and the electric current interface and a Frequency Domain study step are chosen for designing. This combination is useful for the modeling of AC problems when inductive effects are negligible. In the simulations also purely capacitive effect of the electrodes were considered based on the parallel plate and the inductive effects were assumed as negligible.

In the AC/DC module the 2D time harmonics analysis of electric current is available which was considered for impedance analysis of the designed device. The module on the assumption of inductive effect is negligible considers the electric field as linear and curl free. This is because, when inductive effect is neglected, the electric field becomes curl free and is termed as the gradient of a scalar potential, *V,* as discussed in [4, 23]. The continuity equation for the conductivity and displacement currents then becomes

$$-\nabla.\{(\boldsymbol{\sigma} + \boldsymbol{j\omega\varepsilon_r\varepsilon_0})\nabla \boldsymbol{V}\} = \mathbf{0} \qquad \textbf{(18)}$$

Where ε_0 denotes permittivity of free space, ε_r denotes relative permittivity, the potential applied on sensor is represented by V, conductivity of the system is denoted by $\boldsymbol{\sigma}$ and $\boldsymbol{\omega}$ represents angular frequency ($\boldsymbol{\omega}$ =2πf, f is input frequency). The following equations represent the equations used for electric field E and displacement D, using the gradient of V:

$$\mathbf{E} = -\nabla \mathbf{V} \qquad (19)$$

$$\mathbf{D} = \varepsilon_0 \varepsilon_r \mathbf{E} \qquad (20)$$

The module obtains the current density J using the Ohm's law as below

$$J = \sigma E + j\omega D + J_e \qquad (21)$$

Here, σ denotes conductivity of the electrolyte PBS and external current density is represented by Je. For this system, because of no external current density was present, the equation could be reduced to

$$J = \sigma E + j\omega D \qquad (22)$$

The equation of the impedance has been taken as the ratio of voltage and total current at the electrode by the COMSOL Multiphysics software and the admittance is taken as the inverse of the impedance by the terminal feature through automatic computations. The coarser mesh was used in this simulation.

3.2.3 BOUNDARY CONDITIONS

In the COMSOL Multiphysics software four gold electrodes are designed on an insulating glass substrate, on a circular surface PBS electrolyte. The PBS has a conductivity of 2×10^{-5} S/m and a relative dielectric constant of 136 as [47] [4]discussed. The outer circumference of the PBS electrolyte was considered to be electrically insulated as a boundary condition to prevent the contact with the Pyrex cylinder which will be used in the fabrication for holding the electrolytic PBS solution. On the counter electrode and reference electrode the ground potential boundary condition was applied. The WE and SE were assigned as the terminals and there voltages of 5mV, 10mV, 15mV, 20mV were applied respectively. The gold electrodes were simulated with thicknesses of 500,1000,1500,2000 μm. Thus an electric connection was built, connecting the working and counter electrode, establishing an electric field.

3.2.4 FINDING THE OPTIMIZED PARAMETERS USING ZSIMPWIN

ZsimpWin is a software for the data analysis of electrochemical impedance. It can extract and analysis various electrical parameters by iterations and provides the equivalent circuit model of the given electrochemical system. To extract the equivalent circuit model of the ECIS device of this project work also ZsimpWin software was used. The values of different electrical parameters were extracted with the help of this software by a number of iterations where the value of chi-square (χ^2) value plays significantly in validating the equivalent circuit model of an electrochemical system. The standard value of χ^2 has been found to be 1.5×10^{-3} or below by the research works [4, 48].

.

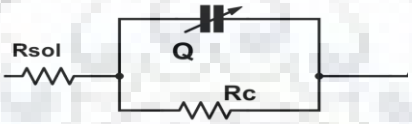

Figure 3.2: Equivalent Circuit model used for the experiment [4].

3.2.5 PROCEDURE OF OPTIMIZATION

Four designs of 50µm, 100µm, 150µm and 200µm geometry for the ECIS device were designed and simulated in COMSOL Multiphysics software. The geometry basically denotes the size of the square shaped electrodes used in the device. For the optimization simulations have been done varying the parameters like applied voltage, thickness of electrodes and diameter of the circular PBS region. Different voltages like 5mV, 10mV, 15mV, 20mV have been applied on electrodes with thickness of 500µm, 1000µm, 1500µm, 2000µm and PBS diameters of 2000µm, 4000µm, 6000µm and 8000µm. To find the optimized design one parameter has been varied keeping the other two parameters constant and the output of the simulation in COMSOL Multiphysics have been obtained. Finally the simulation outputs are compared with the equivalent circuits in the ZsimpWin software and the optimized design parameters are obtained.

3.3 DESIGNED FOUR ELECTRODE ECIS DEVICE

As per the previous discussions in figure 3.3 and 3.4, a four electrode ECIS device has been designed in COMSOL Multiphysics .The design consists of four square shaped gold electrodes- WE, RE, SE, CE etc. The sensing electrode is included as an extra electrode basically for the improvement of sensing of the impedance. The electrodes are placed at 100µm distance from each other on the circular PBS electrolyte region. The circular electrolyte surface has PBS as the material with a conductivity of 2×10^{-5} S/m and a relative dielectric constant of 136. As the boundary condition of the present work, the outer circumference of the PBS electrolyte surface has been kept electrically insulated.

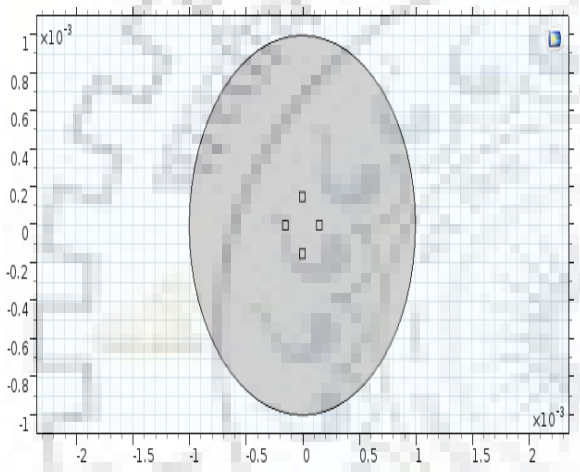

Figure: 3.3 Designed Four Electrode ECIS in COMSOL Multiphysics software.

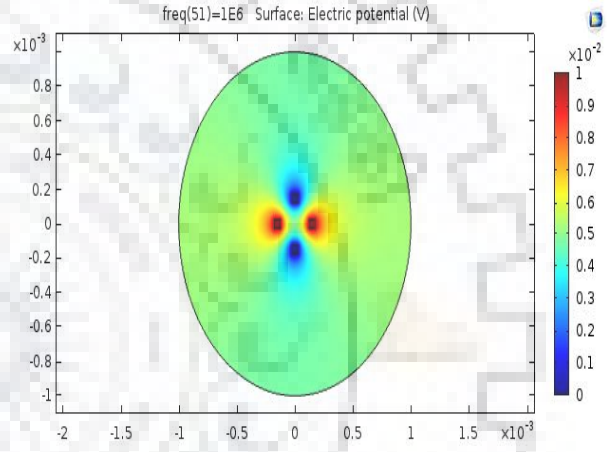

Figure: 3.4 ECIS device after applying proper input parameters and voltage.

For understanding the characteristics of the electrochemical system the impedance of the system should be measured by simulating the impedance for a wide range of frequency. Generally applying an AC voltage or current on the electrodes is considered to be a standard technique and then the response of the electrochemical system is simulated over a range of frequency. From the current or voltage response of the ECIS device the impedance can be calculated. Also from the real and imaginary components of the impedance the in phase and out of phase impedance of the system can be known, which describes the system more profusely. For the simulation of the device, a frequency of 100Hz to 1MHz was applied. On the WE and SE voltages were applied in millivolts. Ground was applied to CE and RE. Figure 3.2 shows the device after all the necessary parameters and electric fields were

applied. The WE and the SE are red colored with the highest applied electric potential, whereas the CE and the RE are blue colored denoting the ground condition. The device was simulated varying the diameters of the PBS surface area, voltage applied and thickness of the electrodes. A coarser mesh was applied for the mesh on the device. The impedance and phase plots were obtained as the outputs from these simulations which were further taken into ZSimpWin to compare with standard equivalent circuit models, hence to find the optimized design parameters.

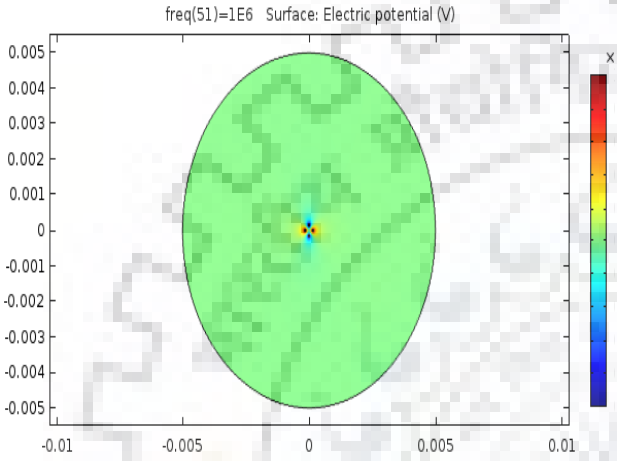

Figure: 3.5 Design with Various Diameters.

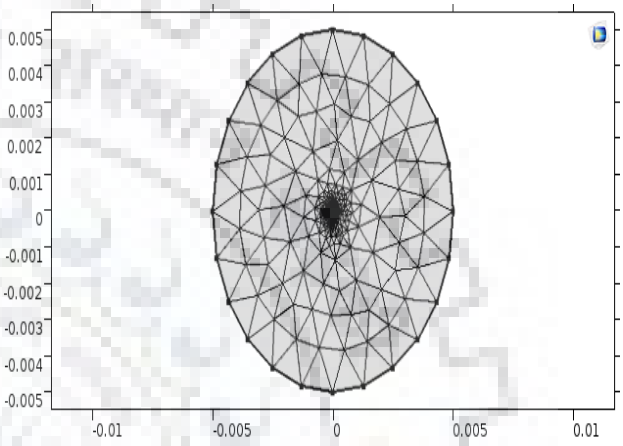

Figure: 3.6 Application of Mesh.

The electrochemical systems can be properly described with its impedance and phase shifts. For this purpose two popular systems are to find the Nyquist and Bode plots of the device. [49]In the device the solution resistance, termed by R_s , is present between the working and the reference electrodes, the charge transfer resistance ,denoted by R_c , is present at the interface of the electrode and the electrolyte. The constant phase element is present in the system representing the double layer capacitance which expresses the absorption and desorption of the ions in between the electrode/electrolyte during electrochemical reactions. These all three key electrical components acting in the device create impacts on the overall impedance and phase shift of the device.

3.4 SIMULATION OUTPUTS AND ANALYSIS

For extracting the impedance and phase angle values of the designs the simulations have been done for all the given parameters according to the table.

Designs (Length of sensor square)	Voltage(mV)	Thickness(µm)	Diameter of PBS(µm)
50µm	5mV	500µm	2000µm
100µm	10mV	1000µm	4000µm
150µm	15mV	1500µm	6000µm
200µm	20mV	2000µm	8000µm

Table 3.1: Parameters used for design considerations and simulations.

a) SIMULATION OUTPUTS OBTAINED FOR VARIOUS APPLIED VOLTAGES

Impedance outputs for 50µm design

Following impedance outputs were obtained from the simulation for the device with 50µm geometry varying the voltages while keeping the thickness and the diameter of the PBS surface diameter constant.. The plots consists of the impedance output from device designed in COMSOL and the plots of standard equivalent R-Q-R circuit model obtained from the

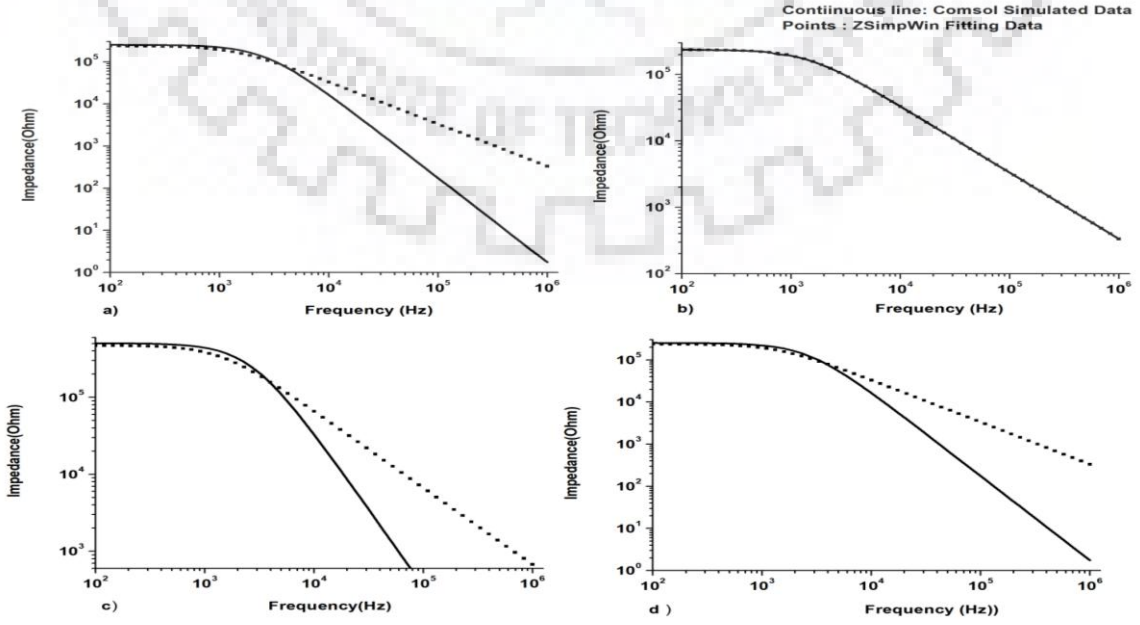

Figure 3.7: Impedance for 50µm Geometry for 5mv, 10mv, 15mv, 20mv.

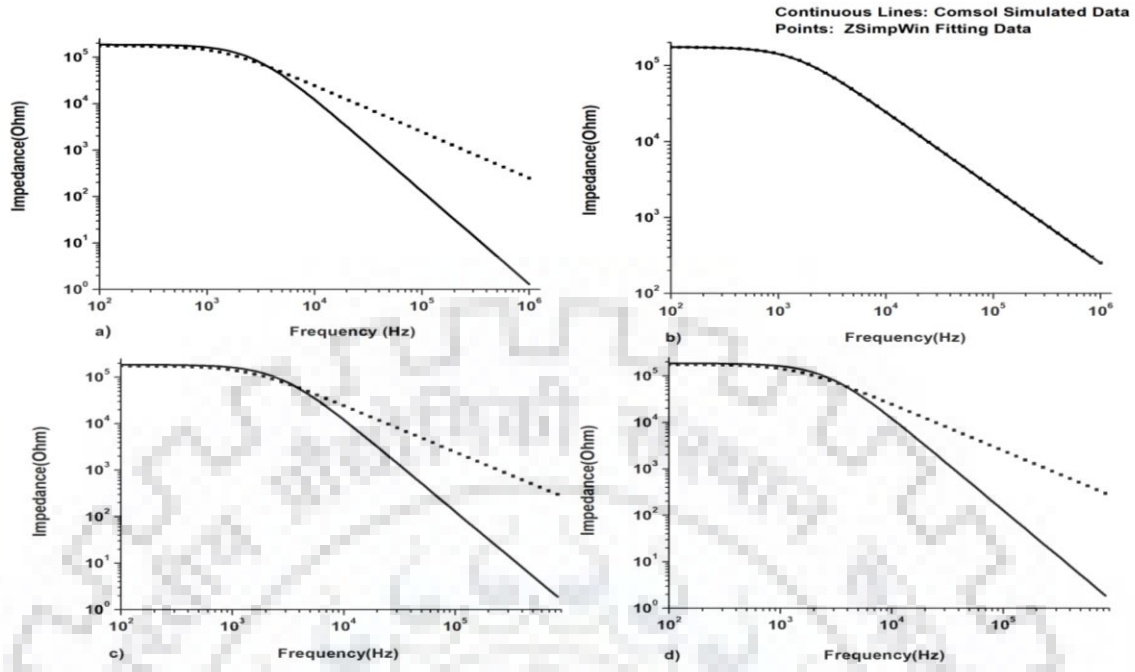

Figure 3.8: Impedance for 100µm Geometry for 5mv, 10mv, 15mv, 20mv.

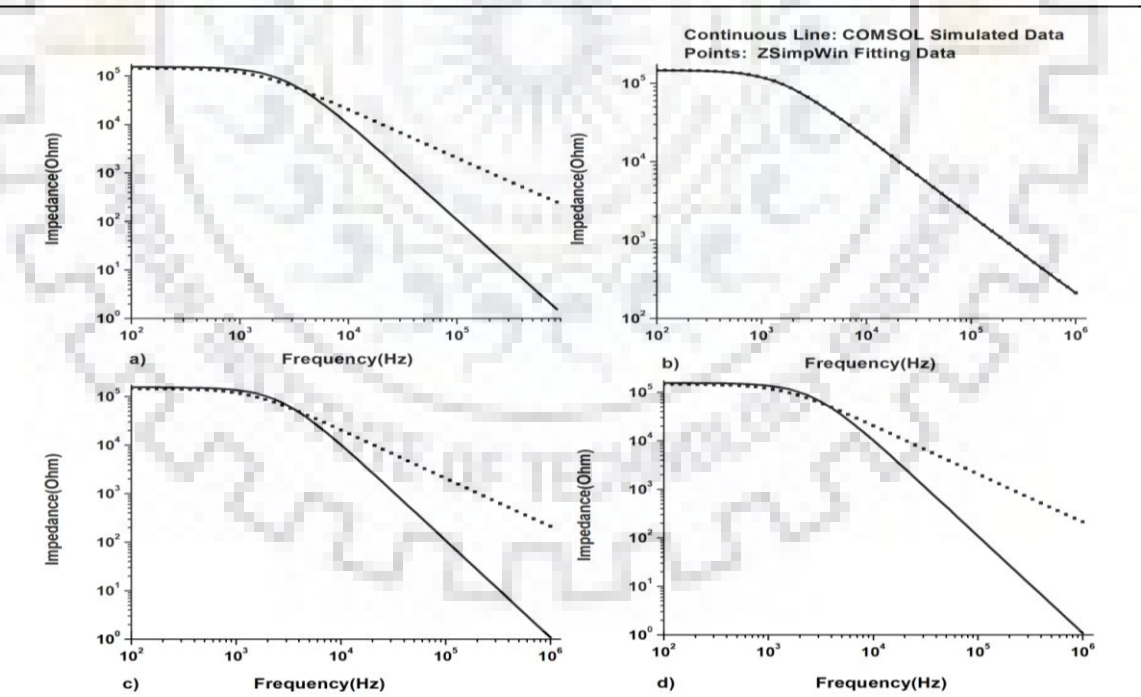

Figure 3.9: Impedance for 150µm Geometry for 5mv, 10mv, 15mv, 20mv.

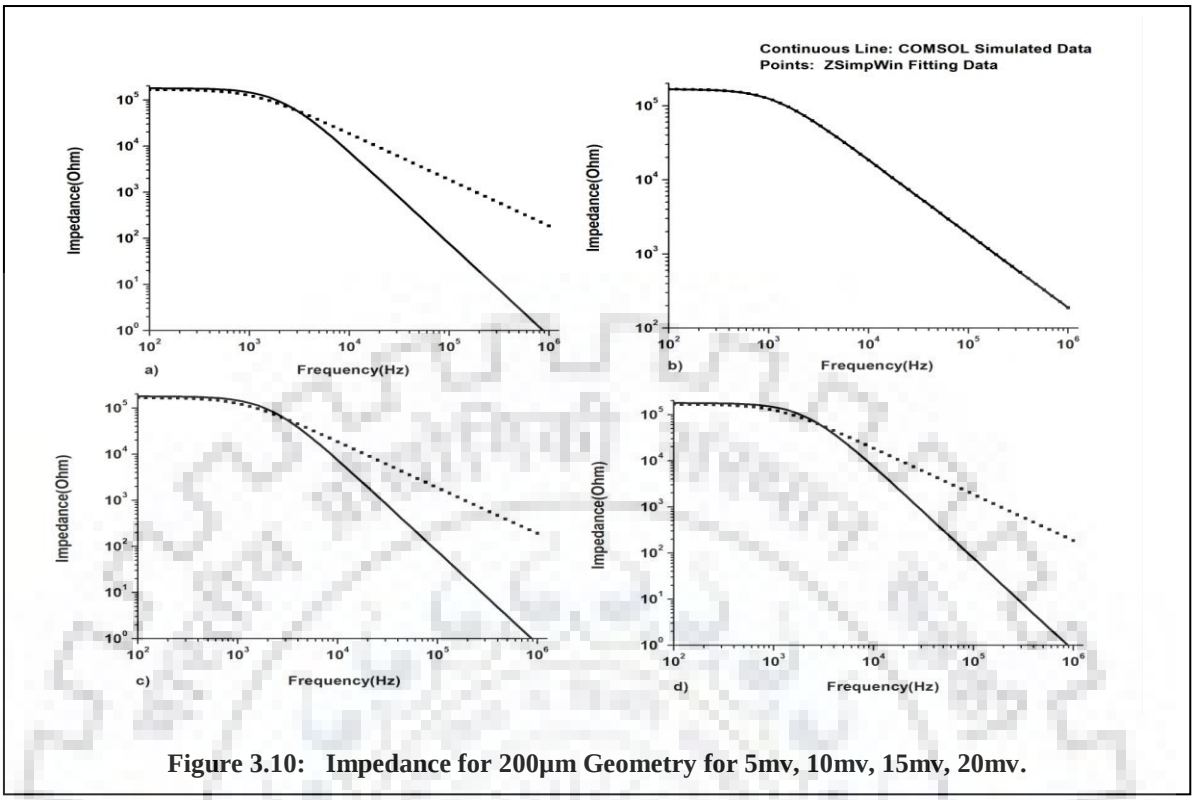

Figure 3.10: Impedance for 200µm Geometry for 5mv, 10mv, 15mv, 20mv.

Observations

- The above figures represent the bode plots of both designed and equivalent circuits impedance values of four electrode ECIS for various designs. The bode plots show the dependency of the magnitude of impedance with the input frequency. In the figures it can be observed that the impedance magnitude decreases as the frequency gets increased. Also with increasing the area of electrodes the impedance values decreases as interfacial capacitance gets decreased for increasing the area of electrodes.

- Since the impedance of the resistance is independent of the frequency and the impedance of the capacitance being a function of the frequency, it is observed that as frequency increases, the impedance of the capacitance decreases and the only the impedances of the resistances are acting in that region.

- At higher frequency the capacitor which is in parallel with the R_c is shorted and removes the R_c resistor from the circuit. Hence the impedance of only the R_s is acting in the system and lower impedance is observed. Also at higher frequency it is understood that the system is basically controlled by the solution resistance R_s.

- At the lower frequency the capacitor acts as a open circuit leaving the (R_s + R_c) resistors in the circuit and the impedance of the system is controlled by the impedance of both of the resistance of the circuit. Hence impedance magnitude is also higher at the lower frequency.

- At the intermediate frequency range the curve has slope of -1 and by extrapolating the plot the value of the capacitance can be obtained from the formula $|Z| = \frac{1}{C_{dl}}$

- It is also observed that the 10 mV plot of the designed device is overlapping with plot of the equivalent circuit data.

Nyquist Plots for the Impedances for Different Voltages

The Nyquist plots have been attained after plotting all the obtained real and negative value of imaginary components of the impedance along X –axis and Y- axis. For each input the points are obtained which represent the impedance at one frequency, though the frequency value cannot be known from the Nyquist plot.[50] The values of the R_s and R_c can be easily known from it. The frequency decreases from left to right. At higher frequency the effect of the solution resistance can be seen. As the frequency lowers the effect of R_c is visible and at the lowest frequency both of the resistances influences the system impedance.

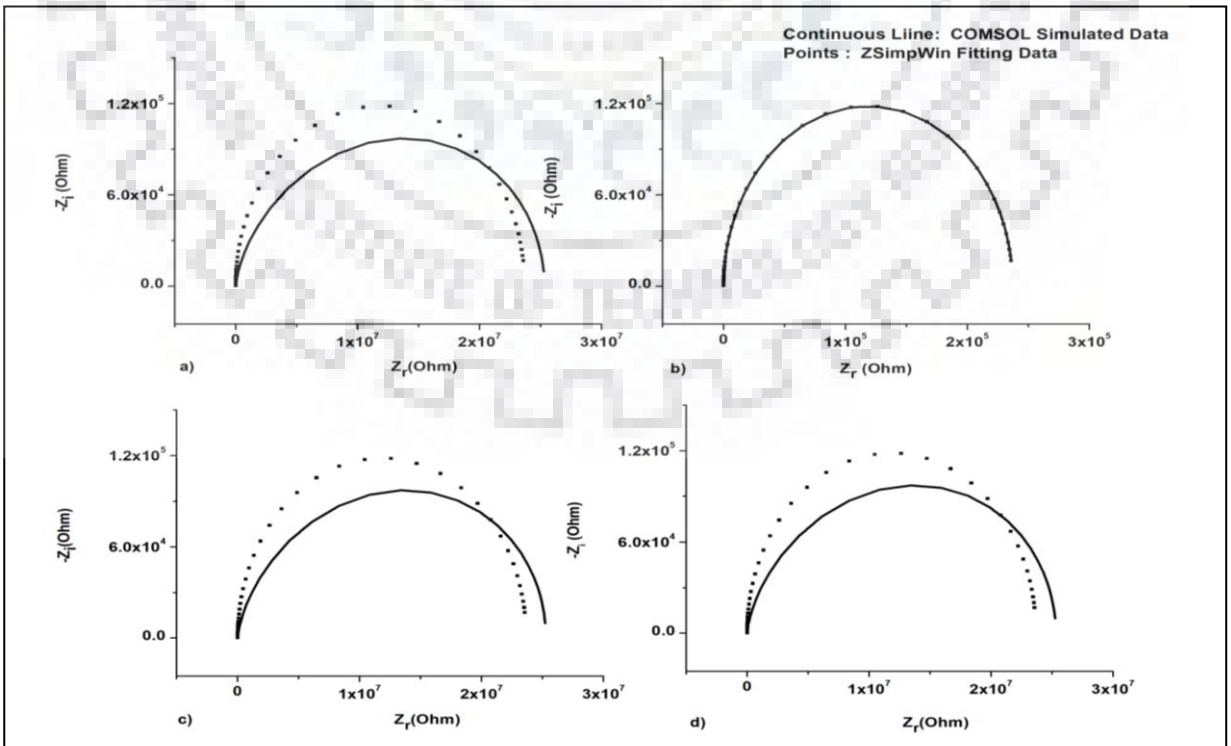

Figure 3.11: Nyquist Plot for 50µm Geometry for 5mv, 10mv, 15mv, 20mv.

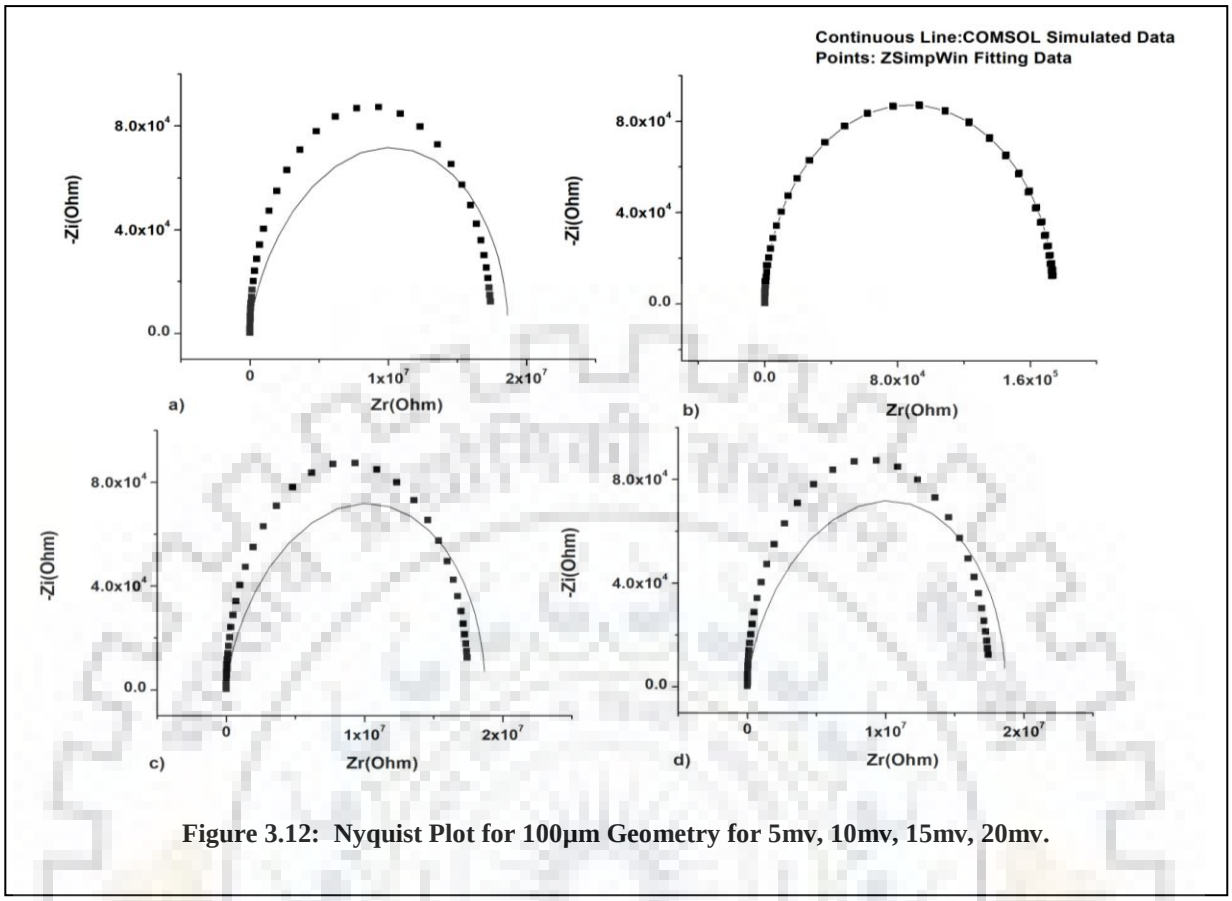

Figure 3.12: Nyquist Plot for 100µm Geometry for 5mv, 10mv, 15mv, 20mv.

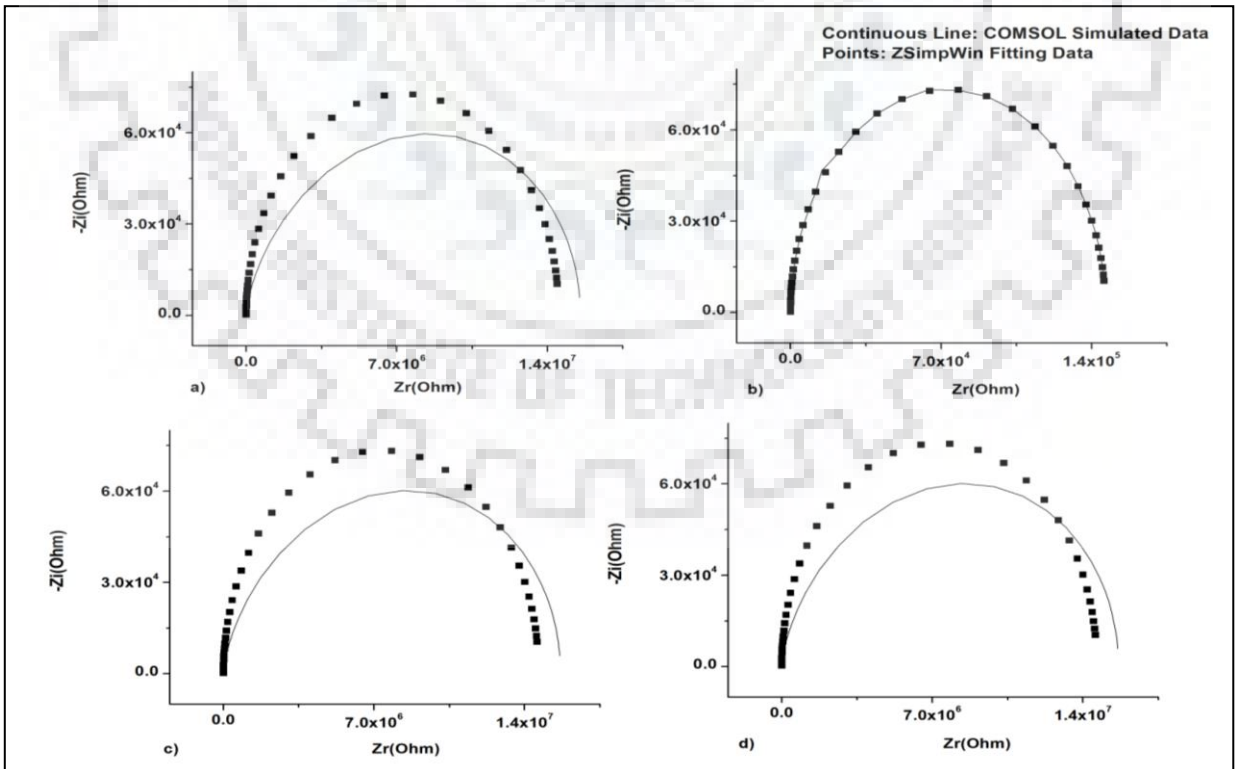

Figure 3.13: Nyquist Plot for 150µm Geometry for 5mv, 10mv, 15mv, 20mv.

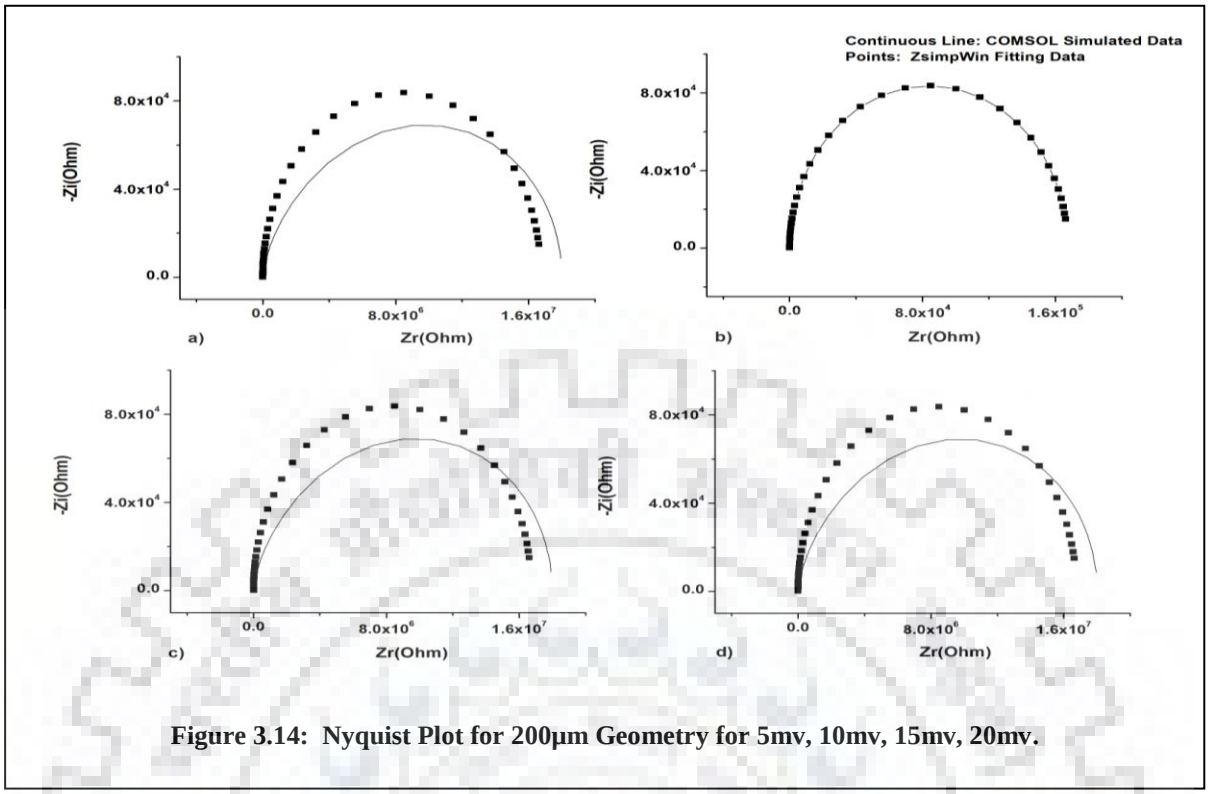

Figure 3.14: Nyquist Plot for 200µm Geometry for 5mv, 10mv, 15mv, 20mv.

Observations

- In the bode plots at highest frequency the R_s only controls the impedance. Whereas at the lowest frequency the (R_s + R_c) act for the overall impedance.
- For the voltage of 10mv the plot matches with the equivalent circuit plot for the designs.

a) OUTPUTS FOR VARIOUS DIAMETERS

Impedance Outputs for Different Diameters

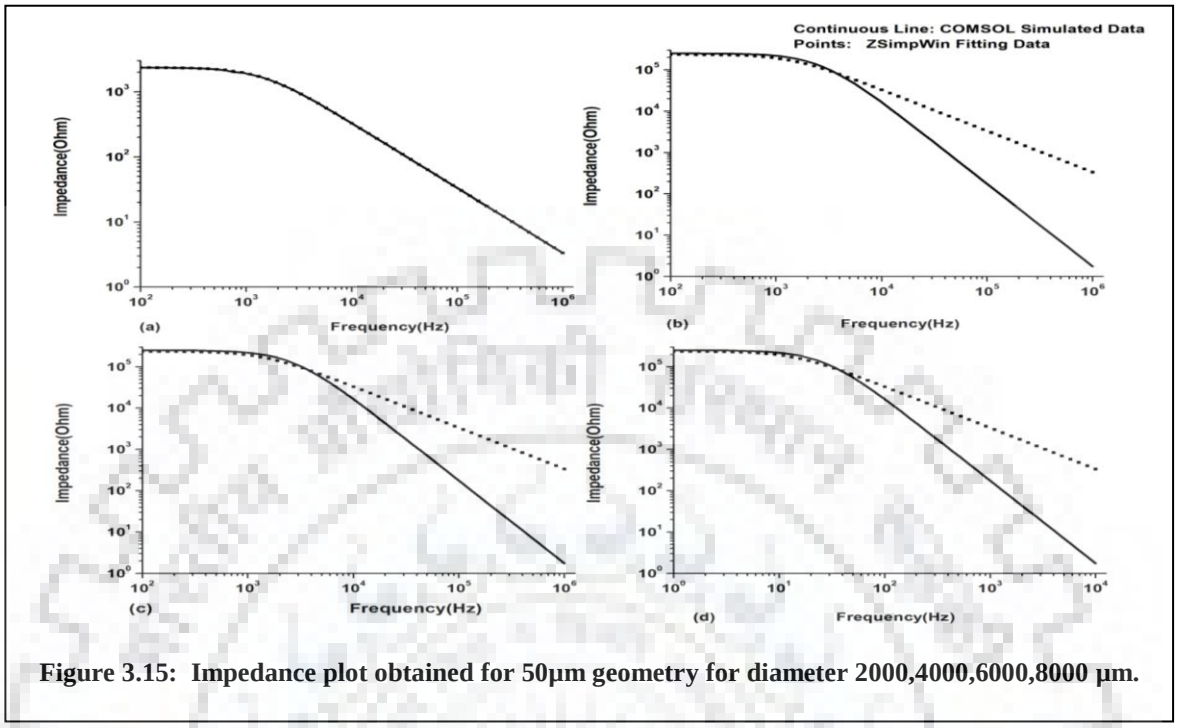

Figure 3.15: Impedance plot obtained for 50µm geometry for diameter 2000,4000,6000,8000 µm.

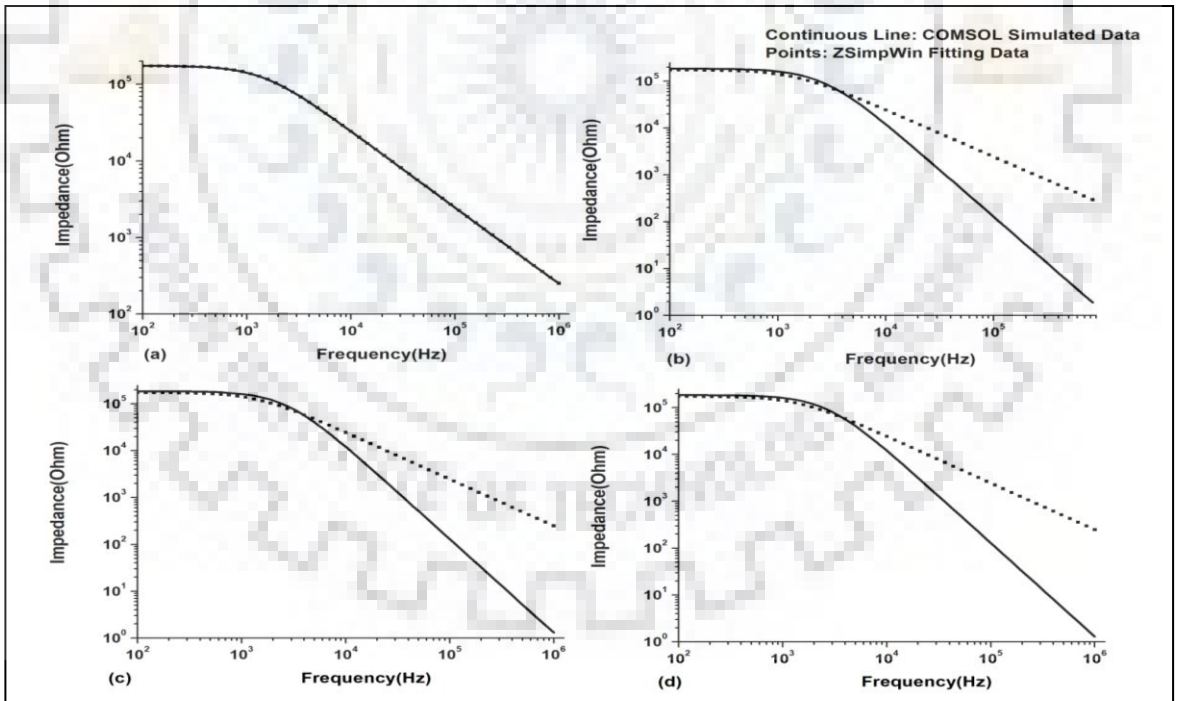

Figure 3.16: Impedance plot obtained for 100µm Geometry for diameter 2000,4000,6000,8000 µm.

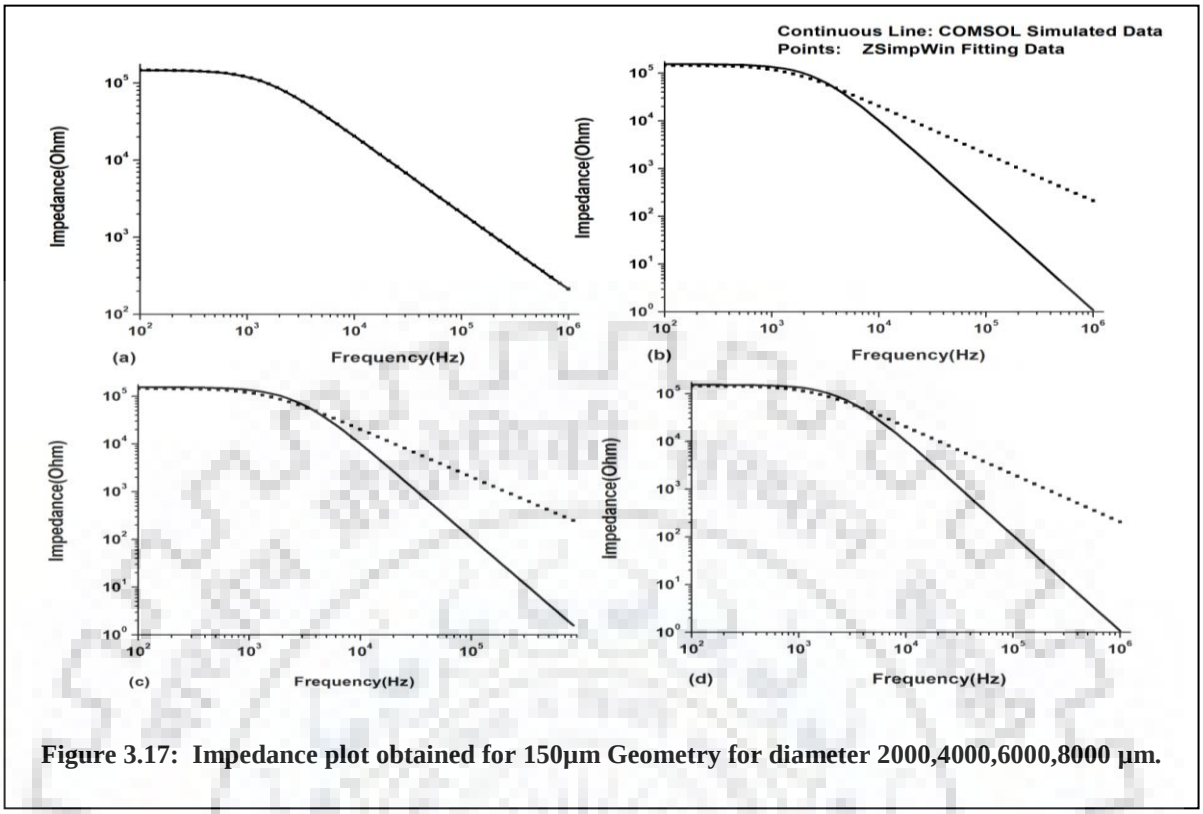

Figure 3.17: Impedance plot obtained for 150µm Geometry for diameter 2000,4000,6000,8000 µm.

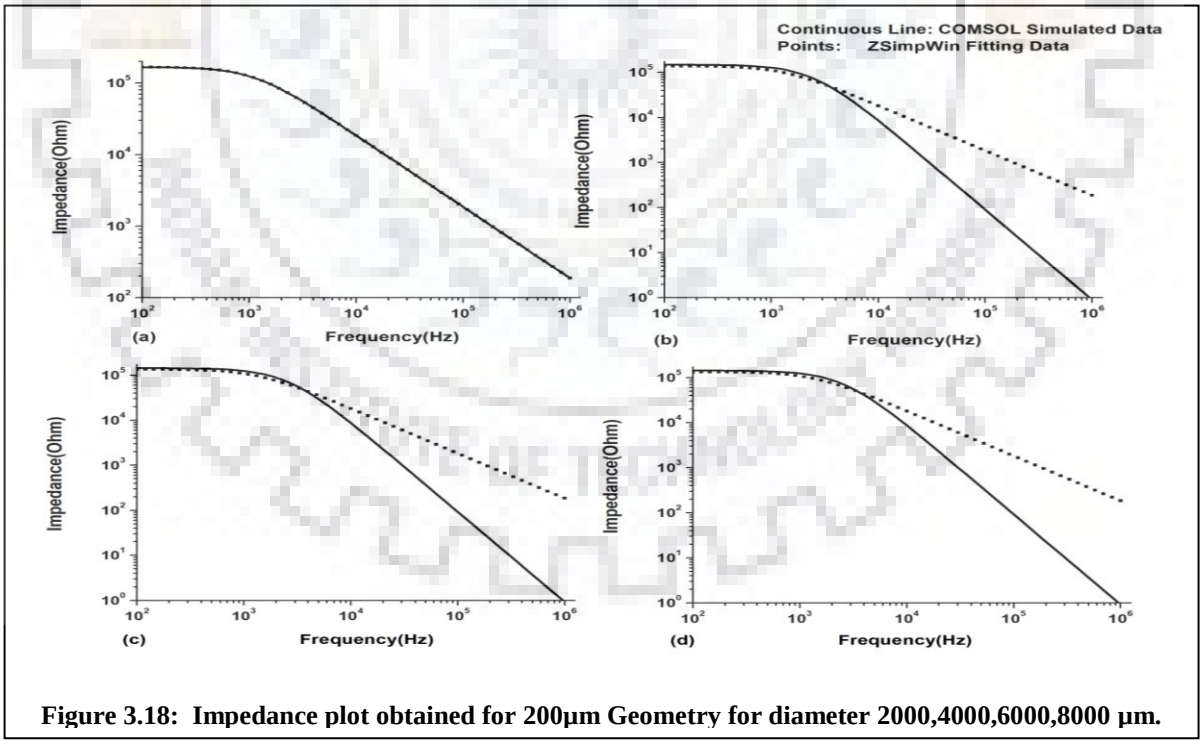

Figure 3.18: Impedance plot obtained for 200µm Geometry for diameter 2000,4000,6000,8000 µm.

Observation: In the bode plot for the diameter of 2000µm the outputs are coming better with the equivalent circuit plot for the designs**.**

- **Nyquist Plots For Different Diameters**

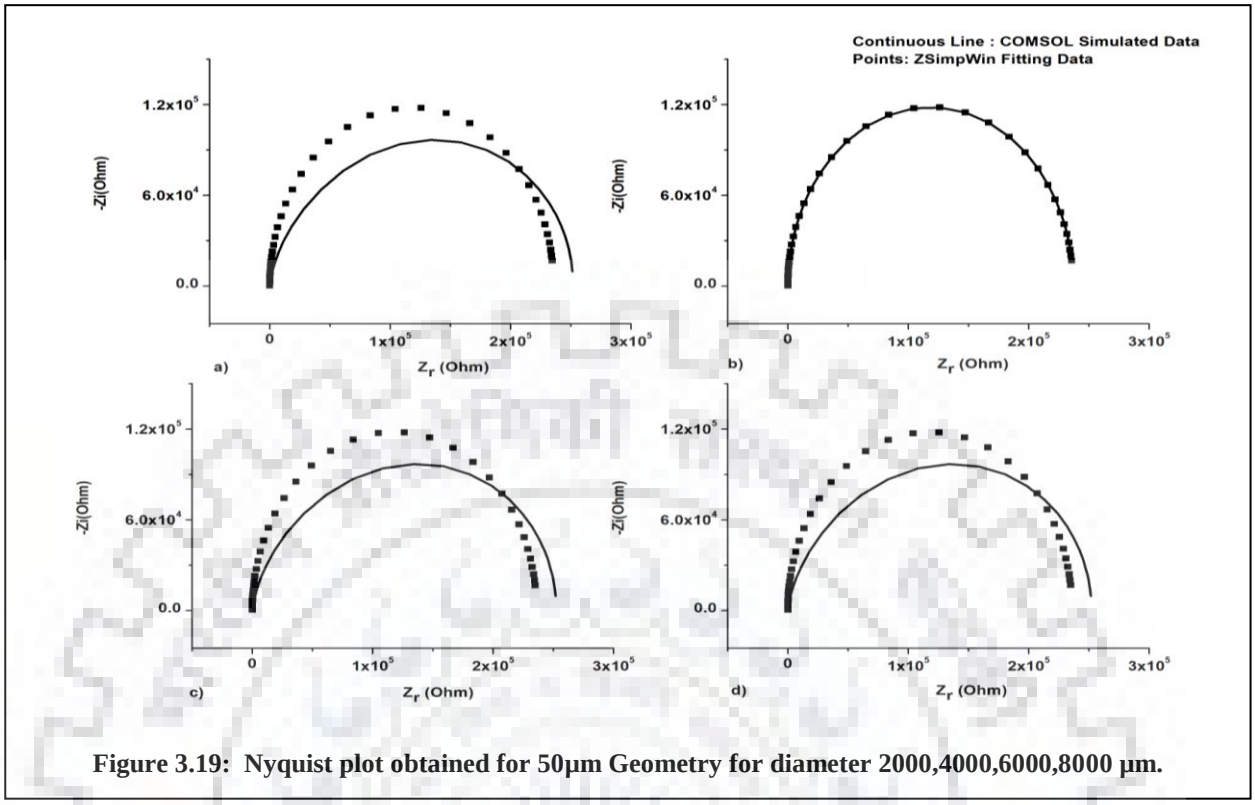

Figure 3.19: Nyquist plot obtained for 50µm Geometry for diameter 2000,4000,6000,8000 µm.

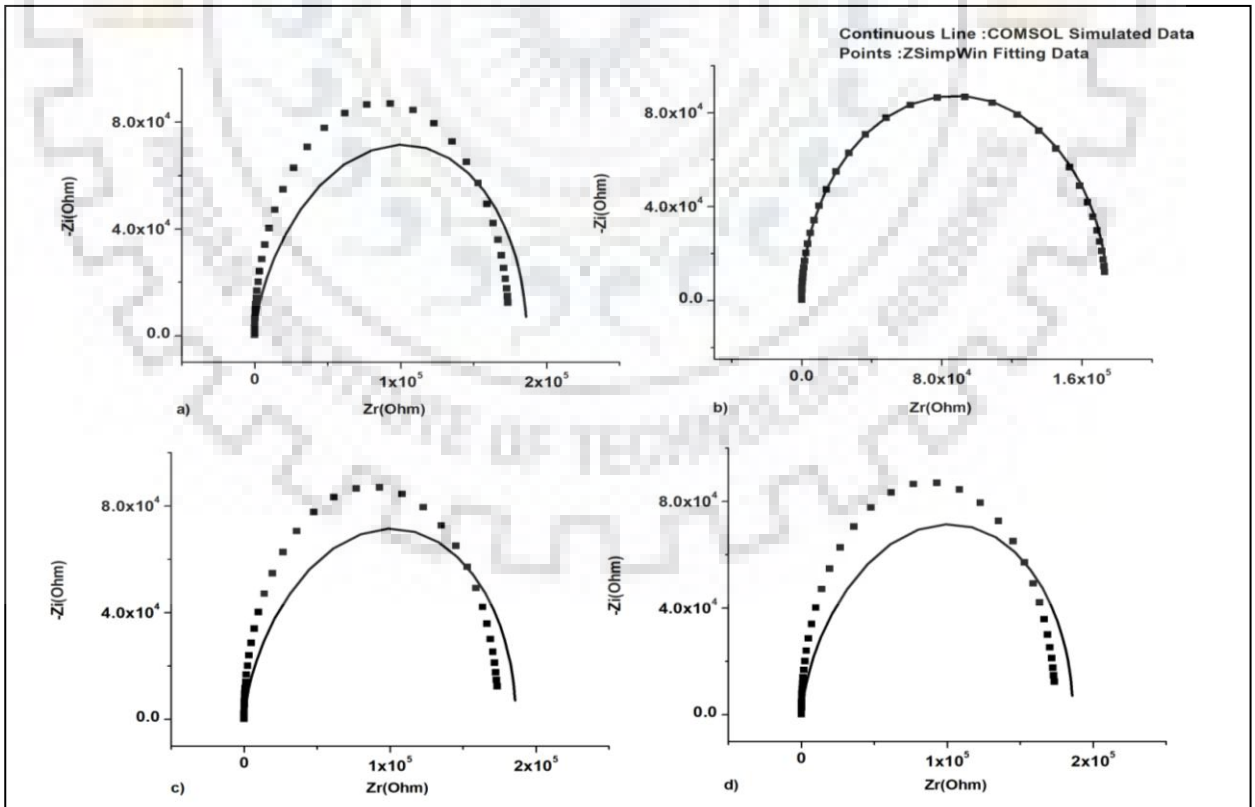

Figure 3.20: Nyquist plot obtained for 100µm Geometry for diameter 2000,4000,6000,8000 µm.

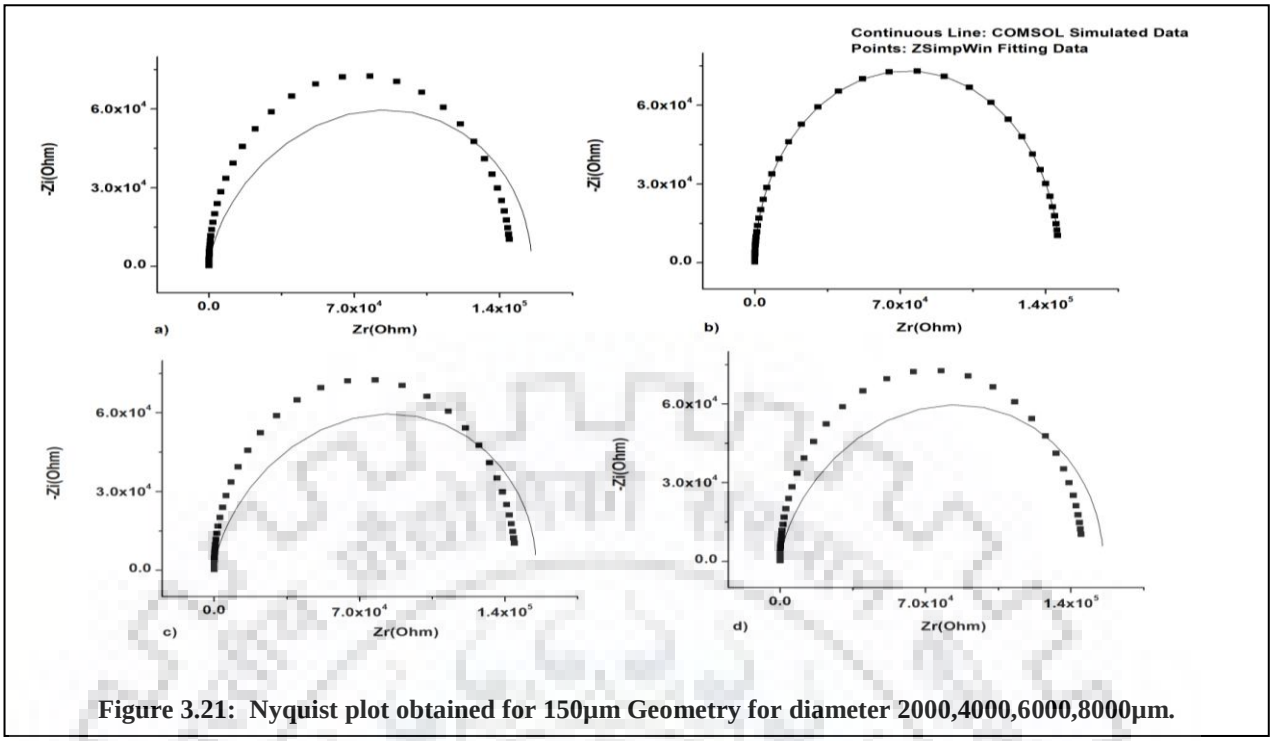

Figure 3.21: Nyquist plot obtained for 150µm Geometry for diameter 2000,4000,6000,8000µm.

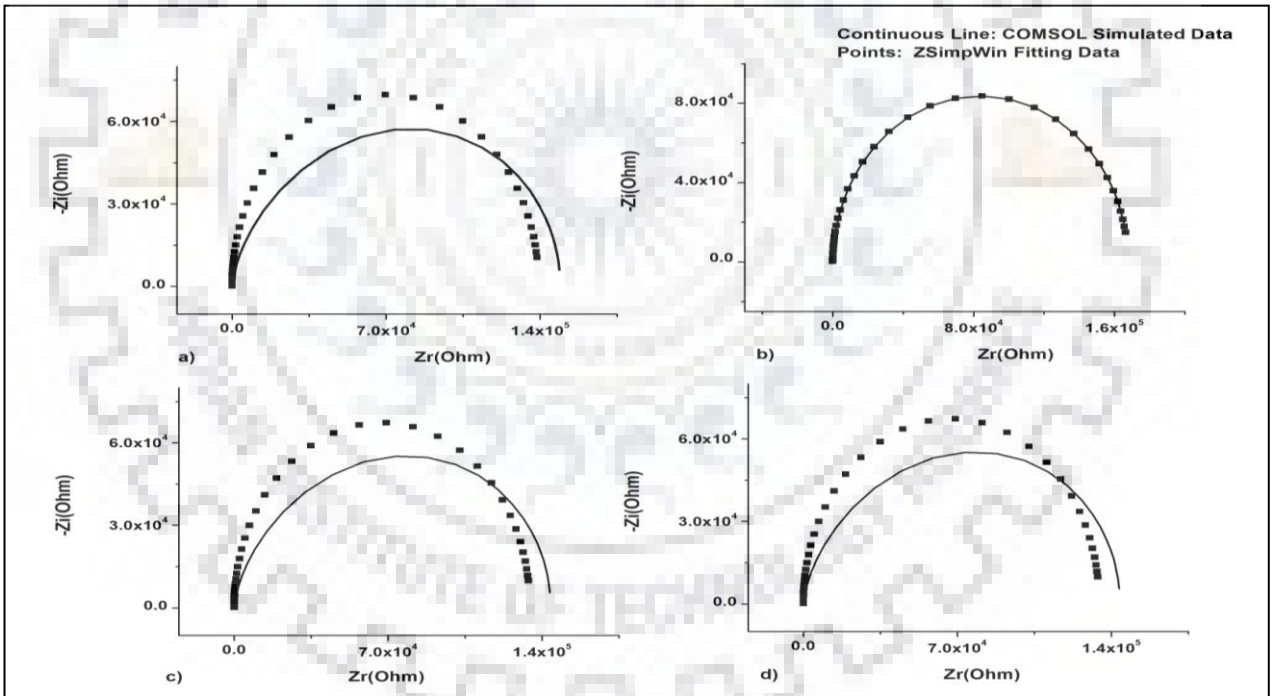

Figure 3.22: Nyquist plot obtained for 200µm Geometry for diameter 2000,4000,6000,8000 µm.

Observation: For 2000um diameter the plots are coming exact as the equivalent one for all the geometries.

b) IMPEDANCE OBTAINED BY CHANGING PBS THICKNESS

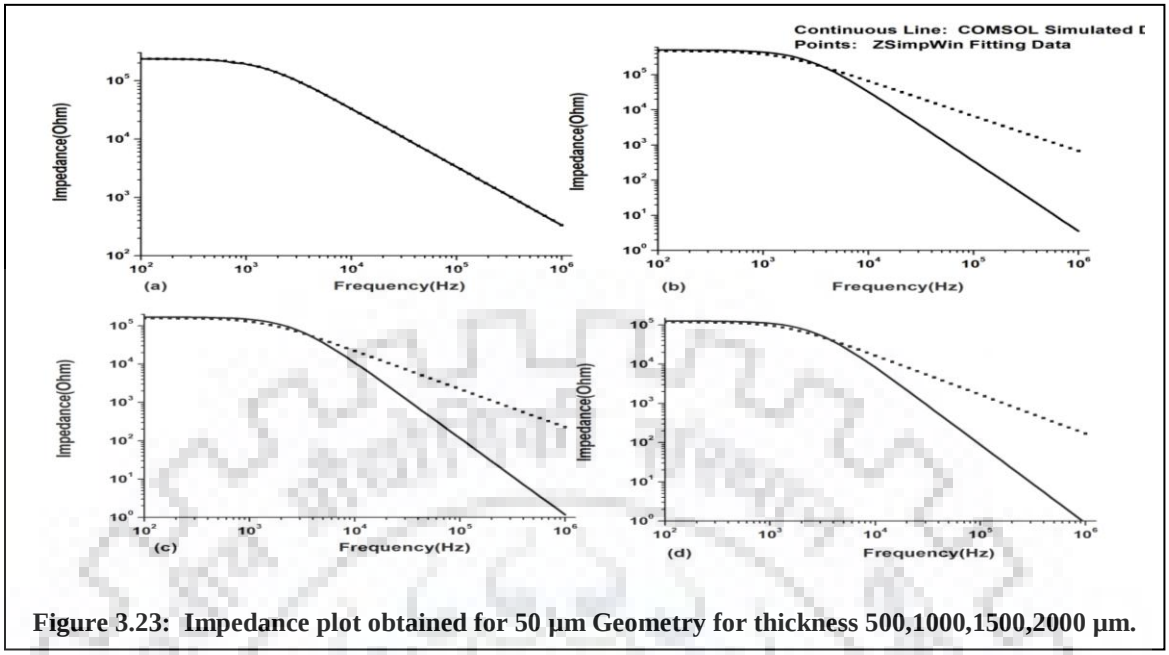

Figure 3.23: Impedance plot obtained for 50 µm Geometry for thickness 500,1000,1500,2000 µm.

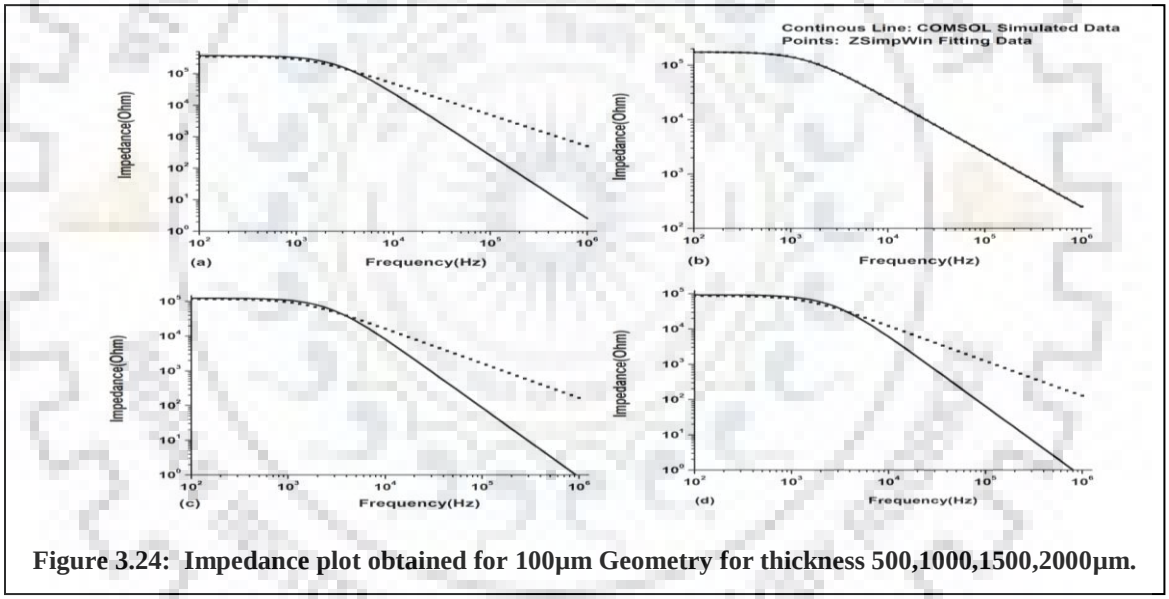

Figure 3.24: Impedance plot obtained for 100µm Geometry for thickness 500,1000,1500,2000µm.

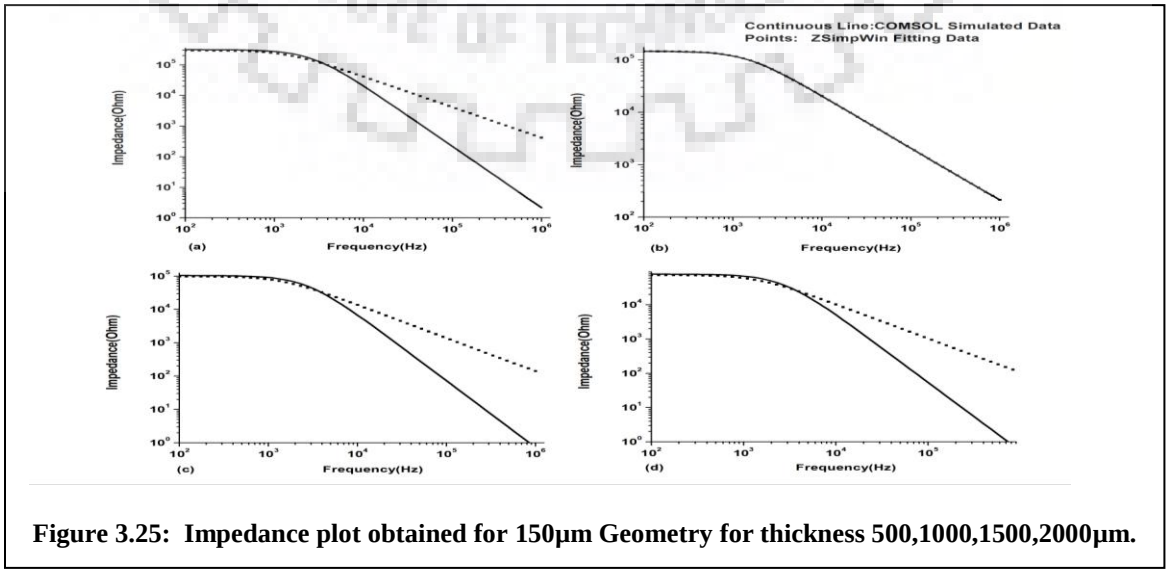

Figure 3.25: Impedance plot obtained for 150µm Geometry for thickness 500,1000,1500,2000µm.

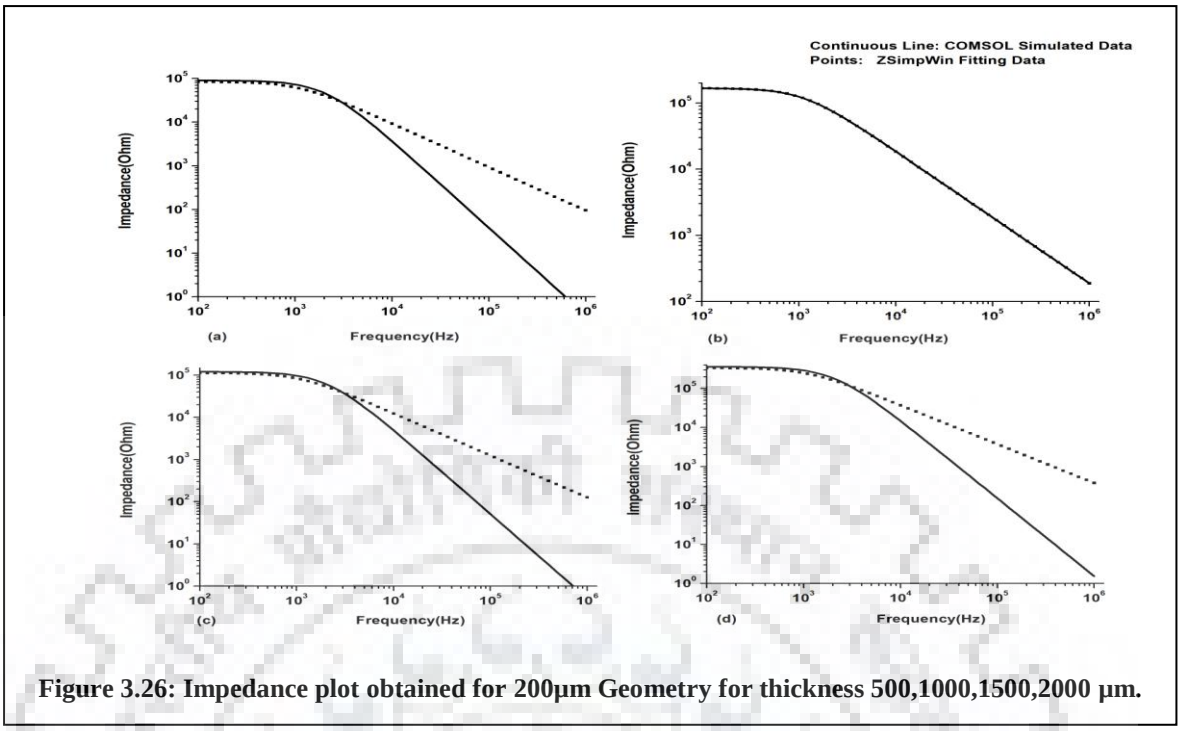

Figure 3.26: Impedance plot obtained for 200µm Geometry for thickness 500,1000,1500,2000 µm.

For different thickness of the electrodes the designs show better outputs for 1000µm electrode thickness for the designs.

- **Nyquist plots Obtained Changing the Thickness**

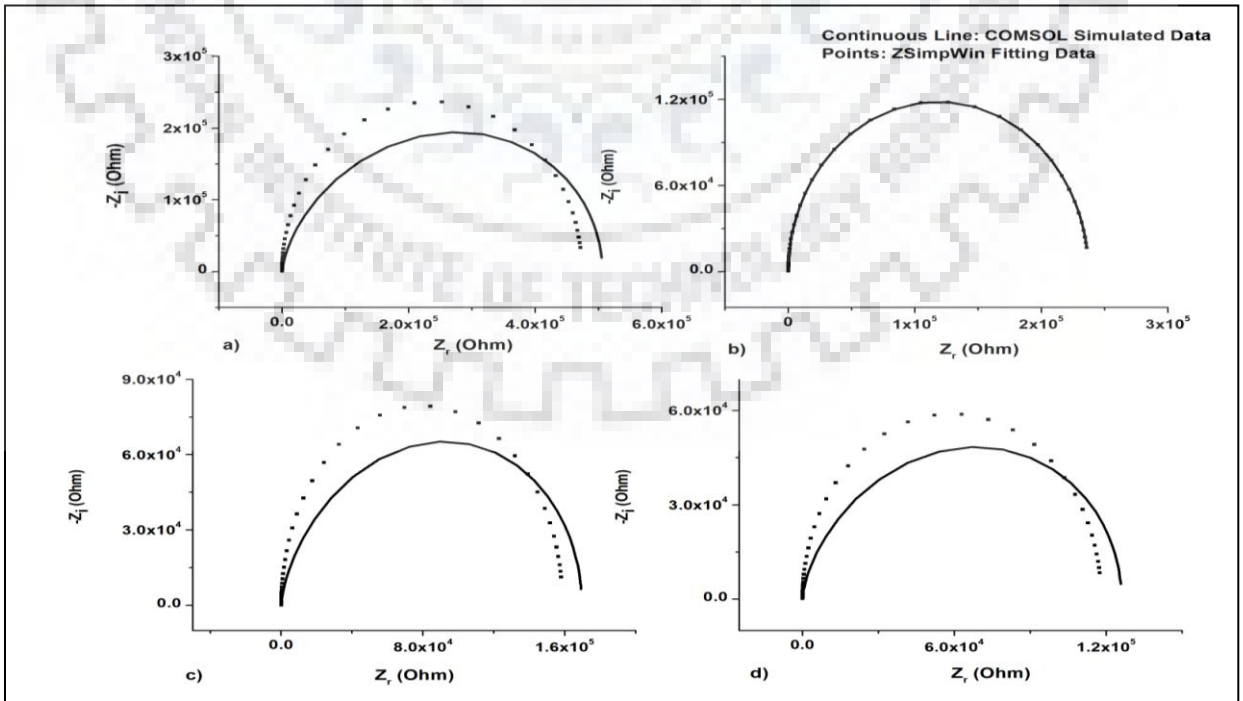

Figure 3.27: Nyquist plot obtained for 50µm Geometry for thickness 500,1000,1500,2000 µm.

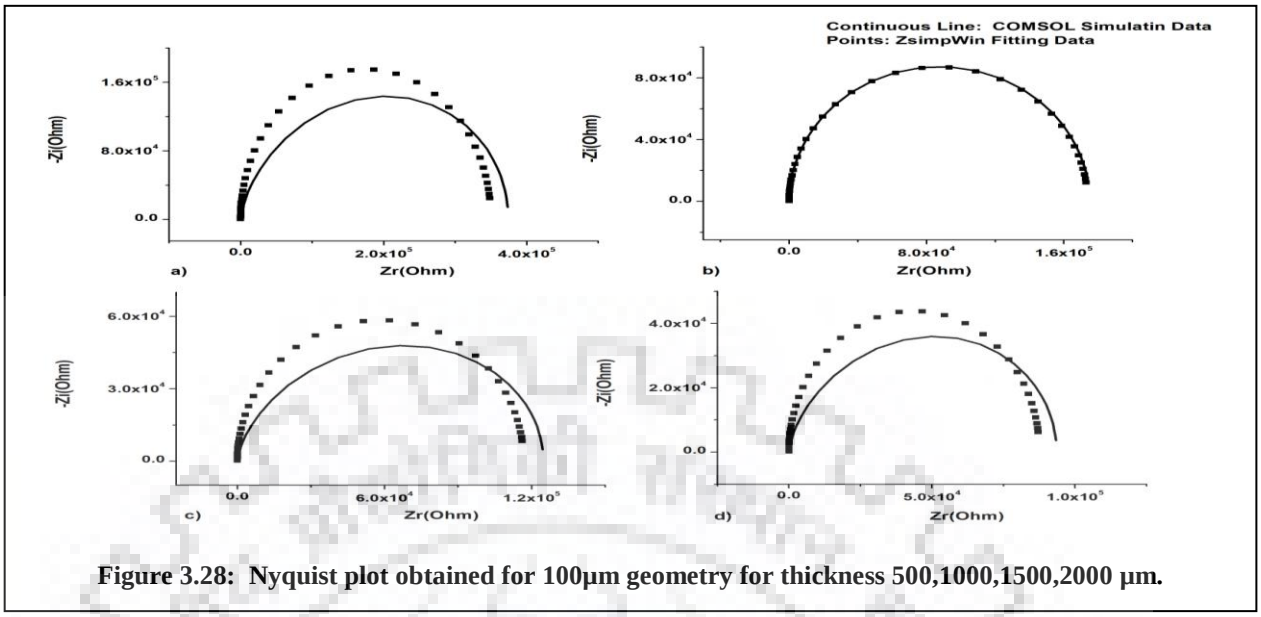

Figure 3.28: Nyquist plot obtained for 100µm geometry for thickness 500,1000,1500,2000 µm.

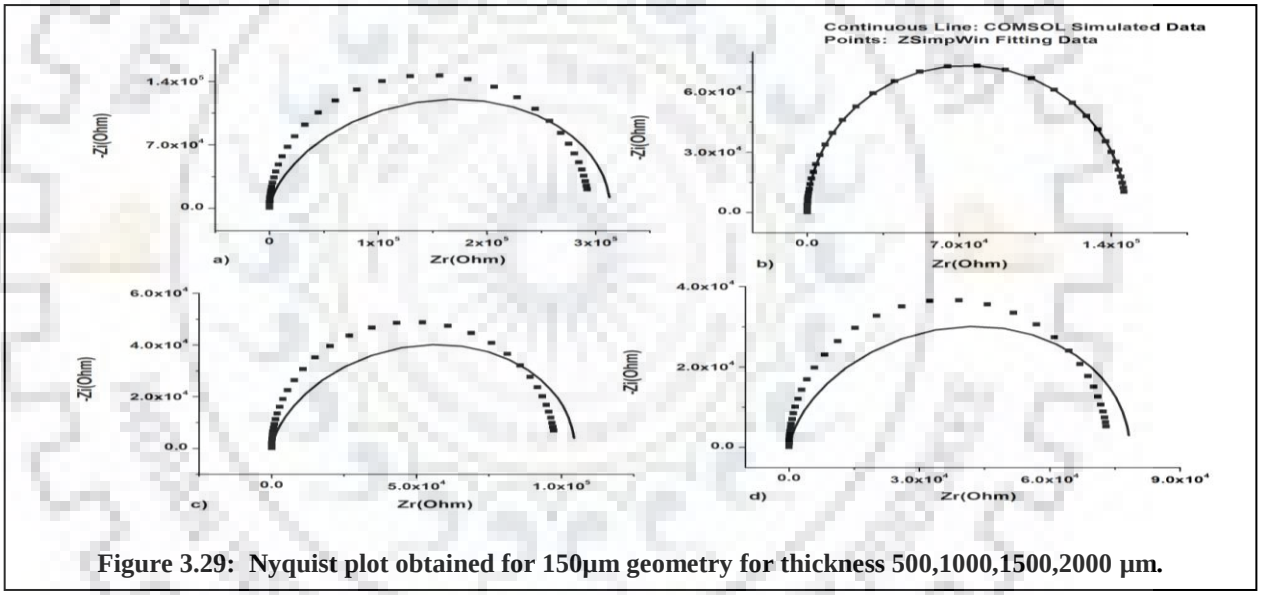

Figure 3.29: Nyquist plot obtained for 150µm geometry for thickness 500,1000,1500,2000 µm.

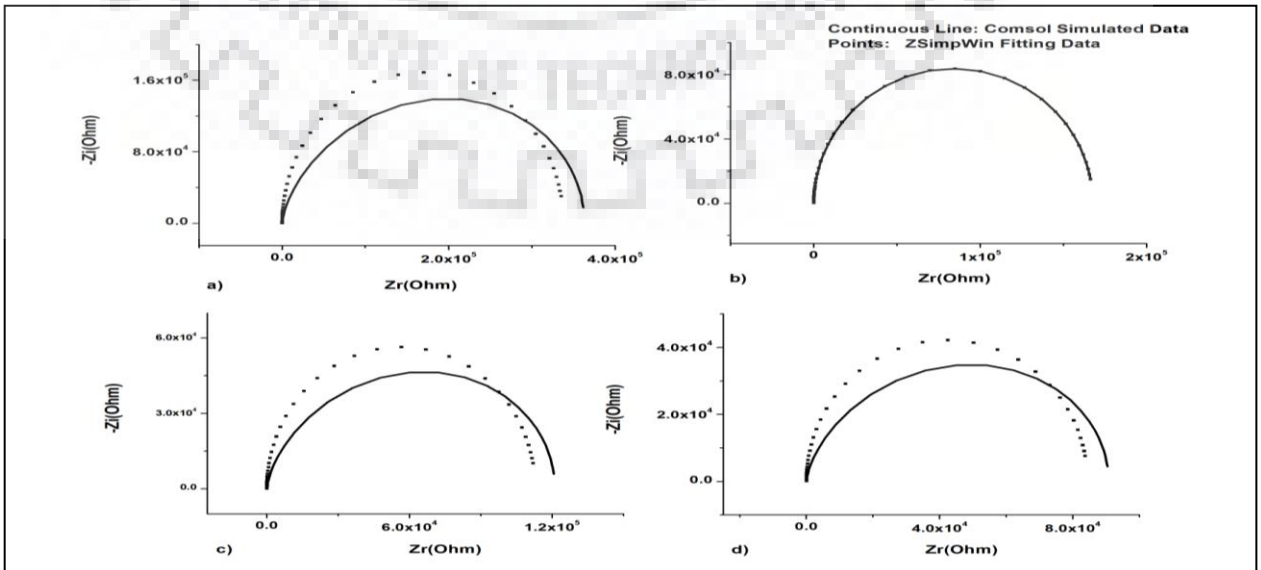

Figure 3.30: Nyquist plot obtained for 200 µm Geometry for thickness 500,1000,1500,2000 µm.

c) Final Output Plots for Optimized Designs

Following outputs were obtained after conducting the simulations varying the design parameters. Satisfactory outputs came for the simulations conducted with applied voltage of 10mV, 1000µm electrode thickness and 1000µm diameter of PBS electrolyte surface.

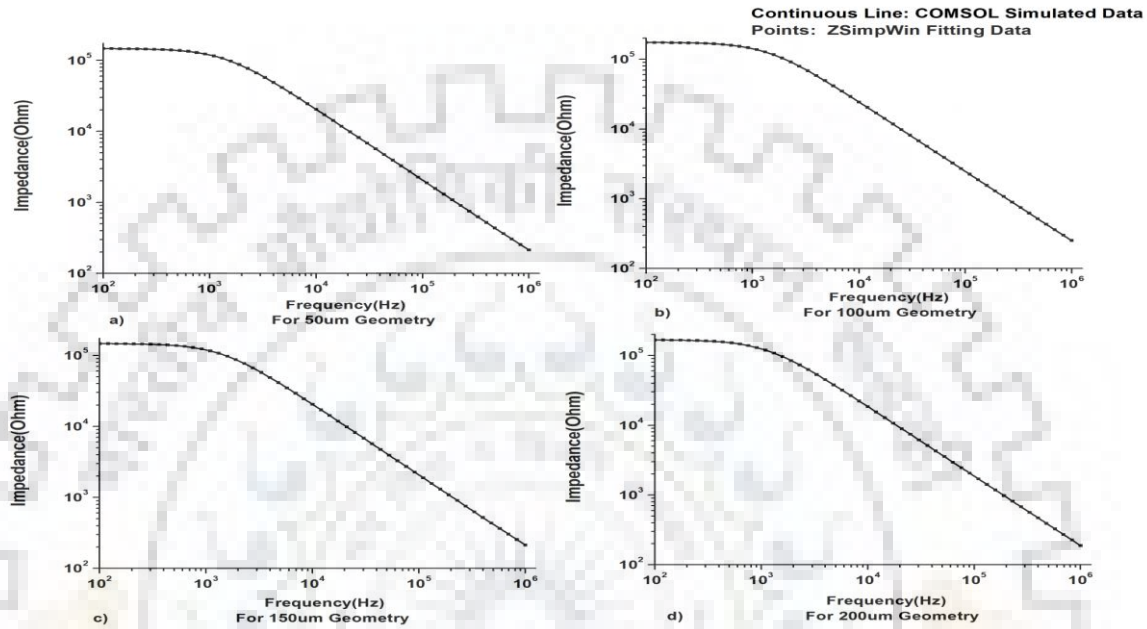

Figure 3.31: Impedance plot obtained for all geometries with voltage 10mV, thickness 1000µm and Diameter of PBS 1000µm.

The impedance of the devices decreases as the frequency increases. This is because at higher frequency only the impedance of the solution resistance acts. There is a sharp change after the 10^3 Hz, as then the signal crosses electrode/electrolyte interface and the charge transfer resistor does not act anymore hence only the impedance also lowers.

- The bode plots also gives the information about the phase shift of the system. At highest and lowest frequency where the device acts mainly resistive as a result the phase angle of the system is zero at those frequencies. Whereas at the intermediate frequencies, mostly the impedance for the capacitive effect of the device acts, hence a negative phase shift of the device impedance is also observed.
- Moreover, the imaginary component of the impedance increases at intermediate frequencies, thus obtained phase angle also increases with the imaginary component.
- The two types of electrochemical reactions that are occurring can also be understood from the nature of the impedance with the frequencies from these plots.

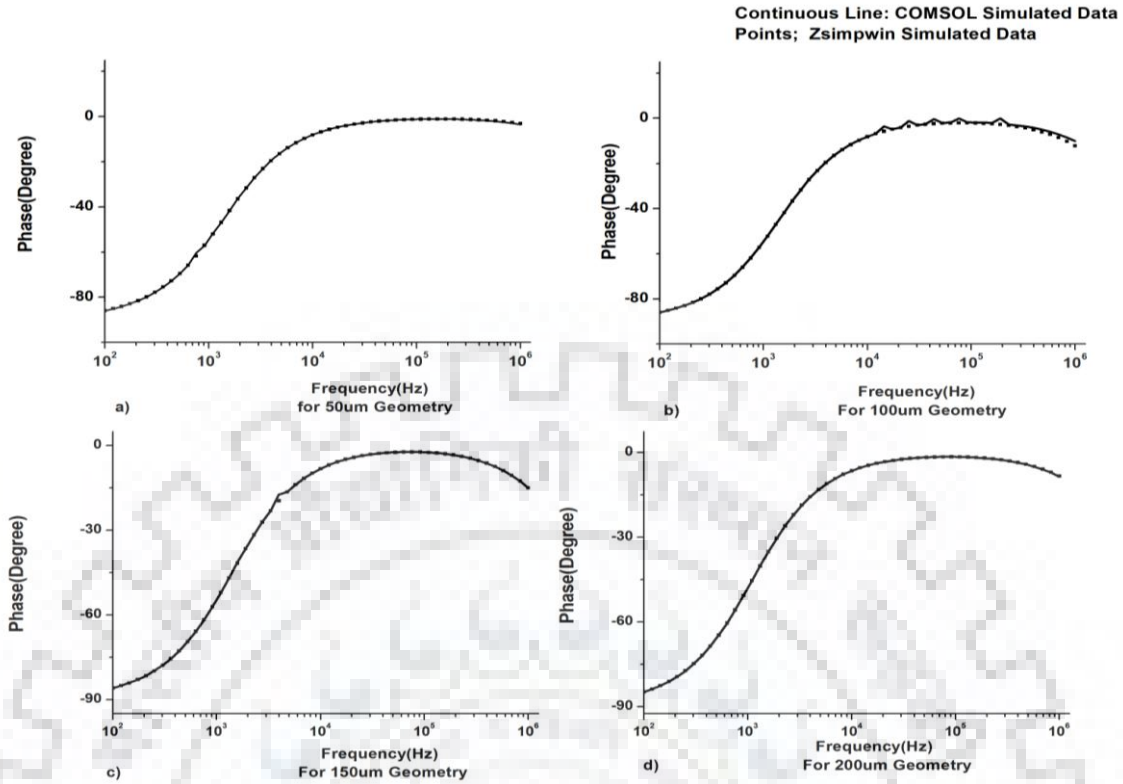

Figure 3.32: Phase output plot obtained for all geometries with voltage 10mV, thickness 1000µm and Diameter of PBS 1000µm.

- From the above bode plots for the phase of the designed devices the capacitive effect, influenced by the double layer capacitance at the electrode/electrolyte interface can be observed which shows the negative slope.
- The frequency $\omega_{(\theta=MAX)}$, at which the phase shift is maximum , can give the value of C_{DL} -the double layer capacitance, using that frequency. Following equation can be used.

$$\omega_{(\theta=MAX)} = \sqrt{(1 / C_{Dl}\ R_c)(1 + R_c/R_s)} \qquad (23)$$

- As the capacitor basically acts as the constant phase element and it is supposed to exhibit 80°-90° phase shift, that is also visible in the obtained plots.

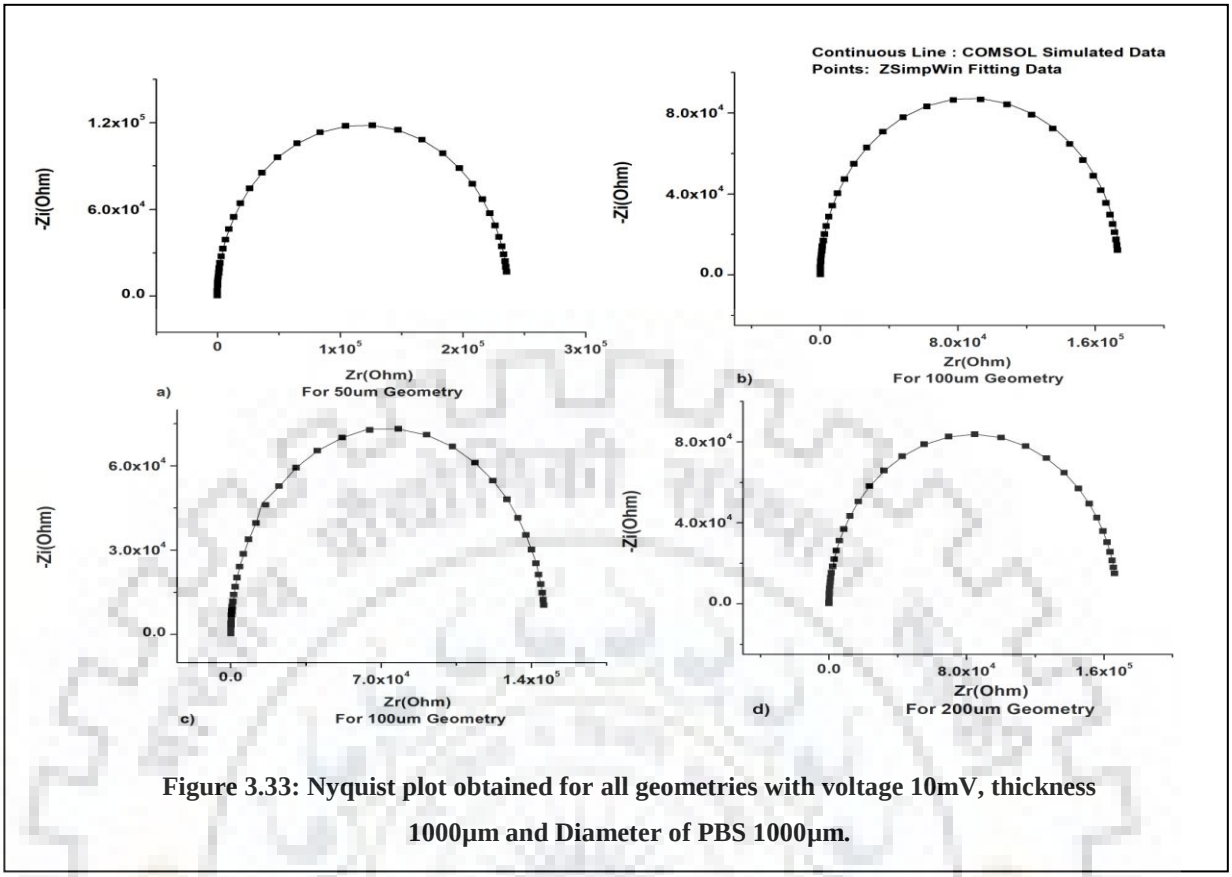

Figure 3.33: Nyquist plot obtained for all geometries with voltage 10mV, thickness 1000µm and Diameter of PBS 1000µm.

- From the Nyquist plot also though the frequency data cannot be known but the effect of the real and imaginary parts of the impedance will be known. For the lower frequency the imaginary components of the electrode/electrolyte interface is more which can be seen in the plots also for all the designs.
- The semicircle shows the single time constant characteristics of the curve.
- From the Nyquist plot the magnitude of impedance can be obtained from the vector drawn from left corner and the length represents the |Z| .Phase angle also can be obtained by getting the angle between the vector drawn and x- axis.
- The values of R_s and R_c the can also be obtained from the Nyquist plots which are tabulated for further analysis. The value of R_s can be obtained by knowing the high frequency intercept at the real axis value which is at the rightmost representing the high frequency region. At the low frequency region (left) the real axis intercept can give the value of the sum of solution resistance and polarization resistance.
- The charge transfer resistance is R_c basically the diameter of the semicircle.

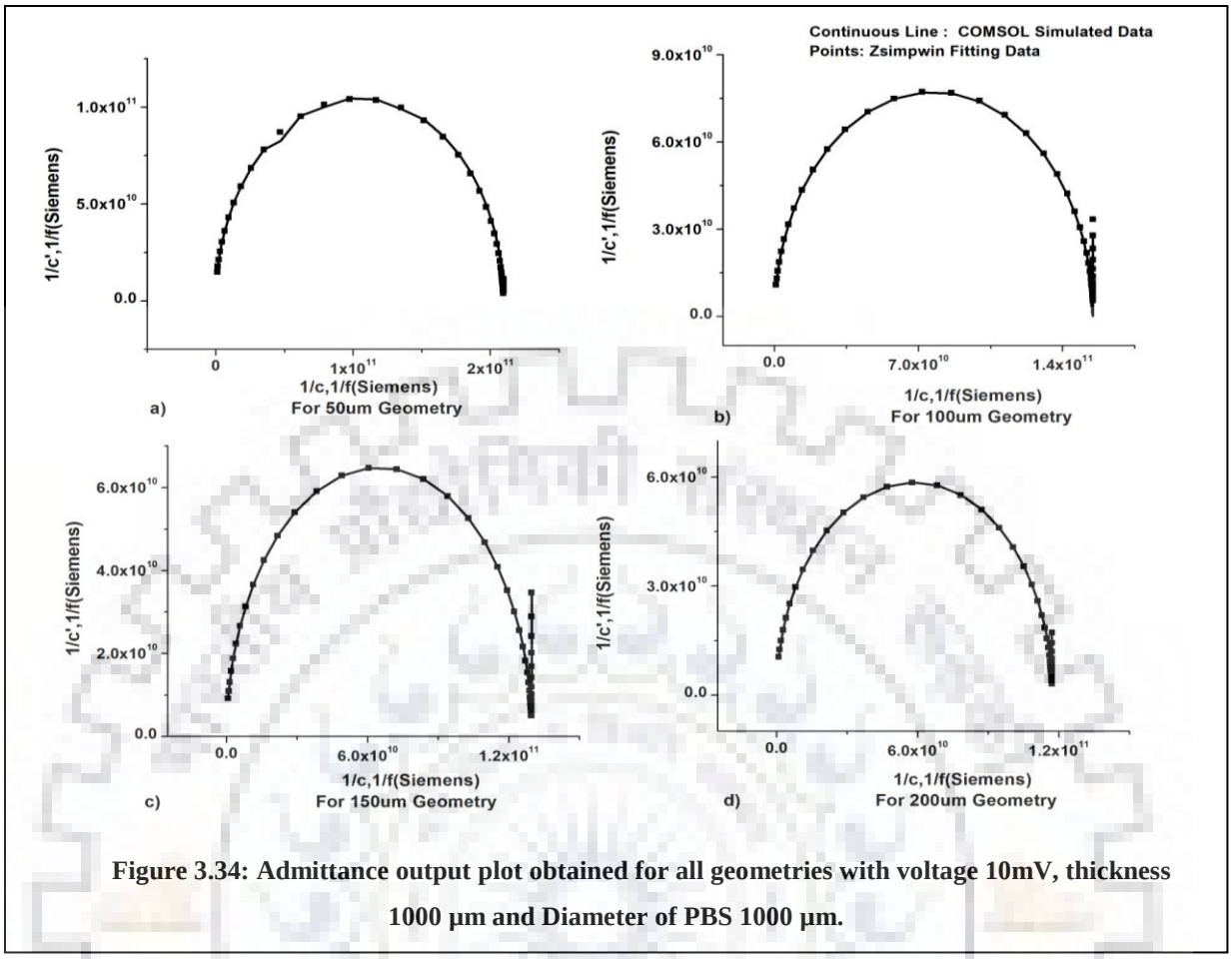

Figure 3.34: Admittance output plot obtained for all geometries with voltage 10mV, thickness 1000 µm and Diameter of PBS 1000 µm.

- The admittance also can also be extracted from the obtained values which are showing the inverse of the impedance plots. In the higher frequencies the imaginary components are more. Hence the effects of solution resistance and charge transfer resistance on admittance are more in higher frequency region.

- In summary, the value of voltage of 10mV, thickness of 1000um and diameter of 1000um showed the closest overlap with the equivalent circuit. Which can be kept in consideration while the fabrication of the device for best output.

d) Obtained Value of Electrical Components and Error Percentage

From the conducted output plots the following parameters and the error percentage were extracted for different thickness of electrodes, applied voltages and diameter of PBS and from there the final optimized design parameters were extracted for different geometries. The feasibility of the design depends largely on the value of the chi square which should be within the range of 1×10^{-3}. The final parameters were finalized keeping that in consideration. The values of $R_{s,}$ R_c and CPE were also obtained from the plots. For each data individual error percentage were also tabulated.

Parameters Obtained For Different Thickness of Electrodes

Electric Components	Design 1(Thickness 500um)		Design 2(Thickness 1000um)		Design 3(Thickness 1500 um)		Design 4(Thickness 2000um)	
	Data	Error %	Data	Error %	Data	Error %	Data	Error%
$R_s(\Omega)$	1.018×10^{4}	201.9	5279	4.577	2113	322.1	3459	150.3
CPE($S.Sec^{n}$)	3.237×10^{-12}	62.4	6.463×10^{-12}	1.465	9.723×10^{-12}	62.3	1.294×10^{-11}	62.52
$R_c(\Omega)$	3.501×10^{7}	18.64	1.739×10^{7}	0.436	1.167×10^{7}	18.64	8.76×10^{6}	18.65
Freq power,n [0<n<1]	1	4.969	1	0.1166	1	4.958	1	4.982
χ^2(Value)	4.89×10^{-01}		2.68×10^{-04}		4.89×10^{-01}		4.89×10^{-01}	

Table 3.2: Parameters Obtained For Different Thickness of Electrodes.

Parameters Obtained Designs with Different Voltages

Electric Components	Design 1(5mV)		Design 2(10mV)		Design 3(15mV)		Design 4(20mV)	
	Data	Error%	Data	Error%	Data	Error%	Data	Error%
$R_s(\Omega)$	4345	4.577	5279	4.577	6962	177.4	4216	293.9
CPE($S.Sec^n$)	6.47×10^{-12}	62.37	$6.463E^{-12}$	1.465	$6.47E^{-12}$	63.43	$6.495E^{-12}$	63.33
$R_c(\Omega)$	1.747×10^{7}	18.63	1.739×10^{7}	0.436	1.752×10^{7}	18.46	1.75×10^{7}	18.44
Freq power,n [0<n<1]	1	4.965	1	0.1166	1	5.094	1	5.081
χ^2(Value)	4.89×10^{-01}		2.68×10^{-04}		4.78×10^{-01}		1.52×10^{-06}	

Table 3.3: Parameters Obtained for Different Voltages.

Parameters Obtained for Designs with Different Diameters

Electric Components	Design 1(Diameter 2000um)		Design 2(Diameter 4000um)		Design 3(Diameter 6000um)		Design 4(Diameter 8000um)	
	Data	Error%	Data	Error%	Data	Error %	Data	Error %
$R_s(\Omega)$	5279	4.577	5497	222.7	3608	282.2	3114	328.3
CPE($S.Sec^n$)	6.463×10^{-12}	1.465	6.477×10^{-12}	63.38	6.488×10^{-12}	62.33	6.505×10^{-12}	62.32
$R_c(\Omega)$	1.739E 7	0.436	1.744×10^{7}	18.45	1.743E 7	18.63	1.743×10^{7}	18.63
Freq power,n [0<n<1]	1	0.1166	1	5.087	1	4.961	1	4.959
χ^2(Value)	2.68×10^{-04}		4.78×10^{-01}		4.89×10^{-01}		1.52×10^{-06}	

Table 3.4: Parameters Obtained for Different Diameters.

Final Design Parameters for Optimized of ECIS Device

Electric Components	Design 1(50um)		Design 2(100um)		Design 3(150um)		Design 4(200um)	
	Data	Error%	Data	Error %	Data	Error%	Data	Error%
$R_s(\Omega)$	4257	4.577	4195	4.092	5487	1.504	2751	0.4938
CPE($S.Sec^n$)	6.463×10^{-12}	1.465	6.474×10^{-12}	1.045	7.74×10^{-12}	0.5934	8.554×10^{-12}	0.1045
$R_c(\Omega)$	1.739×10^{7}	0.436	1.749×10^{7}	0.3124	1.464×10^{7}	0.1769	1.675×10^{7}	0.03432
Freq power,n [0<n<1]	1	0.1166	1	0.8322	0.9998	0.04729	0.9999	0.008388
χ^2(Value)	2.68×10^{-04}		1.37×10^{-04}		4.40×10^{-05}		1.52×10^{-06}	

Table 3.5: Parameters for Optimized Designs.

Discussions:

- From the tables above, the final design parameters, that is the obtained impedance data of experimental and fitted values exhibit a good agreement. The values of $\chi 2$, which measures the error for the fitting values, of the equivalent model are extracted by the ZsimpWin software. The obtained values of $\chi 2$ for different designs, the values reside in the range from 1.5×10^{-3} to 2.30×10^{-5} which is the acceptable range.
- The values of the solution resistance, charge transfer resistance and the double layer capacitance are obtained from these tabulated values. With the increase of the area of the electrodes, the solution resistance and charge transfer resistance values exhibit a decrease as studied.
- With the increase of electrode area the value of CPE also increases. This is because capacitance and area of electrodes are directly proportional.
- At higher frequency the solution resistance basically dominates whereas the value of the charge transfer resistance was very low compared to that.
- The error percentage is acceptable up to 5 percent as the previous studies. So the error obtained here can be considered to be in an acceptable range.

3.5 MASK DESIGN FOR FABRICATION OF DEVICE

For the fabrication of the device the masks which have been used for the project were designed with the help of Clewin 4 software where a 5 inch wafer has been taken for drawing the mask. In the mask the sensors has been drawn along with the connecting wires. The connecting wires make the connection of the electrodes with contact pads and from there the connections are made with an electrochemical work station.

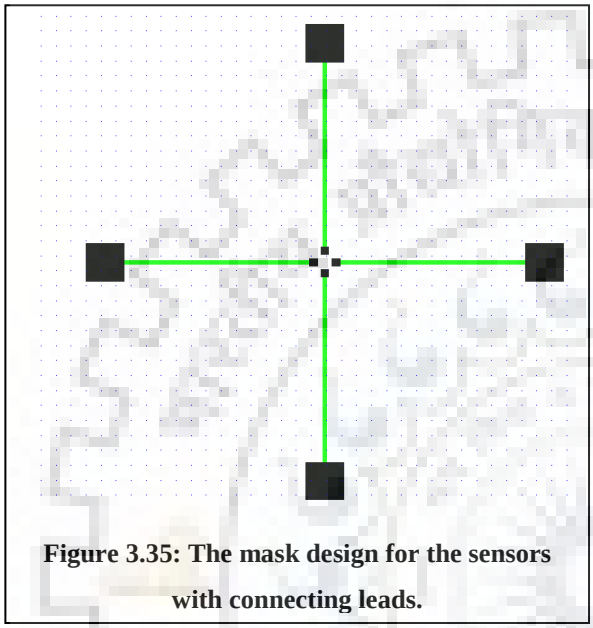

Figure 3.35: The mask design for the sensors with connecting leads.

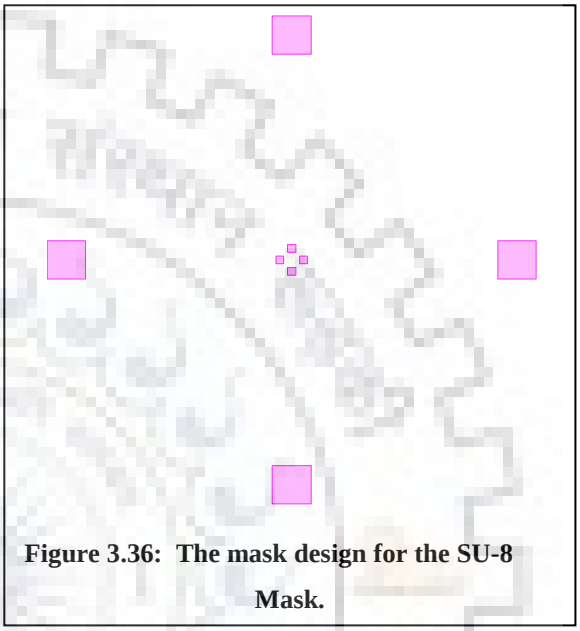

Figure 3.36: The mask design for the SU-8 Mask.

For the fabrication the mask layouts which were drawn in the Clewin software consisted of two layers. One for using the positive photoresist and the other for the negative photoresist during the fabrication, as per the simulated designs and outputs. The centre part consists of the electrodes and the green lines were the connecting lines and the outward bigger squares are the layouts for the contact pads. The layout were made for 50 um, 100um,150 um and 200 um geometries and then were printed in transparent plastic sheets with high resolution printer with 2400 × 2400 dpi resolution.

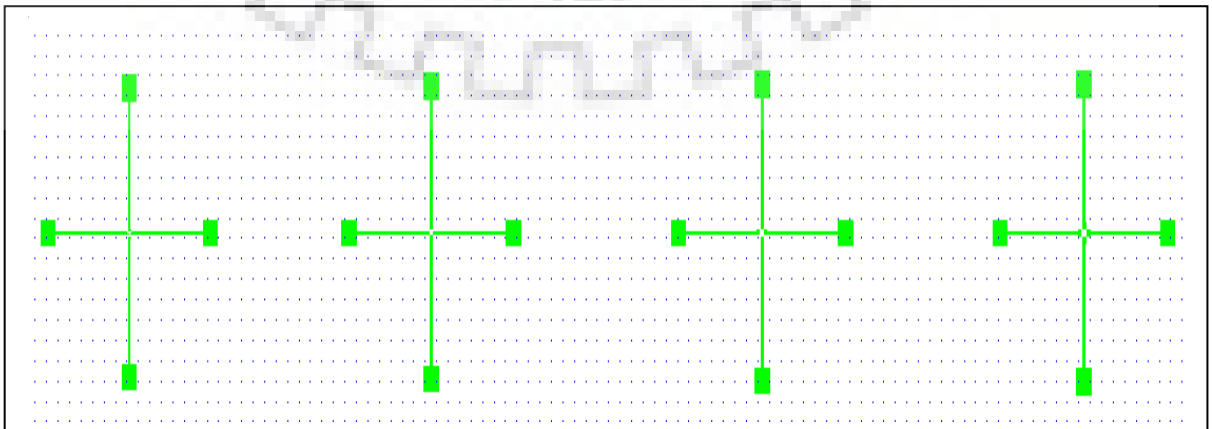

Figure 3.37: The mask design for the sensors with connecting leads for positive photoresist application.

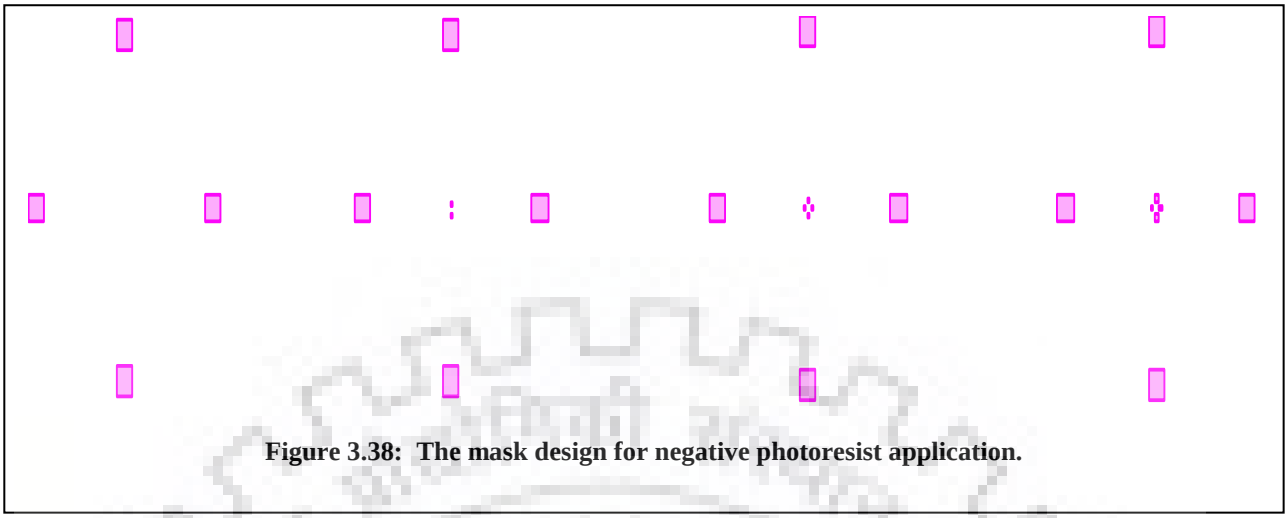

Figure 3.38: The mask design for negative photoresist application.

Two layers have been used here one for the electrode to connecting leads for the positive photoresist and another (pink one) for the negative photo resist. The length of connecting lead wire is 5mm. width 100um.

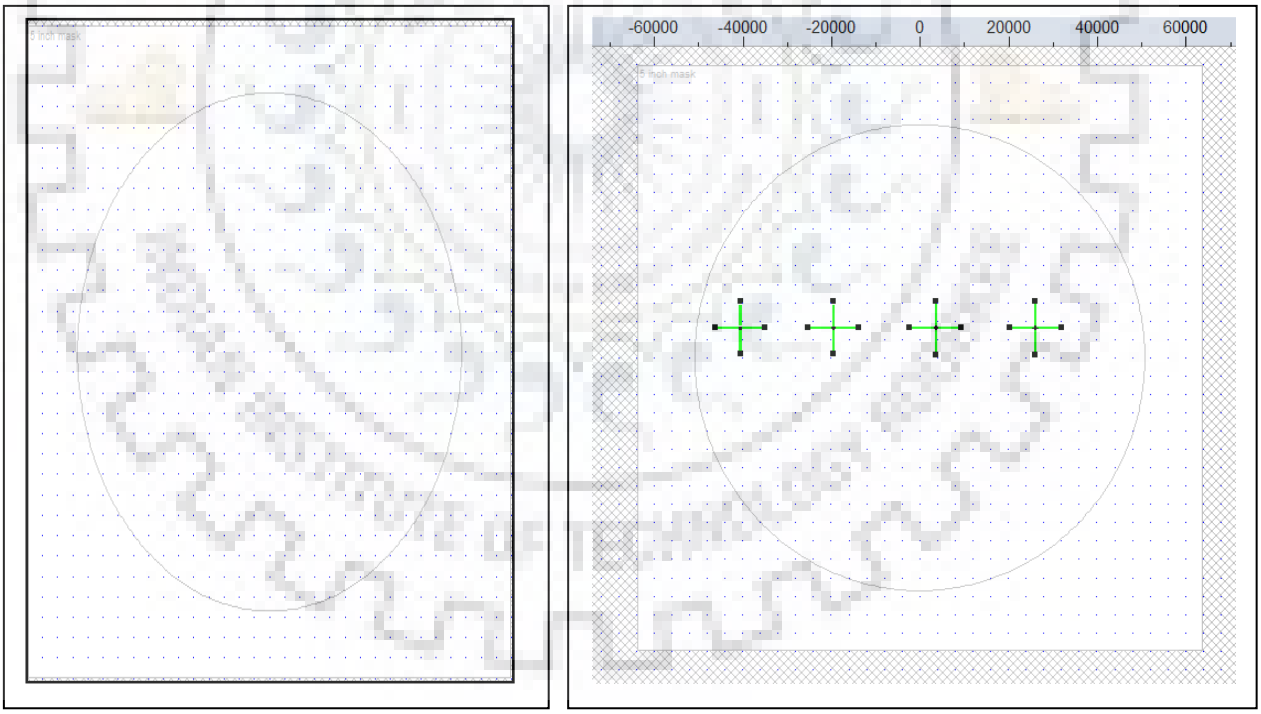

Figure 3.39: 5 inch diameter wafer drawn (left) and layout of masks for the four electrode ECIS on the wafer for different designs in CleWin 4 software (right).

The following steps were finally implemented to design and fabricate the four electrode ECIS device.

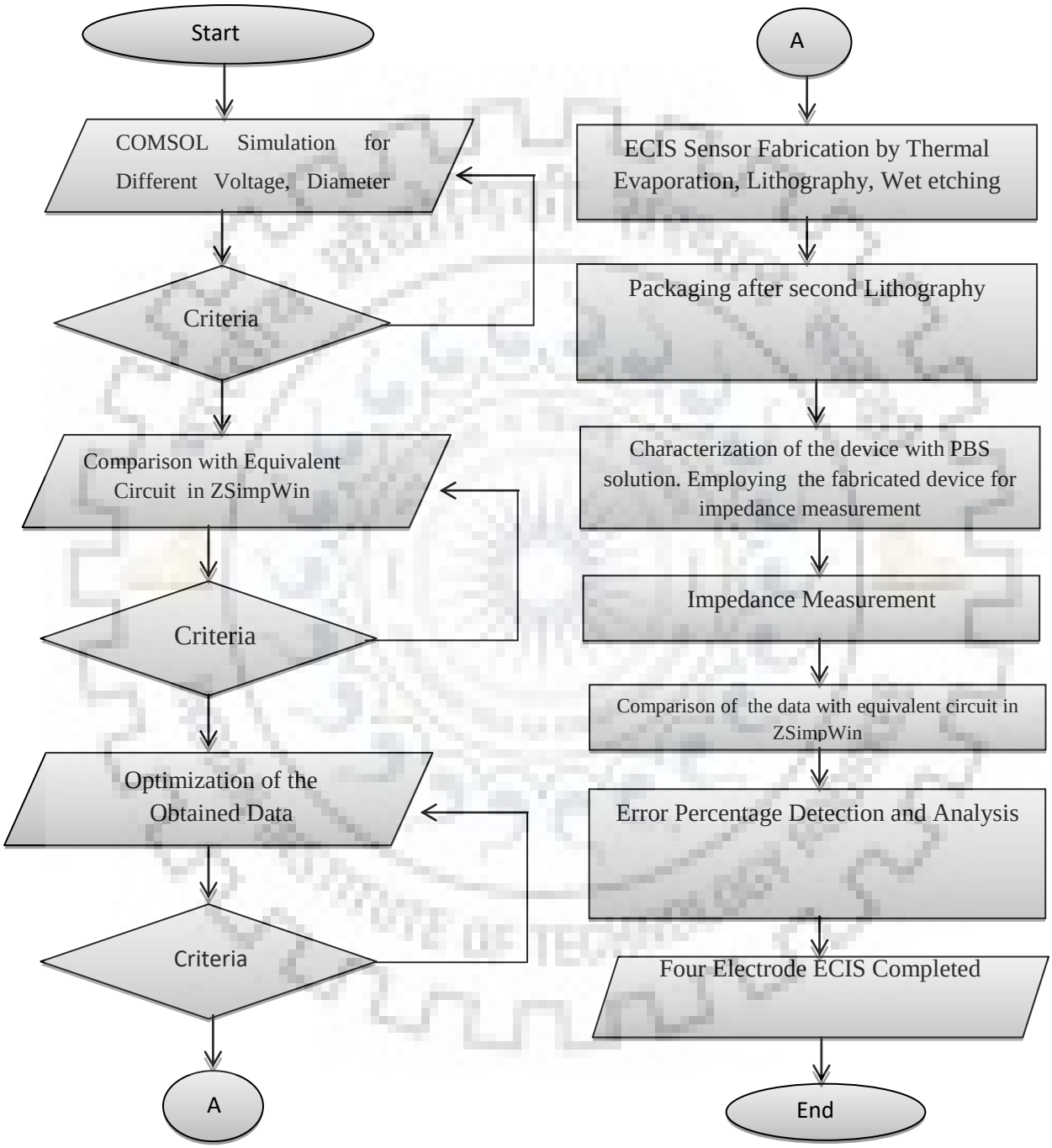

Figure 3.40: Flow chart of Design and Implementation of a Four Electrode ECIS.

CHAPTER-4
FABRICATION AND CHARACTERIZATION OF DEVICE

4.1 FABRICATION OF DEVICE

The four-electrode ECIS device was fabricated adopting the processes of thermal evaporation, lithography, wet etching and finally packaging after second lithography. Then it was taken for characterization. The electrodes and the connecting leads are fabricated and then patterned with a gold metal film deposited on a glass substrate with a layer of titanium as the adhesive. As [4] stated in their work that , by keeping the metallic active electrode area separated from the electrolytic solution which contains the ions, the formation of the double layer capacitance is possible to prevent. Therefore to prevent this contamination a coating of polymer or passivation layer (SU8) has been applied on the connecting leads of the device and the active electrode region are kept separated for current flowing.[4] The fabrication process was completed by the following steps:

1. Chemical Materials Collection

For its inertness with biological samples, gold was selected as the material for the electrodes, interconnecting lines and the contact pads for the fabrication. Glass was selected as the substrate material on which the gold was deposited. As the adhesive for depositing gold Titanium was deposited beforehand on the glass substrate.To select the gold major considering factors is the purity. Approximately Gold of 10gm and of 24 carat was required.

2. Mask Making

In the device fabrication two masks of the device layout was made for the positive and the negative photoresist. The layouts were further patterned on the glass substrate with thin film of gold. Two masking steps were adopted. In the first step the metallic electrode and the interconnecting lines were patterned as Mask 1.In the second step the regions for the

passivation coating of SU8 was marked on the metallic line region. The mask was made in a transparent plastic sheet with a high resolution printer of 2400 × 2400 dpi. The layouts were made beforehand with the Clewin software, where one was made for the positive photoresist and the other for the negative photoresist. Later on they were printed by the high resolution printer. For the positive photoresist the part below the layout was kept unchanged and the rest part was made soluble and later on was etched. For the negative photoresist the part below the layout was hardened and the rest part was made soluble and was etched off.

3. Cleaning of materials used

1 mm glass slides were taken as the insulating substrate for the deposition of gold. At the beginning, cleaning of the glass slides were accomplished with Piranha solution, removing the organic components from the glass slides. The Piranha solution is a strong oxidizing agent which consists of solutions of 98% concentrated H_2So_4 and 30% concentrated H_2O_2 in 3:1 ratio and then was dried with Nitrogen gas. The gold plates were cleaned with acetone and then were passed through ultrasonification and ozonification for further cleaning and then were dried with nitrogen air gun. The titanium palettes were also cleaned with acetone and afterwards were dried with nitrogen air gun.

4. Thermal Evaporation

After that Titanium was at first thermally deposited on the glass slides heated at 1650° Celsius temperature by the thermal evaporator. Titanium worked as an adhesive for depositing gold on the glass. Following that gold was deposited over it with temperature of 1064° Celcius by thermal evaporation.

5. Spin Coating

A coating of positive photoresist AZ1512HS was applied on the sample substrate uniformly by spin coating at 3000 rpm for 20 seconds in the spin coater.

6. Soft Bake

The sample was soft baked being heated at 90° Celcius for 2.5 mins.

7. UV Exposure

The mask was kept over the glass slides and UV exposure was given for 20 seconds to transfer the pattern from the mask to photoresist.

8. Developing the Pattern

The pattern was developed with the developer by keeping the sample immersed for 50 sec.

9. Etching

- The photoresist was removed with acetone cleaning.
- To etch the gold Potassium Iodide, Iodine and distilled water for KI:I_2:DI water in 4gm,1gm and 40ml amount.
- To etch the Titanium from the glass slides Hydrogen Fluoride acid, Hydrogen peroxide and DI water solution was used in HF:H_2O_2:DI water in 1:1:20 ratio for 20 sec.
- After etching the glass slides were dried with nitrogen gas.

10. Second Lithography

To apply the negative photoresist SU8, which is a photosensitive and biocompatible polymer another lithography step was accomplished. This SU8 layer acts as the passivation layer over the metal electrodes. This negative photoresist which makes the part below it hardened on UV exposure while the rest part is made soluble hence compatible for etching. To accomplish the process, only the electrode sensors and contact pads were exposed. This was done so that they can make contact with electrolyte surface. Hard baking was done for photoresist to make the polymer more stable and inert. The thickness of SU8 has been kept 50 µm and was applied over the metal electrodes to prevent any contamination.

11. Packaging

Finally for culturing the cells a cylinder shaped Pyrex well of 78.5 mm^2 area of boundary was placed surrounding the active electrodes. The Pyrex cloning cylinders got aligned and attached for serving as the reservoir of the 1mL PBS electrolyte solution surrounding the active area of four electrodes. As the glue PDMS was used. The device was further provided with electrical connections using thin metal wires which connected the device with the impedance measurement instrument. Subsequent packaging for further measurements were done for the devices.

The following devices were finally fabricated for the four geometries as per the studies and the simulations conducted.

Figure 4.1: Fabricated devices after attaching with cloning cylinder and the close view of the electrodes of 200 µm in electron microscope.

The process flow adopted for the fabrication of the four electrode device is appended in the following flow chart:

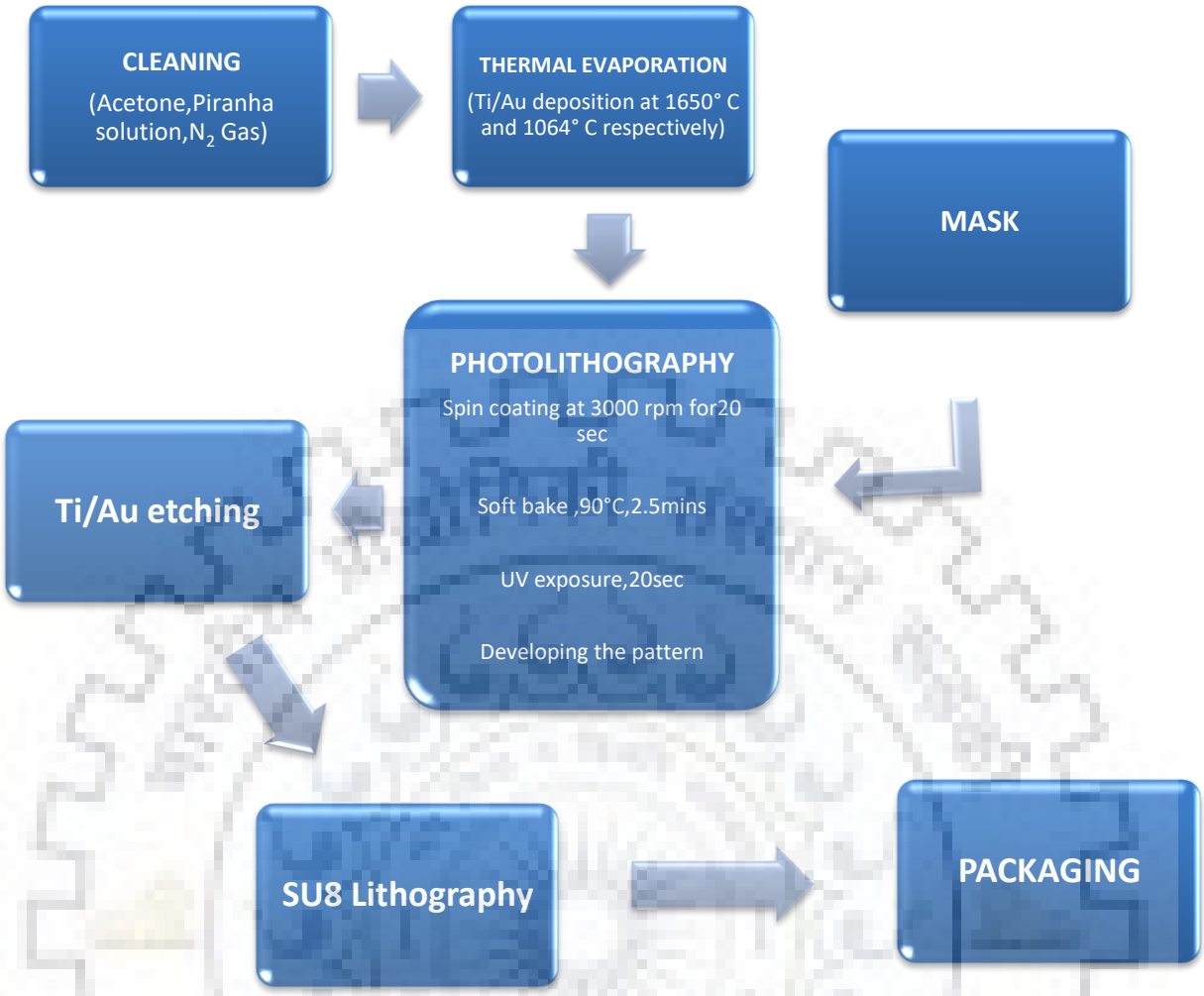

Figure 4.2: Process Flow for the fabrication of ECIS Device.

4.2 IMPEDANCE MEASUREMENT AND DEVICE CHARACTERIZATION WITH PBS

The characterization of the device was using the electrolytic test solution of Phosphate Buffer Saline (PBS) which is a biocompatible chemical substance. Living cells can survive in the PBS solution for 5-6 hrs. So a 1ml solution of PBS was chosen as the electrolyte and hence for the characterization of the device. As per [4] the electrical impedance of PBS of the fabricated device was measured by the electrochemical work station Zahner Zennium (Germany). Small voltages of 10mV (peak-to-peak) respectively and the range of input frequency applied on the device was 100 Hz to 1 MHz having 51 sample points. The impedance analyzer can give the measured value of two parameters those are the real part of the impedance and the phase of the impedance. The instrument is capable of reducing the

noise margin of the data. The data obtained was further compared in the ZsimpWin software extracting its equivalent circuit mode, followed by the curve fitting of the obtained data. The Nyquist data was obtained from the devices of four designs and subsequently the experimental data was exported to, for further analysis using equivalent circuit simulations in ZsimpWin software.

4.3 FINAL IMPEDANCE AND MEASUREMENT OF OTHER PARAMETERS OF OPTIMIZED ECIS DEVICE

For the four geometries finally the following bode plots for the four impedance curves were obtained where the COMSOL simulated data and the experimental data were plotted together and they were matched properly with slight deviations. In this curves both the magnitude of impedance, |Z| and frequency were plotted in logarithmic scale for 51 sample points. Input frequency range was 100Hz to 1MHz. So the plot displays the information and the relation between both the frequency and the impedance unlike Nyquist plot.

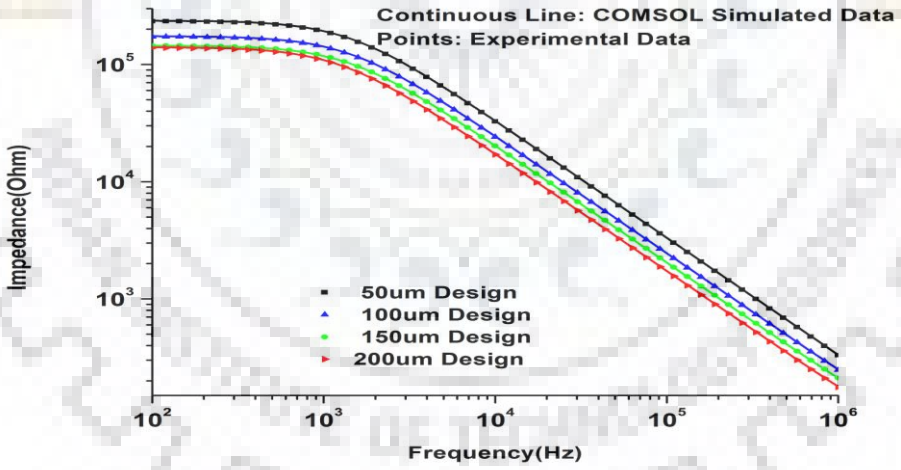

Figure.4.3: Bode plot for impedance of the optimized designs for the 10mV applied voltage.

Figure 4.3 represents the bode plot of both experimental and simulated impedance values of four electrode ECIS for various designs. Observing the output plots it can be found that, magnitude of impedance decreases with the increasing input frequency. Also the

electrode/electrolyte system exhibits linearity in impedance as a function of electrode area for all the designs after 10^3 Hz frequency.

The region of interest between for impedances in the above bode plot is the range of frequencies between 10^3 to 10^7 Hz. For the higher frequency range the impedance is low as only the solution resistance is acting here. Whereas for the lower frequency both the solution resistance and the charge transfer resistance are acting and resulting higher impedance there.

4.4 COMPARISON OF THE DATA WITH EQUIVALENT CIRCUIT IN ZSIMPWIN

4.4.1 COMPARISON OF COMSOL DATA WITH PRACTICAL DATA

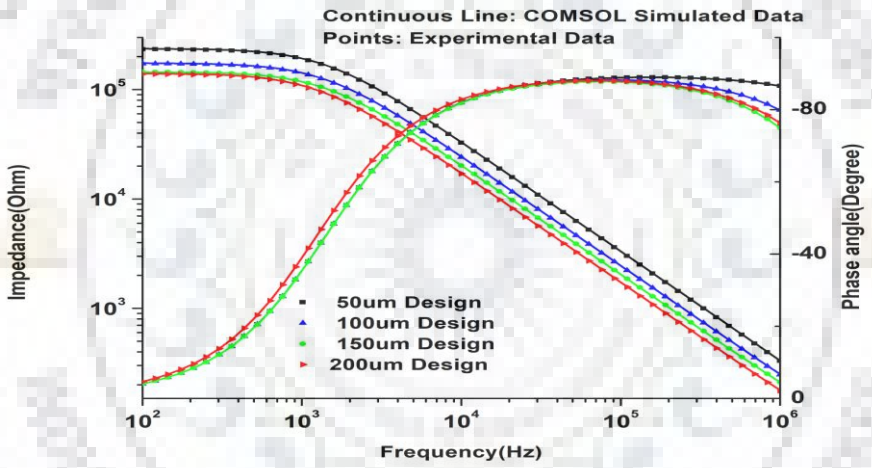

Figure.4.4: Bode plot for the simulations and experiment results for PBS.

In Figure 4.4 the bode plot for the impedance and phase shifts are obtained from the simulations of the designs and the data got from the experiments , after the characterization of the device with PBS sample. The two curves are almost overlapped with each other. From the impedance curve the drastic decrease of magnitude is observed after the exchange of ions at the interface of electrode/electrolyte. For lower range of frequencies the effect of the solution and the charge transfer resistance are visible. The intermediate frequency range with the negative slope of -1 depicts the impedance due to the double later capacitance and finally the higher frequency range shows the effect of the solution resistance. The polarization effects of both the electrolyte and electrode give the total impedance of the ECIS device. We can see with the increase of the frequency the impedance decreases that means the current through

the fabricated ECIS device can flow smoothly for the higher frequencies. The phase angle decreases from zero to negative value showing the capacitive effect of the device. Since impedance is inversely proportional to area, device having electrodes with smallest area shows higher impedance and the electrode with higher area shows lesser impedance allowing more charge to flow through it. Thus here the 200um geometry electrode has the lower polarization impedance and lower electrolytic resistance. A small deviation has been found with the experimental and simulated data. To calculate the error percentage for the impedance and phase values of the COMSOL software simulated data and experimental data following formula was used as per **[4]** which gives the relative standard error (RSE %) percentage of the two compared data sets.

$$RSE = (\text{COMSOL simulated data} - \text{Experimental data}) \times 100 \times (\text{Experimental data})\text{-}1$$

Table 1 comprises all the RSE of different electrical parameters of the electrical components of the equivalent circuit model of both the data sets.

4.5 ANALYSIS OF RESULTS

After fabricating the device data was collected considering different cases. All the data was analyzed focusing on impedance, resistance, capacitance and error percentage analysis.

4.5.1 EQUIVALENT CIRCUIT FITTING RESULTS

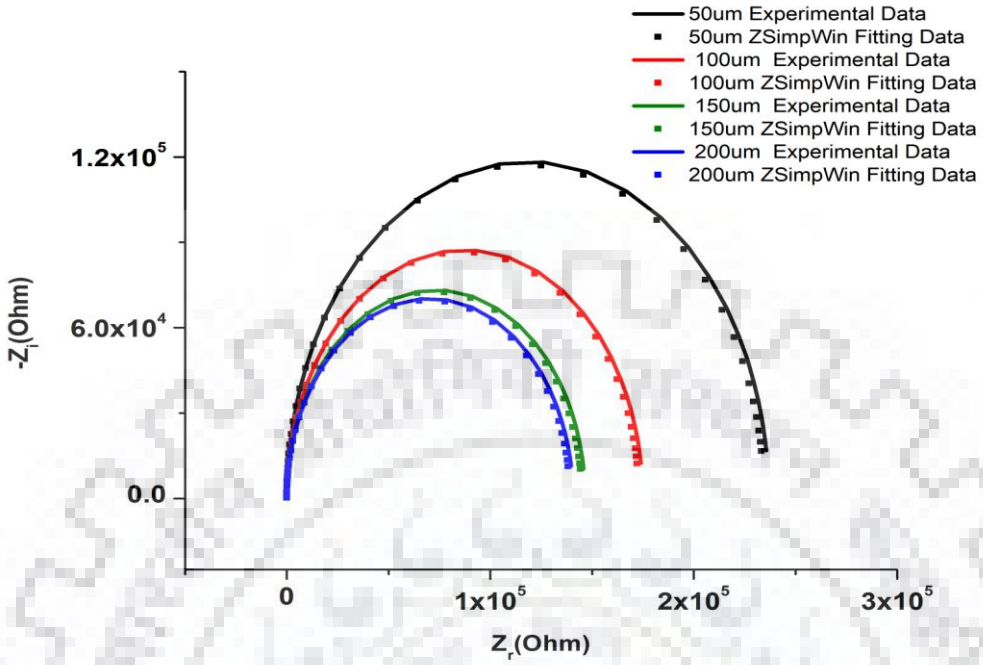

Figure.4.5. Nyquist plots obtained from the equivalent circuit fitted data of the ZsimpWin Data simulations and experimentally obtained values.

Figure 4.5 exhibits output Nyquist plots from the data obtained by COMSOL simulations and experimentation curve fitted by the ZsimpWin equivalent circuit models which consist of constant phase element (CPE, Q) as the double layer capacitance which is parallel to the charge transfer resistance (R_c) and together having a series connection with the resistance (R_s) which denotes the solution resistance. The circuit is the interpretation of the theoretical model of the electrode/electrolyte circuit proposed by [51].

Figure 4.6 exhibits the impedance and phase bode plots for the final experimental value after the characterization of the device. Both the curves matched with the ZSimpWin fitting data which means the device can be used for the further research using a living cell on the device. The impedance after 10^3 Hz took a negative slope which represents the characteristics of the CPE effect. Also the lower frequency region shows the effect of the solution and charge transfer resistance characteristics and finally the higher region of frequency shows the effect of the solution resistance which mainly dominates after the current passes the electrode/electrolyte interface and enters the solution of electrolyte. Hence in the higher

frequency region the impedance is lower which means that the device will have a better result for the higher frequency input which working with a living cell.

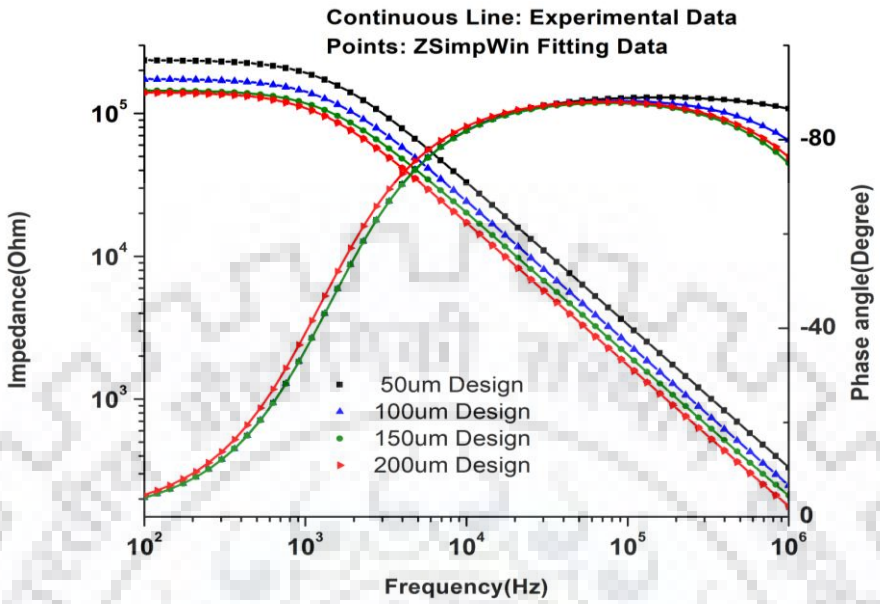

Figure 4.6: Bode plots obtained from the equivalent circuit fitted data of the ZSimpWin simulations and experimentally obtained values.

The phase shift also shows the capacitive effect of the CPE and it is also giving the value from -90 degree which goes with the previous literature studies.

In Table 4.1 the data and error percentage of the electrical components have been given and it is observed that the simulated and the experimental data has got aligned with slight deviation and the $\chi 2$ value is below 1.5×10^{-3} for the accomplished designs which is in the satisfactory range. It is also visible that the CPE values exhibit an increase along with increasing electrode area as capacitance is directly proportional to the electrode area. Also the error percentage is acceptable upto 5 percent as the previous studies. So the error obtained here can be considered in a satisfactory range.

From the table, increase of the electrode area results a decrease in R_s and R_c can be comprehended.

Electric Components	Design 1(50um)		Design 2(100um)		Design 3(150um)		Design 4(200um)	
	Data	RSE%	Data	RSE %	Data	RSE%	Data	RSE %
$R_s(\Omega)$	19.36	2.291	43.23	2.796	54.38	2.486	41.73	1.043
CPE(S.Sec^n)	4.825×10^{-10}	2.025	6.539×10^{-10}	1.008	7.8×10^{-10}	2.09819	9.27×10^{-10}	1.674
$R_c(\Omega)$	2.344×10^{5}	1.611	1.73×10^{5}	3.012	1.45×10^{5}	2.926	1.391×10^{5}	1.01154
N	1	0.0006056	1	0.0008027	1	0.07823	1	0.02939
χ^2	5.21×10^{-10}		1.27×10^{-08}		1.20×10^{-08}		1.77×10^{-09}	

Table 4.1: Values of Different Electric Components of the Final Circuit Obtained and RSE.

The relative standard error shows the least percentage for the 200um geometry and highest for the 50um geometry. The same is also showed in the Nyquist plot where the impedance for the smallest design of 50um is the highest whereas the impedance for the largest design is the lowest. But larger surface area also creates more contamination problems, also for the low resistive bio-samples it might not give the exact result which thus paves the way to emphasize on the optimization of the device so that these problems can be overcome.

4.5.2 DERIVED RELATION BETWEEN AREA OF ELECTRODES, IMPEDANCE AND PHASE FOR THE DESIGNED DEVICE

The relation of electrode area with the impedance and phase of the optimized ECIS device can be shown by a mathematical expression by plotting the magnitude of the impedance, also the phase angle of the device against the variables, frequency and the area of the electrodes. To obtain this LAB Fit curve fitting software was adopted. This software using the Levenberg Marquardt algorithm between the independent and dependant variables finds the best fitted equation for the given data. For this study the following 3D plots have been obtained for impedance and phase angle, to depict their relation with the area of electrodes for the fabricated device. For the plotting a frequency range from 100Hz to 1MHz was taken and the area of the electrodes were considered for the 50 µm, 100µm, 150µm and 200µm etc. The mathematical relation for magnitude of impedance represented by Z, the electrode area denoted by A_W and frequency f , for the obtained plot can be given as

$$\mathbf{Z=A_1\times(B_1^{f})\times A_W^{C1} + D1} \qquad \mathbf{(24)}$$

Where the values of the constants are, $A_1= 0.1292\times10^{7}$, $B_1= 0.9997$, $C_1= -0.2128$, $D_1= 0.4555\times10^{4}$ respectively. For the phase angle (θ) and the electrode area (A_w) are equation is obtained as follows for the output plot

$$\mathbf{\theta=(M_2+A_w)/(N_2+O_2\times f)+P_2\times f} \qquad \mathbf{(25)}$$

The values of the constants are $M_2=-0.1246\times10^{7}$, $N_2=0.1268\times10^{5}$, $O_2=0.1119\times10^{2}$, $P_2=-0.1031\times10^{-4}$.A sharp rise for the phase in the low frequency is observed from the plot in the following page.

a)

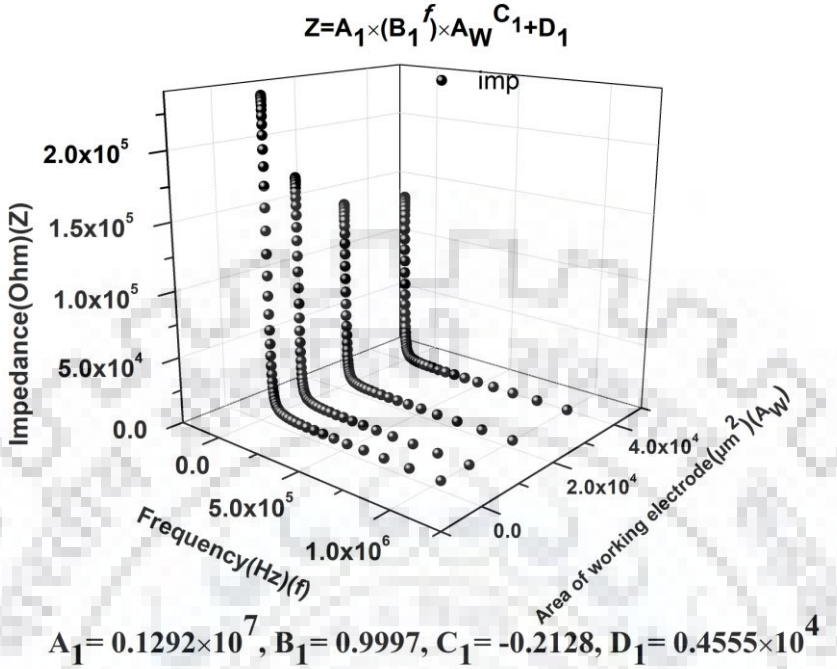

$A_1 = 0.1292\times10^{7}$, $B_1 = 0.9997$, $C_1 = -0.2128$, $D_1 = 0.4555\times10^{4}$

b)

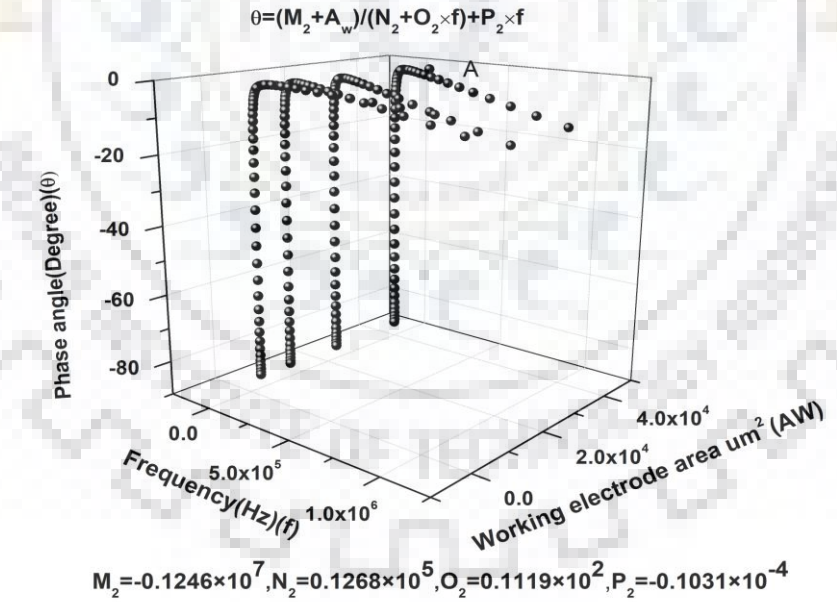

$M_2 = -0.1246\times10^{7}$, $N_2 = 0.1268\times10^{5}$, $O_2 = 0.1119\times10^{2}$, $P_2 = -0.1031\times10^{-4}$

Figure 4.7: 3D plot showing the dependence of (a) Impedance (b) Phase angle of the device with the working electrode area and derived mathematical equations with value of constants.

CHAPTER-5

CONCLUSION AND FUTURE SCOPE OF WORK

An optimized four electrode ECIS device has been designed, fabricated and characterized including obtaining an empirical relation of the impedance and the phase angle of the device with the area of electrodes. The design has been verified by conducting simulations for various voltages applied on the electrodes, diameters of PBS electrolyte surface and thickness of the electrodes and analyzing the error percentages comparing with the equivalent circuit models. The values of electrical components for the electrical circuit of the designed device were also extracted. The optimized design depicted a satisfactory result for the impedance and phase angle of the sensors with the equivalent circuit models.

The impact of electrode area on the impedance, phase shift and capacitance of the device was also studied in details. A frequency range of 100Hz to 1MHz was applied on the device for conducting the simulations. The magnitude of impedance of the device exhibited a decrease with an increase of the input frequency. It was observed that for the lower frequency range the effect of the solution resistance and the charge transfer resistance was more. For higher frequency range the effect of mostly the solution resistance was prominent. Whereas for the intermediate frequency the double layer capacitance mainly dominated for the impedance and phase shift of the device. Therefore for the operation of the device with a living cell the frequency range should be kept in consideration. The device was also fabricated with inert material gold for the electrodes and connecting pads on a glass substrate. Titanium was used as the adhesive during the deposition. The fabricated device was further characterized with the PBS solution as the electrolyte for the system and showed a good agreement with the simulated design output up to an extent. The obtained values after the device characterization were again analyzed and an empirical relation with the obtained design parameters for the impedance, phase shift and the area of the electrodes was established.

The device can be further employed with actual living cells to find the impedance of the living cells and hence study their behavior and characteristics on the application of different electrical inputs. The device can also be improved by considering the device for more complex circuits and making the whole system along with the connection with electrical inputs more biocompatible for the living cells. By using this optimized design a complete electromechanical device can be developed for the complete analysis of the bioimpedance of the living cells.

REFERENCES

[1] Q. Liu and P. Wang, *Cell-based biosensors: principles and applications*: Artech House, 2009.

[2] P. Wang, C. Wu, N. Hu, and K. J. Hsia, *Micro/Nano Cell and Molecular Sensors*: Springer, 2016.

[3] A. Touhami, "Biosensors and nanobiosensors: design and applications," *Nanomedicine*, vol. 15, pp. 374-403, 2014.

[4] R. Pradhan, A. Mitra, and S. Das, "Characterization of electrode/electrolyte interface of ECIS devices," *Electroanalysis*, vol. 24, pp. 2405-2414, 2012.

[5] Y. Xu, X. Xie, Y. Duan, L. Wang, Z. Cheng, and J. Cheng, "A review of impedance measurements of whole cells," *Biosensors and Bioelectronics*, vol. 77, pp. 824-836, 2016.

[6] J. Hong, K. Kandasamy, M. Marimuthu, C. S. Choi, and S. Kim, "Electrical cell-substrate impedance sensing as a non-invasive tool for cancer cell study," *Analyst*, vol. 136, pp. 237-245, 2011.

[7] Q. Liu, C. Wu, H. Cai, N. Hu, J. Zhou, and P. Wang, "Cell-based biosensors and their application in biomedicine," *Chemical reviews*, vol. 114, pp. 6423-6461, 2014.

[8] D. Das, F. A. Kamil, S. Agrawal, K. Biswas, and S. Das, "Fragmental frequency analysis method to estimate electrical cell parameters from bioimpedance study," *IEEE Transactions on Instrumentation and Measurement*, vol. 63, pp. 1991-2000, 2014.

[9] L. Robilliard, D. Kho, R. Johnson, A. Anchan, S. O'Carroll, and E. Graham, "The Importance of Multifrequency Impedance Sensing of Endothelial Barrier Formation Using ECIS Technology for the Generation of a Strong and Durable Paracellular Barrier," *Biosensors*, vol. 8, p. 64, 2018.

[10] G. Harsanyi, *Sensors in biomedical applications: fundamentals, technology and applications*: CRC press, 2000.

[11] B. Ghane-Motlagh and M. Sawan, "A review of microelectrode array technologies: design and implementation challenges," in *Advances in Biomedical Engineering (ICABME), 2013 2nd International Conference on*, 2013, pp. 38-41.

[12] M. Kaisti, "Detection principles of biological and chemical FET sensors," *Biosensors and Bioelectronics*, vol. 98, pp. 437-448, 2017.

[13] T. Yoshinobu, K.-i. Miyamoto, T. Wagner, and M. J. Schöning, "Recent developments of chemical imaging sensor systems based on the principle of the light-addressable potentiometric sensor," *Sensors and Actuators B: Chemical*, vol. 207, pp. 926-932, 2015.

[14] A. Alassi, M. Benammar, and D. Brett, "Quartz crystal microbalance electronic interfacing systems: A review," *Sensors*, vol. 17, p. 2799, 2017.

[15] R. Szulcek, H. J. Bogaard, and G. P. van Nieuw Amerongen, "Electric cell-substrate impedance sensing for the quantification of endothelial proliferation, barrier function, and motility," *Journal of visualized experiments: JoVE*, 2014.

[16] S. L. Swisher, M. C. Lin, A. Liao, E. J. Leeflang, Y. Khan, F. J. Pavinatto, *et al.*, "Impedance sensing device enables early detection of pressure ulcers in vivo," *Nature communications*, vol. 6, p. ncomms7575, 2015.

[17] W. G. Jiang, *Electric cell-substrate impedance sensing and cancer metastasis* vol. 17: Springer Science & Business Media, 2012.

[18] J. I. Alvarez, A. Dodelet-Devillers, H. Kebir, I. Ifergan, P. J. Fabre, S. Terouz, *et al.*, "The Hedgehog pathway promotes blood-brain barrier integrity and CNS immune quiescence," *Science*, vol. 334, pp. 1727-1731, 2011.

[19] G. E. Slaughter and R. S. Hobson, "Artificial Neural Network for Temporal Impedance Recognition of Neurotoxins," in *IJCNN*, 2006, pp. 2001-2008.

[20] S. F. Lempka, S. Miocinovic, M. D. Johnson, J. L. Vitek, and C. C. McIntyre, "In vivo impedance spectroscopy of deep brain stimulation electrodes," *Journal of neural engineering*, vol. 6, p. 046001, 2009.

[21] L. Yang and R. Bashir, "Electrical/electrochemical impedance for rapid detection of foodborne pathogenic bacteria," *Biotechnology advances*, vol. 26, pp. 135-150, 2008.

[22] L. Huang, L. Xie, J. M. Boyd, and X.-F. Li, "Cell-electronic sensing of particle-induced cellular responses," *Analyst*, vol. 133, pp. 643-648, 2008.

[23] A. F. M. Mansor, I. Ibrahim, A. A. Zainuddin, I. Voiculescu, and A. N. Nordin, "Modeling and development of screen-printed impedance biosensor for cytotoxicity studies of lung carcinoma cells," *Medical & biological engineering & computing*, vol. 56, pp. 173-181, 2018.

[24] O. G. Martinsen and S. Grimnes, *Bioimpedance and bioelectricity basics*: Academic press, 2011.

[25] D. Andre, M. Meiler, K. Steiner, C. Wimmer, T. Soczka-Guth, and D. Sauer, "Characterization of high-power lithium-ion batteries by electrochemical impedance spectroscopy. I. Experimental investigation," *Journal of Power Sources*, vol. 196, pp. 5334-5341, 2011.

[26] J.-L. Hong, K.-C. Lan, and L.-S. Jang, "Electrical characteristics analysis of various cancer cells using a microfluidic device based on single-cell impedance measurement," *Sensors and Actuators B: Chemical*, vol. 173, pp. 927-934, 2012.

[27] H. C. Lukaski and M. Moore, "Bioelectrical impedance assessment of wound healing," *Journal of diabetes science and technology*, vol. 6, pp. 209-212, 2012.

[28] A. R. A. Rahman, C.-M. Lo, and S. Bhansali, "A micro-electrode array biosensor for impedance spectroscopy of human umbilical vein endothelial cells," *Sensors and Actuators B: Chemical*, vol. 118, pp. 115-120, 2006.

[29] M. W. Shinwari, D. Zhitomirsky, I. A. Deen, P. R. Selvaganapathy, M. J. Deen, and D. Landheer, "Microfabricated reference electrodes and their biosensing applications," *Sensors*, vol. 10, pp. 1679-1715, 2010.

[30] R. Lind, P. Connolly, C. Wilkinson, and R. Thomson, "Finite-element analysis applied to extracellular microelectrode design," *Sensors and Actuators B: Chemical*, vol. 3, pp. 23-30, 1991.

[31] H. P. Schwan, "Electric characteristics of tissues," *Biophysik*, vol. 1, pp. 198-208, 1963.

[32] J. Martinez, A. Montalibet, E. McAdams, M. Faivre, and R. Ferrigno, "Effect of electrode material on the sensitivity of interdigitated electrodes used for Electrical Cell-Substrate Impedance Sensing technology," in *2017 39th Annual International Conference of the IEEE Engineering in Medicine and Biology Society (EMBC)*, 2017, pp. 813-816.

[33] X. Jiang and M. G. Spencer, "Electrochemical impedance biosensor with electrode pixels for precise counting of CD4+ cells: A microchip for quantitative diagnosis of HIV infection status of AIDS patients," *Biosensors and Bioelectronics*, vol. 25, pp. 1622-1628, 2010.

[34] A. Mansor, I. Ibrahim, I. Voiculescu, and A. Nordin, "Screen printed impedance biosensor for cytotoxicity studies of lung carcinoma cells," in *International Conference for Innovation in Biomedical Engineering and Life Sciences*, 2015, pp. 122-126.

[35] K. Cheung, S. Gawad, and P. Renaud, "Impedance spectroscopy flow cytometry: On-chip label-free cell differentiation," *Cytometry Part A*, vol. 65, pp. 124-132, 2005.

[36] M. Brischwein, S. Herrmann, W. Vonau, F. Berthold, H. Grothe, E. R. Motrescu, *et al.*, "Electric cell-substrate impedance sensing with screen printed electrode structures," *Lab on a Chip*, vol. 6, pp. 819-822, 2006.

[37] M. Taghinejad, H. Taghinejad, M. Abdolahad, and S. Mohajerzadeh, "A nickel–gold bilayer catalyst engineering technique for self-assembled growth of highly ordered silicon nanotubes (SiNT)," *Nano letters*, vol. 13, pp. 889-897, 2013.

[38] S. Siddiqui, Z. Dai, C. J. Stavis, H. Zeng, N. Moldovan, R. J. Hamers, *et al.*, "A quantitative study of detection mechanism of a label-free impedance biosensor using ultrananocrystalline diamond microelectrode array," *Biosensors and Bioelectronics*, vol. 35, pp. 284-290, 2012.

[39] J. Hong, D. S. Yoon, S. K. Kim, T. S. Kim, S. Kim, E. Y. Pak, *et al.*, "AC frequency characteristics of coplanar impedance sensors as design parameters," *Lab on a Chip*, vol. 5, pp. 270-279, 2005.

[40] Y. Yun, Z. Dong, V. N. Shanov, and M. J. Schulz, "Electrochemical impedance measurement of prostate cancer cells using carbon nanotube array electrodes in a microfluidic channel," *Nanotechnology*, vol. 18, p. 465505, 2007.

[41] H. E. Ayliffe, A. B. Frazier, and R. Rabbitt, "Electric impedance spectroscopy using microchannels with integrated metal electrodes," *Journal of Microelectromechanical systems*, vol. 8, pp. 50-57, 1999.

[42] G. Rondelli, P. Torricelli, M. Fini, and R. Giardino, "In vitro corrosion study by EIS of a nickel-free stainless steel for orthopaedic applications," *Biomaterials*, vol. 26, pp. 739-744, 2005.

[43] A. Han, E. Moss, and A. B. Frazier, "Whole cell electrical impedance spectroscopy for studying ion channel activity," in *The 13th International Conference on Solid-State Sensors, Actuators and Microsystems, 2005. Digest of Technical Papers. TRANSDUCERS'05.*, 2005, pp. 1704-1707.

[44] M. Thein, F. Asphahani, A. Cheng, R. Buckmaster, M. Zhang, and J. Xu, "Response characteristics of single-cell impedance sensors employed with surface-modified microelectrodes," *Biosensors and Bioelectronics*, vol. 25, pp. 1963-1969, 2010.

[45] L. Ding, D. Du, J. Wu, and H. Ju, "A disposable impedance sensor for electrochemical study and monitoring of adhesion and proliferation of K562 leukaemia cells," *Electrochemistry communications*, vol. 9, pp. 953-958, 2007.

[46] D. T. Price, A. R. A. Rahman, and S. Bhansali, "Design rule for optimization of microelectrodes used in electric cell-substrate impedance sensing (ECIS)," *Biosensors and Bioelectronics*, vol. 24, pp. 2071-2076, 2009.

[47] M.-H. Wang and L.-S. Jang, "A systematic investigation into the electrical properties of single HeLa cells via impedance measurements and COMSOL simulations," *Biosensors and bioelectronics*, vol. 24, pp. 2830-2835, 2009.

[48] X. Cui and D. C. Martin, "Electrochemical deposition and characterization of poly (3, 4-ethylenedioxythiophene) on neural microelectrode arrays," *Sensors and Actuators B: Chemical*, vol. 89, pp. 92-102, 2003.

[49] F. Lisdat and D. Schäfer, "The use of electrochemical impedance spectroscopy for biosensing," *Analytical and bioanalytical chemistry*, vol. 391, p. 1555, 2008.

[50] G. Instruments, "Basics of electrochemical impedance spectroscopy," *G. Instruments, Complex impedance in Corrosion*, pp. 1-30, 2007.

[51] W. Franks, I. Schenker, P. Schmutz, and A. Hierlemann, "Impedance characterization and modeling of electrodes for biomedical applications," *IEEE Transactions on Biomedical Engineering*, vol. 52, pp. 1295-1302, 2005.

Mtech thesis

ORIGINALITY REPORT

11%	6%	8%	%
SIMILARITY INDEX	INTERNET SOURCES	PUBLICATIONS	STUDENT PAPERS

PRIMARY SOURCES

Pradhan, Rangadhar, Analava Mitra, and Soumen Das. "Characterization of Electrode/Electrolyte Interface of ECIS Devices", Electroanalysis, 2012. Publication	1%
ethesis.nitrkl.ac.in Internet Source	<1%
www.coursehero.com Internet Source	<1%
"Micro/Nano Cell and Molecular Sensors", Springer Nature, 2016 Publication	<1%
link.springer.com Internet Source	<1%
www.cs.princeton.edu Internet Source	<1%
www.tdx.cat Internet Source	<1%
krishikosh.egranth.ac.in	